Spring 3-11-2013

A Role for Interferon Stimulated Gene-15 (ISG15) During Chikungunya Virus Infection

Scott Werneke
Washington University in St. Louis

WASHINGTON UNIVERSITY IN ST. LOUIS

Division of Biology and Biomedical Sciences

Immunology

Dissertation Examination Committee:
Deborah Lenschow, Chair
Marco Colonna
Michael Diamond
Daved Fremont
Anthony French
Robyn Klein
Robert Schreiber

A Role for Interferon Stimulated Gene-15 (ISG15) During Chikungunya Virus Infection

by

Scott William Werneke

A dissertation presented to the
Graduate School of Arts and Sciences
of Washington University in
partial fulfillment of the
requirements for the degree
of Doctor of Philosophy

May 2013

St. Louis, Missouri

TABLE OF CONTENTS

LIST OF FIGURES AND TABLES

Chapter 1

Chapter 2

LIST OF ABBREVIATIONS

ALT	alanine aminotransferase
AST	aspartate aminotransferase
Atg	Autophagy related gene
BFV	Barmah forest virus
BMDC	Bone marrow-derived dendritic cell
BMM	Bone marrow-derived macrophages
BUN	blood urea nitrogen
CARD	Caspase activation and recruitment domain
CCHFV	Crimean Congo hemorrhagic fever virus
CCL	Chemokine (C-C motif) ligand
CHIKV	Chikungunya Virus
Co-ip	Co-immunoprecipitation
CPE	Cytopathic effect
CRP	C-reactive protein
CXCL	Chemokine (C-X-C motif) ligand
DC	Dendritic cell
DMEM	Dulbecco's Modified Eagle Medium
dsRNA	Double stranded RNA
EAV	Equine arteritis virus
ECSA	Eastern, central, southern African CHIKV clade
Efp	Estrogen-responsive finger protein
γHV68	Murine gama-herpesvirus 68
Herc5	Hect domain and RLD 5
IFN	Interferon
IFNAR	Interferon α/β receptor
IL	Interleukin
i.p.	Intraperitoneally
IRF	Interferon regulatory factor
ISG	Interferon stimulated gene
ISGF	Interferon stimulated gene factor
ISGylation	ISG15 protein conjugation
ISRE	Interferon stimulated response element
kDa	Kilodalton
LC-MS	Liquid chromatography mass spectrometry
LC3	Microtubule associated protein 1 light chain 3
LPS	Lipopolysaccharide
MCP-1	Monocyte chemotactic protein 1
MDA5	Melanoma differentiation associated protein-5
MEF	Murine embryonic fibroblast
MOI	Multiplicity of infection
NF-κB	Nuclear factor κB
NK cells	Natural killer cells
NLR	NOD like receptor
Nsp	non-structural protein

OAS	2’-5’ oligoadenylate synthetase
PAMP	Pathogen associated molecular pattern
PBS	Phosphate buffered saline
PCBP	Poly(C) binding protein
PCR	Polymerase chain reaction
PFU	Plaque forming unit
pIC	Polyinosinic-polycytidylic acid
PKR	Protein kinase RNA activated
PRR	Pattern recognition receptor
PRRSV	Porcine reproductive and respiratory syndrome virus
qRT-PCR	Quantitative real-time PCR
RIG-I	Retinoic acid-inducible gene-1
RLR	RIG-I like receptor
RRV	Ross river virus
s.c.	Subcutaneously
SFV	Semliki Forest virus
SINV	Sindbis virus
ssRNA	Single stranded RNA
STAT	Signal transducer and activator of transcription
TLR	Toll-like receptor
TNF-α	Tumor necrosis factor a
TRAF	TNF receptor associated factor
UBA	Ubiquitin associated
Ubc	Ubiquitin conjugating
UbE1L	Ubiquitin enzyme 1-like
UBL	Ubiquitin-like
UIM	Ubiquitin-interacting motif
VEEV	Venezuelan equine encephalitis
VHS	Vps27, HRS, STAM
VLP	Virus-like particle
WT	Wild type
Y2H	Yeast 2 hybrid

ACKNOWLEDGEMENTS

I would like to thank all of the members of my thesis committee, Marco Colonna, Mike Diamond, Daved Fremont, Anthony French, Robyn Klein and Bob Schreiber for their continued support and guidance. To be able to work with such leaders in the field of immunology has been an incredible opportunity and has allowed me to become a better scientist. In addition, I would also like to thank Daved Fremont and Robyn Klein for allowing me to do a rotation in their labs, which helped me early on in my scientific career.

This thesis would not have been possible without the contribution of many different collaborators. First and foremost, I would like to thank Clementine Schilte, Pierre-Emmanuel Joubert and Dr. Matthew Albert from the Pasteur Institute. Our collaboration with Matthew's lab has resulted in two publications, both of which have contributed greatly to my thesis. I consider both Clementine and Matthew valuable mentors and truly appreciate being able to work with them. Visiting the Pasteur Institute is easily one of the highlights of my graduate studies and I would like to thank Matthew for welcoming me into his lab and Clementine for showing me the sights. I would like to thank Dr. Stephen Higgs (Kansas State University, recombinant CHIK-GFP) and Dr. Michael Gale (University of Washington, FLAG-MDA5/RIGI) for contributing reagents for my studies. Dr. Kathryn Stone (Yale MS & Proteomics) and Dr. Sophia Alvarez (Danforth Plant Science Center) generated the mass spec data for Chapter 3. I would also like to thank the many collaborators that we've had at Wash U. I have obtained reagents and advice from many different people, including members from the following labs: Diamond (Szretter, Brien, Pal), Klein (Daniels), Virgin (Hwang), Murphy, Fremont, and French. I would also like to thank Suellen Greco for her help with the necropsy and blood chemistry analysis.

I am indebted to my mentor, Deborah Lenschow. It's fun to reflect on how it all started, back at a poster session in 2007. I was drawn to Debbie's lab from her apparent passion and excitement for science. As my first rotation, I was given the freedom to go where the science took me, and made a ton of mistakes. With Debbie's guidance, I was able to bounce back and really started to grow as a scientist. After joining the lab, Debbie challenged me to do my best and helped me to develop my critical thinking skills. I learned early on that it was not enough to just present data; I needed to identify my own strengths and weaknesses and to look ahead to find the relevance of my research. Debbie was always around to discuss science, life, or how badly the Cubs were doing that year. I admire her ability to maintain a balance in her life and will strive for the same. I am extremely grateful for being able to learn from and work with Debbie and would like to thank her for making my graduate experience a positive one.

Now on to the Lenschow lab, the crazy, fun, dysfunctional family that we are: Jessea Campbell, Dave Morales, Kristen Monte, Mari Rodriguez, Anjali Rohatgi, and Jessica Struckhoff. I really appreciate being able to walk in to a lab knowing that I can participate in a lively discussion on science, politics, sports, sitcoms, or anything really. To be able to share our reagents, ideas, opinions and time made for a great working environment and has definitely contributed to my thesis. Time spent outside of the lab was just as fun. I will remember lab lunches, Cardinals games, science conferences, the St. Louis half marathon, Cowboys & Aliens, the Atlas Shrugged book club and a couple of epic paintball battles.

Grad school life would not be complete without the contribution of my family and friends. I would like to thank all of my Wash U and St. Louis friends that have supported me along the way. I am grateful for all of the adventures we've shared: snowboarding trips, softball games, movies, salsa dancing, etc. Most importantly, I would like to thank my family for always

being there. I am incredibly thankful for the encouragement of my parents Mark and Kathy, my brother Brian, and all of the Taylors and the Wernekes. I couldn't have done it without their continuous love and support.

ABSTRACT OF THE DISSERTATION

A Role for Interferon Stimulated Gene-15 (ISG15) During Chikungunya Virus Infection

by

Scott William Werneke

Doctor of Philosophy in Biology and Biomedical Science

Immunology

Washington University in St. Louis, 2013

Professor Deborah J. Lenschow, Chairperson

Chikungunya fever is caused by Chikungunya virus (CHIKV), an infectious disease that is characterized by severe joint and muscle pain in humans. The latest outbreak of CHIKV, which began in 2005, has affected millions of people across India, Singapore, and the Indian Ocean Island region. Type I interferon (IFN), which mediates protection against many different viruses through the upregulation of interferon stimulated genes (ISGs), has been shown to be essential for the control of CHIKV infection. As the role of ISGs during CHIKV infection is largely unknown, we investigated the activity of the interferon stimulated gene ISG15.

ISG15 is a ubiquitin like molecule that has the ability to conjugate to intracellular proteins and can also be found as a free form both intra- and extracellularly. ISG15 conjugation has previously been shown to be essential for protection against influenza B and Sindbis virus infections. We demonstrate that neonatal ISG15$^{-/-}$ mice are profoundly more susceptible to CHIKV infection compared to WT mice. Unlike other viral models, mice lacking the ability to form ISG15 conjugates through the deletion of the E1 enzyme UbE1L, do not display an increase in CHIKV induced lethality. In addition, we observed no differences in viral loads between wild type and ISG15$^{-/-}$ mice during the course of the infection. Instead, ISG15$^{-/-}$ mice displayed a

dramatic increase in proinflammatory cytokines and chemokines. Our data suggests that the role of ISG15 during CHIKV infection is conjugation independent and that ISG15 protection is mediated not through its action as an antiviral molecule, but through regulation of the immune response.

To identify potential mechanisms of action for unconjugated free ISG15, we characterized both intra- and extracellular forms of ISG15 using mass spectrometry. We identify phosphorylation as a potential post-translational modification for extracellular ISG15 and identify the secreted 30kDa ISG15 conjugate as ISG15 bound to hemoglobin subunit beta-1. We also identify over 140 potential non-covalent binding partners for intracellular ISG15 that are involved in many different cellular pathways, including innate immunity, vesicular sorting, and cell signaling. Based on our findings, we have generated preliminary data examining a role for ISG15 in autophagy as well as a role for ISG15 in the regulation of cytokine production. Our characterization of both intra- and extracellular ISG15 will hopefully guide future experiments needed to determine the mechanism by which ISG15 regulates the host response to viral infection.

CHAPTER 1

Introduction

Overview

In 2005, a large scale outbreak of Chikungunya Virus (CHIKV) was reported on the Indian Ocean Island of La Reunion, where approximately 1/3 of the 770,000 inhabitants became infected (1, 2). The scale and severity of this outbreak in combination with additional concurrent outbreaks in India and Southeast Asia has brought this virus to the forefront of infectious disease studies. Research on CHIKV has greatly expanded in an attempt to understand both the viral life cycle as well as the host response to infection. Critical to the control of CHIKV infection is the induction of type I interferons (IFN) (3-5). Interferons, named for their ability to "interfere" with viral replication, act by generating an antiviral state within host cells (6-8). Type I IFN mediates protection through the upregulation of hundreds of interferon stimulated genes (ISGs), although how ISGs provide protection is not well understood. In our introduction, we give an overview of our current knowledge of CHIKV, the type I IFN response, as well as the interferon stimulated gene ISG15.

Chikungunya Virus

History of CHIKV outbreaks (Epidemiology)

Chikungunya virus (CHIKV) was originally isolated in Tanzania in 1952 (9). Since then, CHIKV has been documented to be responsible for numerous outbreaks across Africa and Southeast Asia. Repeated isolated outbreaks of CHIKV have been reported in southern, eastern, and western Africa between the 1960s-1990. In the 1960s, CHIKV was reported in Asia, causing major outbreaks in Myanmar, Thailand, Sri Lanka and India (10). Sporadic outbreaks were also reported in Thailand, Indonesia and the Philippines in the 1980s and Malaysia in the 1990s (11). Phylogenic analysis suggests that CHIKV originated in Africa and subsequently spread to Asia. Currently there are three evolutionary clades of CHIKV, including West African strains, Eastern, Central and Southern African strains (ECSA) and a third clade from Asia (12).

The most recent large scale outbreak of CHIKV began in Kenya in 2004, spreading to the Comoros and eventually appearing on La Reunion Island in March of 2005 (13, 14). The peak of the La Reunion outbreak occurred in December 2005-April 2006, where 38% of the population became infected and 237 deaths were attributed to CHIKV infection (15). The epidemic soon spread to surrounding islands, including Comoros, Mayotte, Mauritius and Madagascar. An estimated 1.6 - 6 million cases were reported in India from 2006-2007 (16-18). The epidemic also affected areas of Southeast Asia, with outbreaks in Thailand, Singapore and Indonesia. Phylogenic studies have confirmed that the ECSA clade was responsible for the 2005-2009 epidemic (1, 2).

Imported cases of CHIKV from travelers returning from these areas to the U.S., Europe, and other countries fueled fears of large outbreaks in previously unexposed urban populations. Increased global communication and travel may make it possible for easier spread of the virus,

which was exemplified by a small outbreak (250 cases) in Italy in 2007 and in Southern France in 2010 (19-21). As a result, research on CHIKV has greatly increased over the last ten years in an attempt to gain a better understanding of CHIKV pathogenesis (11).

Transmission and Viral Vectors

CHIKV is an arbovirus, a virus that is transmitted by arthropod vectors. CHIKV is transmitted to humans primarily by mosquitoes. There are two distinct transmission cycles for CHIKV: (1) sylvatic and (2) human-mosquito-human. Sylvatic transmission is confined to Africa, where outbreaks normally affect smaller populations and are dependent on forest-dwelling Aedes mosquito species, including *Aedes furcifer*, *Aedes taylori*, *Aedes luteocephalus*, *Aedes africanus*, and *Aedes neoafricanus*. Monkeys, birds, rodents and other vertebrate species serve as reservoirs for CHIKV outside of epidemic periods (11). The absence of sylvatic transmission in Asia provides additional evidence that CHIKV originated in Africa before being introduced in Asia.

Non-sylvatic transmission, human-mosquito-human transmission, is dependent on mosquitoes that live in urban areas with a close association with humans. In Asia, *Aedes Aegypti* has been described as a predominant vector for CHIKV. However, a new mosquito vector has been described following the La Reunion outbreak: *Aedes Albopictus.* CHIKV La-Reunion shows only 1-2% amino acid changes when compared to the Tanzania CHIKV reference strain (3). The impact of these mutations on the pathogenicity of the La-Reunion CHIKV strain is not well understood, however research has shown that a mutation in the E1 protein of CHIKV is in part responsible for the use of *Aedes Albopictus* as a new viral vector (22). It is postulated that the alanine to valine amino acid change at position 226 in the E1 CHIK protein allows for

decreased dependency on cholesterol for CHIKV growth, allowing for adaptation in *Aedes Albopictus*. Additional mutations found in the E2 La Reunion envelope protein, E2- G60D and E2- I211T, are thought to maximize the effectiveness of the E1 A226V mutation for *Ae Albopictus* infectivity (23).

Aedes Albopictus as a new mosquito vector adds to concerns of increased global outbreaks for CHIKV due to wide distribution of this vector in urban and Western populations. *Aedes Albopictus* is found in temperate regions where *Aedes Aegypti* is scarce, including parts of the U.S., Europe, China and Japan (11). *Ae. Albopictus* has the ability to colonize various ecosystems and may be a difficult vector to control.

Symptoms (Acute and Long Term)

Chikungunya in Makonde language translates to "that which bends up," which refers to stooped posture developed during infection resulting from severe muscle and joint pain (11). More than 95% of CHIKV infected adults are symptomatic (24). Patients that are infected with CHIKV suffer from polyarthralgia, myalgia, asthenia, fever, headache, and rash. Symptoms may also include acute tenosynovitis and gastrointestinal complaints (1, 11). Acute symptoms usually persist for 1-10 days. During the outbreak on La-Reunion, novel disease symptoms were also described that had previously not been reported for CHIKV, including respiratory or kidney failure, lymphopenia, lethal hepatitis and encephalopathy (25). In addition, although CHIKV can normally be resolved by healthy individuals, La-Reunion reported approximately 250 deaths, seen in infants and elderly (26). Several animal models have been developed that mimic the symptoms observed during CHIKV infection in humans (27-30).

Chronic arthralgia can persist weeks, months, or even years after initial infection. Symptoms usually include fluctuating joint pain that does not change in anatomical location. Virus is usually not detected in circulation after 2 weeks by RT-PCR, although IgM specific responses can persist years after infection. Chronic symptoms normally correlate with age, viral load and CRP (C-reactive protein) levels observed during acute infection (31). It remains unclear whether chronic symptoms result from poor regeneration of joint tissue following damage during acute infection, autoimmune disease induced during infection, or whether the virus is able to persist at low levels in select tissues (30).

CHIKV classification

Chikungunya virus belongs to the *Alphavirus* genus and is a member of the *Togaviridae* family. The alphavirus genus can be further subdivided in to 7 antigenic complexes based on serological cross reactivity: Barmah Forest (BF), Eastern equine encephalitis (EEE), Middelburg (MID), Ndumu (NDU), Semliki Forest (SF), Venezuelan equine encephalitis (VEE), and Western equine encephalitis (WEE) (32). CHIKV belongs to the Semliki Forest Complex. Alphaviruses were also once classified by their geographic prevalence in to Old World and New World Viruses. Old world alphaviruses are mostly arthrogenic and include Chikungunya virus, O'Nyong Nyong Virus (ONNV), Semliki Forest (SFV), Sindbis virus (SIN) and Ross River (RRV). In contrast, new world alphaviruses cause encephalitis and include Venezuelan, Eastern and Western Equine Encephalitis viruses (33).

CHIKV genome and replication

Chikungunya, like all alphaviruses, is an enveloped positive sense, single stranded RNA virus. Electron microscopy indicates that CHIKV is about 70nm in diameter (34). General steps regarding the replication cycle for CHIKV is largely deduced from data obtained from other Alphaviruses and is supported by the sequence similarities that are conserved in CHIKV (32).

The genome is enclosed by capsid proteins (C) that form a nucleocapsid, which is enveloped in a host-derived lipid bilayer that contains two viral envelope glycoproteins E1 and E2. These envelope proteins are necessary for receptor binding (E2) and membrane fusion (E1) of host cells. The receptor for CHIKV is unknown, and is likely responsible for restricting the tropism of CHIKV. The primary targets of CHIKV infection are thought to be fibroblasts, found in the muscle and connective tissue (4). Epithelial (HeLa, 293T, Vero) and endothelial (TrHBMEC) cell lines also support CHIKV growth (3). Unlike RRV or VEEV, most hematopoietic cells do not support CHIKV growth, although replication can be seen in primary monocytes and macrophages (3, 30, 35). After receptor binding, virions are endocytosed and the nucleocapsid is released into the cytosol following pH mediated conformational changes in the E1-E2 dimer that allows for fusion (36-38).

Once the nucleocapsid has disassembled, translation of the viral genome and replication occurs. The CHIKV genome is approximately 11.8-kb long and is organized as follows: 5' cap-nsP1-nsP2-nsP3-nsP4-(junction region)-C-E3-E2-6k-E1-poly(A)-3' (32). The four non-structural proteins (nsP1-4) are translated directly from the viral genome to form polyprotein P1234 and P123 precursors. These polyproteins are processed by an internal viral protease, located within nonstructural protein nsP2. The nonstructural proteins are responsible for generation of a complementary minus strand RNA, plus strand RNA and subgenomic RNA. The subgenomic RNA is derived from the minus strand RNA and is used to generate the structural proteins E1,

pE2, Capsid and 6k (a small peptide that may act as a signal sequence for the translocation of E1). pE2 is eventually cleaved to generate E2, which forms a heterodimer with E1, and E3, which is not incorporated into the virion. The function of E3 is unknown, although may share similarities with SINV E3, which is thought to be involved in proper folding of viral envelope glycoprotein spike formation (32).

Following genome replication and viral protein production, virion assembly occurs via nucleocapsid formation in the cytoplasm. Alphavirus capsid proteins contain RNA binding domains that allow for incorporation of the genome into the nucleocapsid. The capsid proteins oligomerize to form an icosahedral shell which then diffuses freely through the cytoplasm to reach the plasma membrane. At the cell membrane, the nucleocapsid obtains a lipid bilayer composed of mature envelope glycoprotein spikes that are composed of trimers of E1-E2 heterodimers. The E2 protein is necessary for interaction with the capsid proteins, leading to maturation of the nucleocapsid which then allows for budding (32).

Pathogen recognition and interferon production

In humans, viremia for CHIKV infection peaks by day 2 p.i., sharply declines during days 3 and 4 p.i. and is undetectable by day 5 (39). This quick decline of viremia suggests that the innate immune response is critical for the early response to CHIKV infection. As a result, current research on CHIKV has focused on understanding the type I interferon response to infection. Here, we review the type I interferon signaling pathway and its importance in controlling CHIKV infection.

Pattern Recognition Receptors and RNA Virus Detection

Production of type I IFN is dependent on the ability to detect invading pathogens through the use of pattern recognition receptors (PRRs). PRR recognize conserved pathogen structures known as pathogen-associated molecular patterns (PAMPs). Toll-like Receptors (TLRs), NOD like receptors (NLRs), and RIG-I-like receptors (RLRs) are well described PRRs that play a role in pathogen detection. Although the signaling components for each PRR can vary, each pathway ultimately leads to the activation of NF-κB and/or IRF3, which are necessary for IFN transcription (40).

TLRs contain a luecine-rich repeat (LRR) for detection of PAMPs, a transmembrane domain and an intracellular Toll/IL-1 receptor (TIR) domain that mediates downstream signaling. TLRs are localized to either the plasma membrane or endosomal compartment and respond to bacterial and/or viral components. The primary TLRs responsible for RNA virus detection are TLR3 (dsRNA) and TLR7/8 (ssRNA rich in G/U residues) and are localized to the endosome. Phagocytosis of nucleic acids from apoptotic or necrotic cells triggers TLR signaling, which leads to macrophage or dendritic cell activation. Downstream signaling of TLR3 and TLR7/8 is mediated by TRIF and MyD88, respectively, which leads to the production of IFN and other pro-inflammatory cytokines (40, 41).

The two best described RLRs, RIG-I (retinoic acid-inducible gene I) and MDA5 (melanoma differentiation-associated gene 5), are both cytosolic RNA sensors that are responsible for detecting intracellular RNA viruses. RIG-I and MDA5 contain a C-terminal DExD/H box RNA helicase domain for viral RNA recognition and N-terminal caspase-recruitment and activation domain (CARDs) which mediate downstream signaling (42). RIG-I recognizes dsRNA with 5' triphosphate and MDA5 recognizes long dsRNA. Engagement of RIG-I or MDA5 allows for the association with Cardif /IPS-1/MAVS/VISA, which leads to the

activation of NF-κB (nuclear factor κB), AP-1 (a heterodimer of activating transcription factor 2 (ATF2) with c-Jun), IRF7 and IRF3 (7, 42).

NLRs are cytosolic sensors that detect a wide array of PAMPs and other physiological stressors and are primarily characterized by their ability to activate the inflammasome. The role for NLRs in RNA virus detection is less defined, although recent literature suggests that the NLR NOD2 plays a role in the detection of Respiratory Syncytial, Influenza A and Parainfluenza viruses (43). NLRX1 has also been shown to regulate IFN production (44). Both NOD2 and NLRX1 interact with Cardif, resulting in a similar downstream signaling cascade as RLRs. Translocation of NF-κB, AP-1 and IRF3/7 to the nucleus allows for type I IFN production (40, 42).

Interferons

There are three classes of IFN: type I, II and III. Type II IFN consists of a single member, IFNγ which signals through the IFNγ receptor complex (IFNGR) and mediates broad immune responses to pathogens. Type III IFNs consist of IFNlambda1-3 and signal through a receptor complex composed of IFNLR1 (IL-28α) and IL-10R2 (IL-10Rβ). The activity of type III IFNs is less well known, however it has been proposed that type III IFNs behave similar to type I IFNs. Type I IFNs are well characterized and are the focus of this section. (45, 46).

Type I IFNs are made up of seven classes: IFNα, IFNβ, IFNε, IFNκ, IFNω, IFNδ, and IFNτ, with IFNα and IFNβ being the focus of antiviral studies. Although there is only one subtype for IFNβ, there are several subtypes of IFNα (13 in humans, at least 10 in mice). Type I IFNs are regulated at the transcriptional level, following PRR activation. The promoter regions of IFNβ and IFNα contain regulatory cis elements called positive regulatory domains (PRDs).

The IFNβ promoter contains 4 PRD domains I-IV, whereas IFNα contains PRDI and PRDIII-like elements (PRD-LE). PRDI and III are the binding sites for the IRF family members, whereas PRDII and PRDIV bind to NF-κB and AP-1, respectively. Binding of transcription factors to the promoter region forms an "enhanceosome," which allows for nucleosome displacement and recruitment of the transcription complex TFIID for gene expression. (42)

After virus has been detected by an infected cell, type I IFN is released, acting in an autocrine and paracrine fashion on both infected and uninfected cells. All type I IFNs mediate there antiviral activity by binding to a common IFNα/β receptor (IFNAR), a complex between IFNAR1 and IFNAR2. IFNAR1 and IFNAR2 associate with intracellular Janus activated kinases (JAKs) tyrosine kinase 2 (Tyk2) and JAK1 respectively. Tyk2 and JAK1 are trans-phosphorylated following IFNAR oligomerization. Activation of Tyk2 and JAK1 allows for phosphorylation of STAT1 and STAT2 (signal transducer and activator of transcription). Phosphorylation of STAT1 and STAT2 allows for dimerization followed by association with IRF9. This complex is known as interferon-stimulated response factor 3 (ISGF3). ISGF3 translocates to the nucleus and activates the transcription of interferon stimulated genes (ISGs) by binding to interferon stimulated response elements (ISRE). Hundreds of ISGs are transcribed in response to type I interferon signaling although the antiviral function for many of these genes remains unknown. (46)

A role for type I IFN during CHIKV infection

Research on CHIKV has demonstrated that interferons play an essential role during viral infection. Pretreatment of the human epithelial Hela cell line with type I or type II interferon inhibits viral replication and viral induced CPE (3). Adult C57Bl/6 mice are resistant to CHIKV infection whereas $IFNAR^{-/-}$ mice die by day 3 p.i. and show wide viral dissemination and high

viral titers (4). IFNAR$^{-/-}$ mice also show high serum levels of IFNα and IFNβ on day2 p.i., which indicates that IFN is induced during CHIKV infection. Wild type mice infected with CHIKV do not show systemic production of IFNα/β, however it's thought that local production of type I IFN is sufficient to protect wild type mice and limit viral dissemination. Sera from CHIKV infected human patients also have elevated type I interferon levels (5). Type II interferon production does not appear to be as critical in controlling CHIKV infection, as IFNγ levels are not elevated in the sera of human patients and IFNγ$^{-/-}$ mice survive CHIKV infection (5).

In order to understand how type I interferon protects against CHIKV infection, mechanistic studies have been done to describe the cell types necessary to produce and respond to type I IFN. Surprisingly, immature and mature monocyte-derived cDCs, isolated pDCs and monocytes are unable to produce type I IFN in response to CHIKV treatment. Instead, robust production of IFNβ can be detected from primary human foreskin fibroblasts and MRC-5 cells following CHIKV infection. This data suggests that hematopoietic cells do not produce type I IFN following direct stimulation with CHIKV and that fibroblasts may be responsible for the initial production of type I IFN. Bone marrow chimera studies have shown that type I IFNs act on non-hematopoietic cells in order to control CHIKV infection. In addition, search for viral sensors for CHIKV has revealed that both Cardif and MyD88 signaling pathways contribute to the control of CHIKV. In terms of the ISGs that mediate these antiviral activities against CHIKV, little is known. To start to address the mechanism by which type I IFNs mediate control of CHIKV infection, we turned our attention to the interferon stimulated gene ISG15. (5)

Interferon Stimulated Genes

Signaling through the IFNAR receptor leads to the induction of over 300 interferon stimulated genes (ISGs) (47). Many of the proteins that are induced by IFN play a role in pathogen recognition (PRRs) and act as transcription factors that amplify IFN production. Additional ISGs also have direct antiviral function. The effector activities of antiviral ISGs include a wide variety of functions, including but not limited to cytoskeletal remodeling, apoptosis induction, RNA regulation (splicing, editing, and degradation), and other post-translational modifications (45).

Some of the best known antiviral effectors include Mx GTPases, PKR, OAS and RNaseL, as well as ISG15. MxA monomers bind to viral nucleocapsid proteins, which leads to their degradation and limits viral replication. 2', 5' –oligoadenylate synthetase 1 (OAS1) is activated by viral dsRNA to generate 2',5' oligadenylates that subsequently bind to and activate RNaseL, which cleaves cellular and viral RNAs. PKR phosphorylates eukaryotic translation factor 2α (EIF2α) after binding to viral RNAs, which results in translation inhibition. Additional ISGs include the translation regulators IFIT1 and IFIT2 (IFN-induced protein with tetratricopeptide repeats), Viperin, APOBEC (apolipoprotein B mRNA-editing enzyme, catalytic polypeptide), ISG20, and members of the tripartite-motif containing (TRIM) proteins such as TRIM1. Below, we discuss in greater detail the activity of ubiquitin like molecule ISG15. (45)

ISG15

One of the most predominant genes induced by type I IFN is ISG15 (47, 48). ISG15 is a 17kDa molecule that contains two ubiquitin-like domains connected by a peptide linker. Both domains of ISG15 contain approximately 30% identity to ubiquitin and assume a β-grasp fold secondary structure that is almost identical to that for ubiquitin (49). ISG15 is generated as a

propeptide that is processed by an unidentified cellular protease (possibly Ubp1) to reveal a conserved C-terminal LRLRGG diglycine motif that allows for ISG15 to be conjugated to target proteins (50, 51). Due to ISG15s structural similarity to ubiquitin, we will briefly review the activity of the ubiquitin family and ubiquitin like proteins (UBLs).

Ubiquitin and UBLs

Ubiquitin is a 7kDa protein that forms isopeptide bonds with lysines of target proteins through a conserved LRLRGG C-terminal motif. Post-translational modification of proteins by ubiquitin can lead to a variety of functional consequences, dependent on the specific type or ubiquitin modification. The most commonly known function of ubiquitin is to target intracellular proteins to the proteasome through the formation of Lys48 poly-ubiquitin chains, which leads to protein degradation. Ubiquitin can also play an important role in many other cellular processes, including apoptosis, endocytosis, histone regulation and viral budding. (52, 53)

Ubiquitin like proteins (UBLs) share the same structural fold as ubiquitin and can also be conjugated to target proteins. Commonly known UBLs include SUMO-1 (small-ubiquitin-related modifier), Nedd8 (also known as RUB1 (related-to-ubiqutin-1)), Fat10, and several members of the autophagy pathway (Atg8, Atg12). Sumoylation (conjugation of proteins to SUMO-1) allows for protein localization around the nucleus and can also compete for ubiquitin binding sites to prevent ubiquitin mediated degradation. Nedd8 modifies subunits of the SCF (Skp1/cullin-1/F-box protein) ubiquitin ligase family and is required for maximal ligase activity. Fat10 is also thought to compete for ubiquitin binding sites. Unlike ubiquitin, UBLs are not known to self-conjugate, therefore act as monomeric conjugates. (54, 55)

Conjugation to target proteins for both ubiquitin and UBLs is mediated through an E1/E2/E3 enzymatic cascade. The C-terminus of the Ubl is activated via adenylation, allowing for the formation of a thioester bond with the Ubl activating enzyme E1. The ubiquitin like molecule is then transferred to a cysteine side chain of the conjugating enzyme E2, which can also bind to an E3 ligase protein. The E3 protein associates with the acceptor protein and allows for transfer of the ubiquitin moiety to the target protein. Modification of ubiquitin or UBLs to target proteins is reversible, as there exists several De-ubiquitinating and related enzymes. (55)

The ISG15 conjugation cascade

Similar to ubiquitin, ISG15 modification (ISGylation) of target proteins requires an E1, E2, E3 enzymatic cascade. UBE1L is thought to be the major E1 activating enzyme for ISG15, which is specific for ISG15 conjugation (56). The ubiquitin E2 protein UbcH8 appears to be the major E2 for ISG15 (57, 58). Herc5 is thought to be the most important E3 protein for ISGylation (59-61), although other additional E3s have been identified (e.g. Rsp5p, Efp) (57, 62). In addition, ISG15 can be removed from targeted proteins by the deconjugating enzyme UBP43 (63). Unlike ubiquitin, ISG15 is not constitutively expressed. All members of the ISG15 cascade, including UBP43, are induced following type I IFN stimulation.

A role for ISG15 during viral infection

The early induction and high levels of expression of ISG15 following IFN stimulation has led to the investigation into ISG15 as an antiviral molecule (Fig 1.1). Neonatal mice infected with the alphavirus Sindbis virus show >100 fold increase in ISG15 RNA as well as robust ISG15 conjugate formation (64-66). The first demonstration that ISG15 could function as an

antiviral molecule was overexpression of ISG15 through the use of a recombinant Sindbis virus construct. It protected IFNAR$^{-/-}$ mice from Sindbis infection (66). Subsequent studies showed that ISG15$^{-/-}$ mice were more susceptible to Sindbis virus (67). ISG15s role as an antiviral molecule is not limited to Sindbis infection, as ISG15$^{-/-}$ mice are also susceptible to herpes simplex virus, gamma herpes virus, and influenza A and B viruses (67).

The ability of ISG15 to form conjugates appears to be critical for its antiviral role during Sindbis virus infection. UBE1L$^{-/-}$ mice, which lack the ability to form ISG15 conjugates (68), have similar lethality as ISG15$^{-/-}$ mice to Sindbis infection (69). ISG15$^{-/-}$ mice infected with a recombinant Sindbis virus that expresses an unconjugatable form of ISG15 (LRLRAA) are not protected from viral induced lethality while the expression of wild type ISG15 (LRLRGG) protects ISG15$^{-/-}$ mice (67, 69). The importance of ISG15 conjugation has also been demonstrated for other viral infections. UBE1L$^{-/-}$ mice infected with influenza B phenocopy ISG15$^{-/-}$ mice, with similar lethality and lung viral titers (70). Further support for the importance of conjugation comes from the immune evasion strategies employed by viruses. The NS1 protein of influenza B has been shown to directly inhibit ISG15 conjugate formation (56). OTU-domain containing viral proteins, such as the L protein of Crimean-Congo hemorrhagic fever virus (CCHFV) or the Nsp2 protein of Equine Arteritis virus (EAV), also reduce the level of ISG15 conjugates (71). The ability of viruses to target ISGylation suggests that this is an important immune evasion strategy.

ISG15 Function

Although ISG15 has been shown to be an important antiviral molecule, the mechanism by which ISG15 inhibits viral infection is not well understood. Due to the apparent similarities

between ISG15 and ubiquitin as well as the demonstrated importance of ISG15 conjugation in vivo, current research has focused on determining the functional consequence of ISG15 modification of target proteins. Over 200 potential targets of ISGylation have been identified using mass spectrometry. Targets of ISGylation take part in a number of cellular processes, including cell cycle, cell metabolism, and immune signaling pathways (72, 73). Viral proteins have also been shown to be targets of ISGylation (74, 75). A potential mechanism by which ISG15 targets such wide array of proteins with only one main E3 has been suggested. Herc5 has been shown to associate with polyribosmes, allowing for modification newly synthesized proteins (75). However, ISG15 modification appears to be specific, as not all newly translated proteins are ISGylated.

ISG15 modification of target proteins has been suggested to cause either a loss or gain of function for the targeted protein. ISGylation of Ubc13 causes a reduction in polyubiquitinated TRAF6, which consequently leads to a decrease in NF-κB activation (76). In addition, ISG15 modification of filamin B disrupts its scaffold function which then downregulates the type I interferon-induced JNK signaling pathway (77). Conjugation of ISG15 to RIG-I has also been suggested to negatively regulate RIG-I mediated IFN induction (78). So far, modification of 4EHP is the only reported gain of function for ISG15 (79). ISGylation of 4EHP enhances its cap-binding activity which allows for inhibition of mRNA translation. Unlike ubiquitin, ISGylation has not been shown to directly lead to degradation of target proteins (80).

Much less work has gone into studying the importance of free ISG15 during viral infection. In vitro studies have demonstrated that expression of ISG15 interferes with budding of HIV-1 and Ebola virus like particles, although it remains unclear if this is conjugation independent (79, 81-83). Free ISG15 has also been shown to be released extracellularly and has

been suggested to have cytokine like activity. Non-conjugated ISG15 can be detected in the sera of humans treated with IFNβ as well as mice infected with certain viruses. PBMCs and non-hematopoietic cell lines secrete ISG15 in response to IFNβ (84). Recombinant ISG15 has been shown to increase NK cell proliferation and lytic activity (85). Extracellular ISG15 has been shown to act as a neutrophil chemoattractant and can upregulate e-cadherin expression on dendritic cells (86, 87). Most recently, recombinant ISG15 in concert with IL-12 stimulation has been shown to upregulate IFNγ (88). Although ISG15 appears to have cytokine activity, a receptor for ISG15 has not been identified.

Data that we have generated indicates that ISG15 is expressed following CHIKV infection. Nine day old wild type neonates were infected with CHIKV and ISG15 induction was assessed by qRT-PCR and western blot analysis. ISG15 mRNA at the site of infection is detected as early as 3hrs p.i. with peak levels obtained after 24hrs. Lung, liver and serum from nine day old wild type neonates show robust ISG15 induction and ISG15 conjugate formation by western blot analysis. The documented role for ISG15 in the host response to viral infection, including Sindbis virus infection, prompted us to evaluate its action in CHIKV pathogenesis.

Figure 1.1 Forms of ISG15 expression during viral infection. Detection of viral infection leads to upregulation of type I IFN, which mediates its activity through the induction of interferon stimulated genes (ISGs). The ubiquitin-like molecule ISG15, shown to play an important role during several viral infections, is upregulated along with members of the ISG15 conjugation cascade: UbE1L (E1), Ubc8 (E2) and Herc5 (E3). This allows ISG15 to be conjugated to many different intracellular proteins. In addition, ISG15 can be found as a free form, both intra- and extracellularly. It is thought that extracellular ISG15 may have cytokine like activity via binding to an unidentified cell surface receptor. Figure generated by Nadia Giannakopoulos.

Figure 1.1

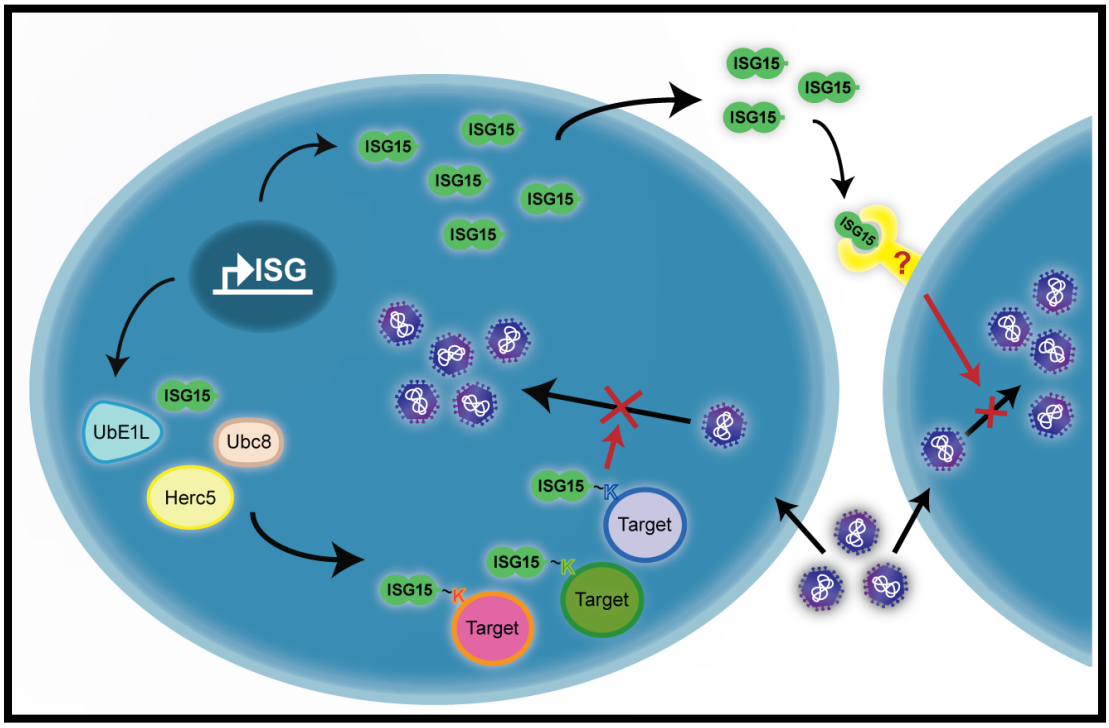
ISG15
ISG15
ISG15
ISG15
ISG15
ISG15
ISG15
ISG15
ISG15
?
ISG
ISG15
UbE1L
Ubc8
Herc5
ISG15 ~K
Target
ISG15 ~K
Target
ISG15 ~K
Target

REFERENCES

1. Bessaud, M., C. N. Peyrefitte, B. A. Pastorino, F. Tock, O. Merle, J. J. Colpart, J. S. Dehecq, R. Girod, M. C. Jaffar-Bandjee, P. J. Glass, M. Parker, H. J. Tolou, and M. Grandadam. 2006. Chikungunya virus strains, Reunion Island outbreak. *Emerg Infect Dis* 12:1604-1606.

2. Schuffenecker, I., I. Iteman, A. Michault, S. Murri, L. Frangeul, M. C. Vaney, R. Lavenir, N. Pardigon, J. M. Reynes, F. Pettinelli, L. Biscornet, L. Diancourt, S. Michel, S. Duquerroy, G. Guigon, M. P. Frenkiel, A. C. Brehin, N. Cubito, P. Despres, F. Kunst, F. A. Rey, H. Zeller, and S. Brisse. 2006. Genome microevolution of chikungunya viruses causing the Indian Ocean outbreak. *PLoS Med* 3:e263.

3. Sourisseau, M., C. Schilte, N. Casartelli, C. Trouillet, F. Guivel-Benhassine, D. Rudnicka, N. Sol-Foulon, K. Le Roux, M. C. Prevost, H. Fsihi, M. P. Frenkiel, F. Blanchet, P. V. Afonso, P. E. Ceccaldi, S. Ozden, A. Gessain, I. Schuffenecker, B. Verhasselt, A. Zamborlini, A. Saib, F. A. Rey, F. Arenzana-Seisdedos, P. Despres, A. Michault, M. L. Albert, and O. Schwartz. 2007. Characterization of reemerging chikungunya virus. *PLoS Pathog* 3:e89.

4. Couderc, T., F. Chretien, C. Schilte, O. Disson, M. Brigitte, F. Guivel-Benhassine, Y. Touret, G. Barau, N. Cayet, I. Schuffenecker, P. Despres, F. Arenzana-Seisdedos, A. Michault, M. L. Albert, and M. Lecuit. 2008. A mouse model for Chikungunya: young age and inefficient type-I interferon signaling are risk factors for severe disease. *PLoS Pathog* 4:e29.

5. Schilte, C., T. Couderc, F. Chretien, M. Sourisseau, N. Gangneux, F. Guivel-Benhassine, A. Kraxner, J. Tschopp, S. Higgs, A. Michault, F. Arenzana-Seisdedos, M. Colonna, L. Peduto, O. Schwartz, M. Lecuit, and M. L. Albert. 2010. Type I IFN controls chikungunya virus via its action on nonhematopoietic cells. *J Exp Med* 207:429-442.

6. Isaacs, A., and J. Lindenmann. 1957. Virus interference. I. The interferon. *Proc R Soc Lond B Biol Sci* 147:258-267.

7. Stetson, D. B., and R. Medzhitov. 2006. Type I interferons in host defense. *Immunity* 25:373-381.

8. Vilcek, J. 2006. Fifty years of interferon research: aiming at a moving target. *Immunity* 25:343-348.

9. Mason, P. J., and A. J. Haddow. 1957. An epidemic of virus disease in Southern Province, Tanganyika Territory, in 1952-53; an additional note on Chikungunya virus isolations and serum antibodies. *Trans R Soc Trop Med Hyg* 51:238-240.

10. Deller, J. J., Jr., and P. K. Russell. 1968. Chikungunya disease. *Am J Trop Med Hyg* 17:107-111.

11. Her, Z., Y. W. Kam, R. T. Lin, and L. F. Ng. 2009. Chikungunya: a bending reality. *Microbes Infect* 11:1165-1176.

12. Powers, A. M., and C. H. Logue. 2007. Changing patterns of chikungunya virus: re-emergence of a zoonotic arbovirus. *J Gen Virol* 88:2363-2377.

13. Sergon, K., A. A. Yahaya, J. Brown, S. A. Bedja, M. Mlindasse, N. Agata, Y. Allaranger, M. D. Ball, A. M. Powers, V. Ofula, C. Onyango, L. S. Konongoi, R. Sang, M. K. Njenga, and R. F. Breiman. 2007. Seroprevalence of Chikungunya virus infection on Grande Comore Island, union of the Comoros, 2005. *Am J Trop Med Hyg* 76:1189-1193.

14. Kariuki Njenga, M., L. Nderitu, J. P. Ledermann, A. Ndirangu, C. H. Logue, C. H. Kelly, R. Sang, K. Sergon, R. Breiman, and A. M. Powers. 2008. Tracking epidemic Chikungunya virus into the Indian Ocean from East Africa. *J Gen Virol* 89:2754-2760.

15. Renault, P., J. L. Solet, D. Sissoko, E. Balleydier, S. Larrieu, L. Filleul, C. Lassalle, J. Thiria, E. Rachou, H. de Valk, D. Ilef, M. Ledrans, I. Quatresous, P. Quenel, and V. Pierre. 2007. A major epidemic of chikungunya virus infection on Reunion Island, France, 2005-2006. *Am J Trop Med Hyg* 77:727-731.

16. Ravi, V. 2006. Re-emergence of chikungunya virus in India. *Indian J Med Microbiol* 24:83-84.

17. Saxena, S. K., M. Singh, N. Mishra, and V. Lakshmi. 2006. Resurgence of chikungunya virus in India: an emerging threat. *Euro Surveill* 11:E060810 060812.

18. Arankalle, V. A., S. Shrivastava, S. Cherian, R. S. Gunjikar, A. M. Walimbe, S. M. Jadhav, A. B. Sudeep, and A. C. Mishra. 2007. Genetic divergence of Chikungunya viruses in India (1963-2006) with special reference to the 2005-2006 explosive epidemic. *J Gen Virol* 88:1967-1976.

19. Mavalankar, D., P. Shastri, and P. Raman. 2007. Chikungunya epidemic in India: a major public-health disaster. *Lancet Infect Dis* 7:306-307.

20. Angelini, R., A. C. Finarelli, P. Angelini, C. Po, K. Petropulacos, G. Silvi, P. Macini, C. Fortuna, G. Venturi, F. Magurano, C. Fiorentini, A. Marchi, E. Benedetti, P. Bucci, S. Boros, R. Romi, G. Majori, M. G. Ciufolini, L. Nicoletti, G. Rezza, and A. Cassone. 2007. Chikungunya in north-eastern Italy: a summing up of the outbreak. *Euro Surveill* 12:E071122 071122.

21. Gould, E. A., P. Gallian, X. De Lamballerie, and R. N. Charrel. 2010. First cases of autochthonous dengue fever and chikungunya fever in France: from bad dream to reality! *Clin Microbiol Infect* 16:1702-1704.

22. Tsetsarkin, K. A., D. L. Vanlandingham, C. E. McGee, and S. Higgs. 2007. A single mutation in chikungunya virus affects vector specificity and epidemic potential. *PLoS Pathog* 3:e201.

23. Tsetsarkin, K. A., C. E. McGee, S. M. Volk, D. L. Vanlandingham, S. C. Weaver, and S. Higgs. 2009. Epistatic roles of E2 glycoprotein mutations in adaption of chikungunya virus to Aedes albopictus and Ae. aegypti mosquitoes. *PLoS One* 4:e6835.

24. Queyriaux, B., F. Simon, M. Grandadam, R. Michel, H. Tolou, and J. P. Boutin. 2008. Clinical burden of chikungunya virus infection. *Lancet Infect Dis* 8:2-3.

25. Pialoux, G., B. A. Gauzere, S. Jaureguiberry, and M. Strobel. 2007. Chikungunya, an epidemic arbovirosis. *Lancet Infect Dis* 7:319-327.

26. Simon, F., H. Tolou, and P. Jeandel. 2006. [The unexpected Chikungunya outbreak]. *Rev Med Interne* 27:437-441.

27. Ziegler, S. A., L. Lu, A. P. da Rosa, S. Y. Xiao, and R. B. Tesh. 2008. An animal model for studying the pathogenesis of chikungunya virus infection. *Am J Trop Med Hyg* 79:133-139.

28. Gardner, J., I. Anraku, T. T. Le, T. Larcher, L. Major, P. Roques, W. A. Schroder, S. Higgs, and A. Suhrbier. 2010. Chikungunya virus arthritis in adult wild-type mice. *J Virol* 84:8021-8032.

29. Morrison, T. E., L. Oko, S. A. Montgomery, A. C. Whitmore, A. R. Lotstein, B. M. Gunn, S. A. Elmore, and M. T. Heise. 2011. A mouse model of chikungunya virus-induced musculoskeletal inflammatory disease: evidence of arthritis, tenosynovitis, myositis, and persistence. *Am J Pathol* 178:32-40.

30. Labadie, K., T. Larcher, C. Joubert, A. Mannioui, B. Delache, P. Brochard, L. Guigand, L. Dubreil, P. Lebon, B. Verrier, X. de Lamballerie, A. Suhrbier, Y. Cherel, R. Le Grand, and P. Roques. 2010. Chikungunya disease in nonhuman primates involves long-term viral persistence in macrophages. *J Clin Invest* 120:894-906.

31. Hoarau, J. J., M. C. Jaffar Bandjee, P. Krejbich Trotot, T. Das, G. Li-Pat-Yuen, B. Dassa, M. Denizot, E. Guichard, A. Ribera, T. Henni, F. Tallet, M. P. Moiton, B. A. Gauzere, S. Bruniquet, Z. Jaffar Bandjee, P. Morbidelli, G. Martigny, M. Jolivet, F. Gay, M. Grandadam, H. Tolou, V. Vieillard, P. Debre, B. Autran, and P. Gasque. 2010. Persistent chronic inflammation and infection by Chikungunya arthritogenic alphavirus in spite of a robust host immune response. *J Immunol* 184:5914-5927.

32. Solignat, M., B. Gay, S. Higgs, L. Briant, and C. Devaux. 2009. Replication cycle of chikungunya: a re-emerging arbovirus. *Virology* 393:183-197.

33. Ryman, K. D., and W. B. Klimstra. 2008. Host responses to alphavirus infection. *Immunol Rev* 225:27-45.

34. Jose, J., J. E. Snyder, and R. J. Kuhn. 2009. A structural and functional perspective of alphavirus replication and assembly. *Future Microbiol* 4:837-856.

35. Her, Z., B. Malleret, M. Chan, E. K. Ong, S. C. Wong, D. J. Kwek, H. Tolou, R. T. Lin, P. A. Tambyah, L. Renia, and L. F. Ng. 2010. Active infection of human blood monocytes by Chikungunya virus triggers an innate immune response. *J Immunol* 184:5903-5913.

36. Glomb-Reinmund, S., and M. Kielian. 1998. The role of low pH and disulfide shuffling in the entry and fusion of Semliki Forest virus and Sindbis virus. *Virology* 248:372-381.

37. Wahlberg, J. M., R. Bron, J. Wilschut, and H. Garoff. 1992. Membrane fusion of Semliki Forest virus involves homotrimers of the fusion protein. *J Virol* 66:7309-7318.

38. Bernard, E., M. Solignat, B. Gay, N. Chazal, S. Higgs, C. Devaux, and L. Briant. 2010. Endocytosis of chikungunya virus into mammalian cells: role of clathrin and early endosomal compartments. *PLoS One* 5:e11479.

39. Carey, D. E., R. M. Myers, C. M. DeRanitz, M. Jadhav, and R. Reuben. 1969. The 1964 chikungunya epidemic at Vellore, South India, including observations on concurrent dengue. *Trans R Soc Trop Med Hyg* 63:434-445.

40. Takeuchi, O., and S. Akira. 2010. Pattern recognition receptors and inflammation. *Cell* 140:805-820.

41. Saito, T., and M. Gale, Jr. 2007. Principles of intracellular viral recognition. *Curr Opin Immunol* 19:17-23.

42. Honda, K., A. Takaoka, and T. Taniguchi. 2006. Type I interferon [corrected] gene induction by the interferon regulatory factor family of transcription factors. *Immunity* 25:349-360.

43. Sabbah, A., T. H. Chang, R. Harnack, V. Frohlich, K. Tominaga, P. H. Dube, Y. Xiang, and S. Bose. 2009. Activation of innate immune antiviral responses by Nod2. *Nat Immunol* 10:1073-1080.

44. Moore, C. B., D. T. Bergstralh, J. A. Duncan, Y. Lei, T. E. Morrison, A. G. Zimmermann, M. A. Accavitti-Loper, V. J. Madden, L. Sun, Z. Ye, J. D. Lich, M. T. Heise, Z. Chen, and J. P. Ting. 2008. NLRX1 is a regulator of mitochondrial antiviral immunity. *Nature* 451:573-577.

45. Sadler, A. J., and B. R. Williams. 2008. Interferon-inducible antiviral effectors. *Nat Rev Immunol* 8:559-568.

46. Platanias, L. C. 2005. Mechanisms of type-I- and type-II-interferon-mediated signalling. *Nat Rev Immunol* 5:375-386.

47. Der, S. D., A. Zhou, B. R. Williams, and R. H. Silverman. 1998. Identification of genes differentially regulated by interferon alpha, beta, or gamma using oligonucleotide arrays. *Proc Natl Acad Sci U S A* 95:15623-15628.

48. Korant, B. D., D. C. Blomstrom, G. J. Jonak, and E. Knight, Jr. 1984. Interferon-induced proteins. Purification and characterization of a 15,000-dalton protein from human and bovine cells induced by interferon. *J Biol Chem* 259:14835-14839.

49. Narasimhan, J., M. Wang, Z. Fu, J. M. Klein, A. L. Haas, and J. J. Kim. 2005. Crystal structure of the interferon-induced ubiquitin-like protein ISG15. *J Biol Chem* 280:27356-27365.

50. Potter, J. L., J. Narasimhan, L. Mende-Mueller, and A. L. Haas. 1999. Precursor processing of pro-ISG15/UCRP, an interferon-beta-induced ubiquitin-like protein. *J Biol Chem* 274:25061-25068.

51. Knight, E., Jr., D. Fahey, B. Cordova, M. Hillman, R. Kutny, N. Reich, and D. Blomstrom. 1988. A 15-kDa interferon-induced protein is derived by COOH-terminal processing of a 17-kDa precursor. *J Biol Chem* 263:4520-4522.

52. Hicke, L. 2001. Protein regulation by monoubiquitin. *Nat Rev Mol Cell Biol* 2:195-201.

53. Jesenberger, V., and S. Jentsch. 2002. Deadly encounter: ubiquitin meets apoptosis. *Nat Rev Mol Cell Biol* 3:112-121.

54. Hochstrasser, M. 2000. Evolution and function of ubiquitin-like protein-conjugation systems. *Nat Cell Biol* 2:E153-157.

55. Welchman, R. L., C. Gordon, and R. J. Mayer. 2005. Ubiquitin and ubiquitin-like proteins as multifunctional signals. *Nat Rev Mol Cell Biol* 6:599-609.

56. Yuan, W., and R. M. Krug. 2001. Influenza B virus NS1 protein inhibits conjugation of the interferon (IFN)-induced ubiquitin-like ISG15 protein. *EMBO J* 20:362-371.

57. Zhao, C., S. L. Beaudenon, M. L. Kelley, M. B. Waddell, W. Yuan, B. A. Schulman, J. M. Huibregtse, and R. M. Krug. 2004. The UbcH8 ubiquitin E2 enzyme is also the E2 enzyme for ISG15, an IFN-alpha/beta-induced ubiquitin-like protein. *Proc Natl Acad Sci U S A* 101:7578-7582.

58. Kim, K. I., N. V. Giannakopoulos, H. W. Virgin, and D. E. Zhang. 2004. Interferon-inducible ubiquitin E2, Ubc8, is a conjugating enzyme for protein ISGylation. *Mol Cell Biol* 24:9592-9600.

59. Dastur, A., S. Beaudenon, M. Kelley, R. M. Krug, and J. M. Huibregtse. 2006. Herc5, an interferon-induced HECT E3 enzyme, is required for conjugation of ISG15 in human cells. *J Biol Chem* 281:4334-4338.

60. Takeuchi, T., S. Inoue, and H. Yokosawa. 2006. Identification and Herc5-mediated ISGylation of novel target proteins. *Biochem Biophys Res Commun* 348:473-477.

61. Wong, J. J., Y. F. Pung, N. S. Sze, and K. C. Chin. 2006. HERC5 is an IFN-induced HECT-type E3 protein ligase that mediates type I IFN-induced ISGylation of protein targets. *Proc Natl Acad Sci U S A* 103:10735-10740.

62. Zou, W., and D. E. Zhang. 2006. The interferon-inducible ubiquitin-protein isopeptide ligase (E3) EFP also functions as an ISG15 E3 ligase. *J Biol Chem* 281:3989-3994.

63. Malakhov, M. P., O. A. Malakhova, K. I. Kim, K. J. Ritchie, and D. E. Zhang. 2002. UBP43 (USP18) specifically removes ISG15 from conjugated proteins. *J Biol Chem* 277:9976-9981.

64. Johnston, C., W. Jiang, T. Chu, and B. Levine. 2001. Identification of genes involved in the host response to neurovirulent alphavirus infection. *J Virol* 75:10431-10445.

65. Labrada, L., X. H. Liang, W. Zheng, C. Johnston, and B. Levine. 2002. Age-dependent resistance to lethal alphavirus encephalitis in mice: analysis of gene expression in the central nervous system and identification of a novel interferon-inducible protective gene, mouse ISG12. *J Virol* 76:11688-11703.

66. Lenschow, D. J., N. V. Giannakopoulos, L. J. Gunn, C. Johnston, A. K. O'Guin, R. E. Schmidt, B. Levine, and H. W. t. Virgin. 2005. Identification of interferon-stimulated gene 15 as an antiviral molecule during Sindbis virus infection in vivo. *J Virol* 79:13974-13983.

67. Lenschow, D. J., C. Lai, N. Frias-Staheli, N. V. Giannakopoulos, A. Lutz, T. Wolff, A. Osiak, B. Levine, R. E. Schmidt, A. Garcia-Sastre, D. A. Leib, A. Pekosz, K. P. Knobeloch, I. Horak, and H. W. t. Virgin. 2007. IFN-stimulated gene 15 functions as a critical antiviral molecule against influenza, herpes, and Sindbis viruses. *Proc Natl Acad Sci U S A* 104:1371-1376.

68. Kim, K. I., M. Yan, O. Malakhova, J. K. Luo, M. F. Shen, W. Zou, J. C. de la Torre, and D. E. Zhang. 2006. Ube1L and protein ISGylation are not essential for alpha/beta interferon signaling. *Mol Cell Biol* 26:472-479.

69. Giannakopoulos, N. V., E. Arutyunova, C. Lai, D. J. Lenschow, A. L. Haas, and H. W. Virgin. 2009. ISG15 Arg151 and the ISG15-conjugating enzyme UbE1L are important for innate immune control of Sindbis virus. *J Virol* 83:1602-1610.

70. Lai, C., J. J. Struckhoff, J. Schneider, L. Martinez-Sobrido, T. Wolff, A. Garcia-Sastre, D. E. Zhang, and D. J. Lenschow. 2009. Mice lacking the ISG15 E1 enzyme UbE1L demonstrate increased susceptibility to both mouse-adapted and non-mouse-adapted influenza B virus infection. *J Virol* 83:1147-1151.

71. Frias-Staheli, N., N. V. Giannakopoulos, M. Kikkert, S. L. Taylor, A. Bridgen, J. Paragas, J. A. Richt, R. R. Rowland, C. S. Schmaljohn, D. J. Lenschow, E. J. Snijder, A. Garcia-Sastre, and H. W. t. Virgin. 2007. Ovarian tumor domain-containing viral proteases evade ubiquitin- and ISG15-dependent innate immune responses. *Cell Host Microbe* 2:404-416.

72. Zhao, C., C. Denison, J. M. Huibregtse, S. Gygi, and R. M. Krug. 2005. Human ISG15 conjugation targets both IFN-induced and constitutively expressed proteins functioning in diverse cellular pathways. *Proc Natl Acad Sci U S A* 102:10200-10205.

73. Giannakopoulos, N. V., J. K. Luo, V. Papov, W. Zou, D. J. Lenschow, B. S. Jacobs, E. C. Borden, J. Li, H. W. Virgin, and D. E. Zhang. 2005. Proteomic identification of proteins conjugated to ISG15 in mouse and human cells. *Biochem Biophys Res Commun* 336:496-506.

74. Zhao, C., T. Y. Hsiang, R. L. Kuo, and R. M. Krug. 2010. ISG15 conjugation system targets the viral NS1 protein in influenza A virus-infected cells. *Proc Natl Acad Sci U S A* 107:2253-2258.

75. Durfee, L. A., N. Lyon, K. Seo, and J. M. Huibregtse. 2010. The ISG15 conjugation system broadly targets newly synthesized proteins: implications for the antiviral function of ISG15. *Mol Cell* 38:722-732.

76. Minakawa, M., T. Sone, T. Takeuchi, and H. Yokosawa. 2008. Regulation of the nuclear factor (NF)-kappaB pathway by ISGylation. *Biol Pharm Bull* 31:2223-2227.

77. Jeon, Y. J., J. S. Choi, J. Y. Lee, K. R. Yu, S. M. Kim, S. H. Ka, K. H. Oh, K. I. Kim, D. E. Zhang, O. S. Bang, and C. H. Chung. 2009. ISG15 modification of filamin B negatively regulates the type I interferon-induced JNK signalling pathway. *EMBO Rep* 10:374-380.

78. Kim, M. J., S. Y. Hwang, T. Imaizumi, and J. Y. Yoo. 2008. Negative feedback regulation of RIG-I-mediated antiviral signaling by interferon-induced ISG15 conjugation. *J Virol* 82:1474-1483.

79. Okumura, A., P. M. Pitha, and R. N. Harty. 2008. ISG15 inhibits Ebola VP40 VLP budding in an L-domain-dependent manner by blocking Nedd4 ligase activity. *Proc Natl Acad Sci U S A* 105:3974-3979.

80. Malakhov, M. P., K. I. Kim, O. A. Malakhova, B. S. Jacobs, E. C. Borden, and D. E. Zhang. 2003. High-throughput immunoblotting. Ubiquitiin-like protein ISG15 modifies key regulators of signal transduction. *J Biol Chem* 278:16608-16613.

81. Malakhova, O. A., and D. E. Zhang. 2008. ISG15 inhibits Nedd4 ubiquitin E3 activity and enhances the innate antiviral response. *J Biol Chem* 283:8783-8787.

82. Okumura, A., G. Lu, I. Pitha-Rowe, and P. M. Pitha. 2006. Innate antiviral response targets HIV-1 release by the induction of ubiquitin-like protein ISG15. *Proc Natl Acad Sci U S A* 103:1440-1445.

83. Pincetic, A., Z. Kuang, E. J. Seo, and J. Leis. 2010. The interferon-induced gene ISG15 blocks retrovirus release from cells late in the budding process. *J Virol* 84:4725-4736.

84. D'Cunha, J., S. Ramanujam, R. J. Wagner, P. L. Witt, E. Knight, Jr., and E. C. Borden. 1996. In vitro and in vivo secretion of human ISG15, an IFN-induced immunomodulatory cytokine. *J Immunol* 157:4100-4108.

85. D'Cunha, J., E. Knight, Jr., A. L. Haas, R. L. Truitt, and E. C. Borden. 1996. Immunoregulatory properties of ISG15, an interferon-induced cytokine. *Proc Natl Acad Sci U S A* 93:211-215.

86. Owhashi, M., Y. Taoka, K. Ishii, S. Nakazawa, H. Uemura, and H. Kambara. 2003. Identification of a ubiquitin family protein as a novel neutrophil chemotactic factor. *Biochem Biophys Res Commun* 309:533-539.

87. Padovan, E., L. Terracciano, U. Certa, B. Jacobs, A. Reschner, M. Bolli, G. C. Spagnoli, E. C. Borden, and M. Heberer. 2002. Interferon stimulated gene 15 constitutively produced by melanoma cells induces e-cadherin expression on human dendritic cells. *Cancer Res* 62:3453-3458.

88. Bogunovic, D., M. Byun, L. A. Durfee, A. Abhyankar, O. Sanal, D. Mansouri, S. Salem, I. Radovanovic, A. V. Grant, P. Adimi, N. Mansouri, S. Okada, V. L. Bryant, X. F. Kong, A. Kreins, M. M. Velez, B. Boisson, S. Khalilzadeh, U. Ozcelik, I. A. Darazam, J. W. Schoggins, C. M. Rice, S. Al-Muhsen, M. Behr, G. Vogt, A. Puel, J. Bustamante, P. Gros, J. M. Huibregtse, L. Abel, S. Boisson-Dupuis, and J. L. Casanova. 2012. Mycobacterial disease and impaired IFN-gamma immunity in humans with inherited ISG15 deficiency. *Science* 337:1684-1688.

CHAPTER 2

ISG15 is critical in the control of Chikungunya Virus infection

independent of UbE1L mediated conjugation

This chapter contains data published in the following publication with significant contribution from Clementine Schilte.

Werneke SW, Schilte C, Rohatgi A, Monte KJ, Michault A, et al. (2011) ISG15 is critical in the control of Chikungunya virus infection independent of UbE1L mediated conjugation. PLoS Pathog 7: e1002322.

Abstract

Chikungunya virus (CHIKV) is a re-emerging alphavirus that has caused significant disease in the Indian Ocean region since 2005. During this outbreak, in addition to fever, rash and arthritis, severe cases of CHIKV infection have been observed in infants. Challenging the notion that the innate immune response in infants is immature or defective, we demonstrate that both human infants and neonatal mice generate a robust type I interferon (IFN) response during CHIKV infection that contributes to, but is insufficient for, the complete control of infection. To characterize the mechanism by which type I IFNs control CHIKV infection, we evaluated the role of ISG15 and defined it as a central player in the host response, as neonatal mice lacking ISG15 were profoundly susceptible to CHIKV infection. Surprisingly, UbE1L$^{-/-}$ mice, which lack the ISG15 E1 enzyme and therefore are unable to form ISG15 conjugates, displayed no increase in lethality following CHIKV infection, thus pointing to a non-classical role for ISG15. No differences in viral loads were observed between wild-type (WT) and ISG15$^{-/-}$ mice, however, a dramatic increase in proinflammatory cytokines and chemokines was observed in ISG15$^{-/-}$ mice, suggesting that the innate immune response to CHIKV contributes to their lethality. This study provides new insight into the control of CHIKV infection, and establishes a new model for how ISG15 functions as an immunomodulatory molecule in the blunting of potentially pathologic levels of innate effector molecules during the host response to viral infection.

Introduction

Chikungunya virus (CHIKV) is a member of the genus Alphavirus, which are enveloped positive-strand RNA viruses transmitted by mosquitoes. It was first isolated in Tanzania in 1952, and reported to cause severe fever as well as myalgias, joint pain and rash within 2-5 days of infection (1, 2). Recently, CHIKV reemerged in Eastern Africa and has developed into a major epidemic in the Indian Ocean region. In 2006, an outbreak on the island of La Réunion resulted in the infection of approximately one-third of the inhabitants (3, 4). It has since spread to India and Southeast Asia with estimates of between 1-6 million people having been infected (5, 6). Concerns for the globalization of this virus has evolved given the continuation of this epidemic, the high serum viremia seen in infected patients, and mutations in the currently circulating strain of CHIKV that have allowed it to adapt to a more widely distributed mosquito vector (7). These concerns have been raised by both an increase in the number of foreign travelers contracting CHIKV and returning to both Europe and the United States, and by the possibility of spread by infected individuals, the latter being exemplified by the outbreak in Italy in 2007 and in Southern France in 2010 (5, 8, 9).

The typical clinical presentation of adults infected with CHIKV includes fever, rash, arthralgias and severe myalgias. Infected neonates, however, display more severe disease, with symptoms including encephalopathy and cerebral hemorrhage, with a subset of these infants developing permanent disabilities (10). During the recent epidemic, it was reported for the first time that CHIKV-infected mothers can transmit the virus to their newborns during delivery, with a vertical transmission rate of approximately 50%, and in some instances infection resulted in mortality (10). This age dependence of disease severity has also been reported for other

alphaviruses and can be reproduced in mouse models through the infection of suckling mice. Indeed, it has been shown that neonatal mice succumb to Ross River Virus (RRV) (11), Semliki Forest Virus (SFV) (12), Sindbis Virus (SINV) as well as CHIKV (13-15). There are likely several factors that contribute to this increased sensitivity in neonates, including alterations in the neonatal immune response.

Regarding immune function in neonates, developmental delays have been described for the adaptive immune responses, however less is known about neonatal innate responses. While still controversial, many reports indicate that neonatal responses are diminished as compared to adults. For example, cord blood cells stimulated with TLR ligands produced low levels of TNFα, IL-1β, and IL-12 (16). Neonatal plasmacytoid DCs have also been shown to have impaired production of type I IFN in response to CpG stimulation (17). It has been shown that LPS does not effectively activate IRF-3 dependent responses, including the production of IFNβ (18). The response to cytokines may also be impaired as there is evidence that STAT-1 recruitment following IFNγ stimulation is less efficient in neonatal than in adult leukocytes (19). Based on the critical role of type I IFN in the control of CHIKV infection (20), we considered the possibility that neonates may have a developmental delay in their type I interferon response, possibly contributing to their increased susceptibility to CHIKV infection and viral dissemination.

In response to CHIKV infection, the production of type I IFNs is triggered by the engagement of the RLR pathway (20, 21). IFNs then stimulate the induction of hundreds of interferon stimulated genes (ISGs) and it is through these ISGs that IFNs mediate their effector function (22). One of the earliest ISGs induced following IFN stimulation is ISG15. ISG15 is a

17kDa protein that contains two ubiquitin-like domains connected by a proline peptide linker (23). Similar to ubiquitin, ISG15 can form conjugates with an array of intracellular host and viral proteins through the use of an E1 (UBE1L), E2 (UbcH8), and E3 (e.g., Herc5, Efp, HHARI) enzymatic cascade (24-28). Conjugation of ISG15 to target proteins has been suggested to cause either a gain or loss of function of the targeted protein, although the consequences of ISG15 conjugate formation are not well understood (29-32). An unconjugated form of ISG15 can also be found in the sera of humans treated with IFN-β_{ser} as well as in virally infected mice (33, 34). The released form of ISG15 has been suggested to have cytokine like activity (35-37), however its role during an antiviral immune response has not been examined.

The rapid induction of ISG15 following IFN stimulation has led to the identification of an antiviral role for ISG15 during infection. ISG15$^{-/-}$ mice display increased susceptibility to SINV, herpes simplex virus-1 (HSV-1), gamma herpes virus (γHV68), influenza A and B viruses, and vaccinia virus (34, 38). ISG15$^{-/-}$ mice infected with influenza B virus display a 2-3 log increase in lung viral titers as well as elevated cytokine and chemokine levels (34). The ability of ISG15 to conjugate to target proteins appears to be essential for ISG15's antiviral activity during certain viral infections, as UbE1L$^{-/-}$ mice, which lack the ability to form ISG15 conjugates, phenocopy ISG15$^{-/-}$ mice during both SINV and influenza B virus infection (39-41). Further support for the importance of ISG15 conjugation during viral infection comes from the evolution of viral proteins that directly target ISG15 conjugate formation. Both the NS1 protein of influenza B virus and the E3L protein of vaccinia virus inhibit ISG15 conjugate formation, while OTU-domain containing viral proteins, such as the L protein of Crimean-Congo hemorrhagic fever virus (CCHFV) or the Nsp2 protein of Equine Arteritis virus (EAV), and the SARS coronavirus

papain-like protease (SARS-CoV PLpro) exert both deubiquitinating and deISGylating activity (24, 38, 42, 43). Therefore, the antiviral activity of ISG15 has been thought to be conjugation dependent.

Herein we demonstrate that despite an increased susceptibility of neonates to CHIKV infection, they produce robust levels of type I IFNs. While insufficient to completely control infection, IFNs participate in limiting the infection. We also show that ISG15 is induced during CHIKV infection and plays a critical role in protecting neonatal mice from viral induced lethality. Surprisingly, the mechanism of action by which ISG15 limits infection is independent of UbE1L mediated conjugation, as UbE1L$^{-/-}$ mice displayed no phenotypic differences as compared to wild-type animals. Furthermore, ISG15 does not directly inhibit viral replication, as suggested by the similar viral loads in WT and ISG15$^{-/-}$ mice. Instead, ISG15 appears to function as an immunomodulatory molecule in this model. These data demonstrate a novel role for ISG15 during viral infection and suggests that prophylactic measures targeting the induction of IFN and ISG15 may help protect neonates during future CHIKV outbreaks.

Results

CHIKV infected infants produce high levels of IFN and IFN-induced chemokines/ cytokines.

Based on the increased severity of neonatal disease that has been observed during the recent epidemic of CHIKV, we assessed the inflammatory response of infants during the acute phase of CHIKV infection. Patients were recruited at the time of presentation in the emergency room and sera samples were collected and stored. CHIKV infection was confirmed by RT-PCR; and all patients were negative for anti-CHIKV IgG and IgM, indicating acute infection. We performed multi-analyte testing using Luminex technology, with a focus on inflammatory cytokines and chemokines. The inflammatory signature was compared to uninfected patients presenting to the emergency room for reasons unrelated to acute infection (e.g., broken bone). The intensity of the immune response in the infant vs. adult cohorts was compared. Non-parametric tests were used for the statistical analysis, and a false discovery rate (FDR) correction was applied to all p-values in order to adjust for multiple testing.

We detected elevated levels of both IFNα and IFNγ in both groups of patients when compared to their respective control group ($p < 0.005$). Interestingly, both IFNα and IFNγ levels were more elevated in infants in comparison to adult patients (Fig. 2.1A). In addition, the chemokines/cytokines known to be induced by IFNs were highly expressed. These included CCL2, CCL4, CXCL9, CXCL10, IL-1Rα, IL-12p40/p70; and strikingly these analytes, with the exception of CXCL9, showed higher plasma concentrations in infants as compared to adult patients (Fig. 2.1B). Despite the clinical presentation including fever (Table S2.1), levels of the pyrogenic cytokines IL-1β and TNFα were not significantly elevated in patients when compared

to their controls; with only IL-6 being slightly upregulated in adult patient as compared to the control group (data not shown). Also of interest, while we observed marked induction of so-called Th1 cytokines, such as IFNγ and IL-12p40/p70, there was no clear skewing toward a Th1 response. In fact, we observed high levels of Th2 cytokines as well as Th17 cytokines (Fig. 2.1C). Notably, these interleukins were upregulated as compared to healthy individuals, but were similarly expressed in the infected infant and adult groups. These data suggest that infants, while developing more severe manifestations of CHIKV, do indeed mount a robust acute response to infection.

One potential caveat to this conclusion is that the viral load is higher in infants, possibly accounting for greater immune activation (median viral load in infants = 1.6×10^8 RNA copies; median viral load in adults = 1.4×10^7 RNA copies). Within the infant group, viral load negatively correlated with age, corroborating the observation that newborns are more susceptible to CHIKV induced disease (Fig. 2.2A). In adults, there was also an age-dependent trend with elderly harboring higher viral loads (Fig. 2.2A). Again this is consistent with the report that increased age is a risk factor for severe CHIKV disease (44). Next, we plotted plasma IFNα concentrations as a function of age. These data demonstrate a strong negative correlation in infants, and followed the pattern seen for CHIKV titers (Fig. 2.2B). We found that IFNα levels correlated with viral loads in both group (Fig. 2.2C). To normalize for CHIKV titers, we separated each cohort in two groups (< global median : low viral load; and > global median : high viral load), in both groups the levels of IFNα were more elevated in infected infants than in infected adults (Fig. 2.2D). Furthermore, we performed univariate linear regression analysis to model the effect of infant status on plasma IFNα concentrations. Infants had higher IFNα concentrations compared to adults (RGM [95% CI] = 5.49 [3.16 - 9.53]; $p<0.001$). This effect

remained significant after adjustment for viral load (adjusted RGM [95% CI] = 3.44 (2.07 - 5.70]; $p<0.001$). Thus for a similar viral load, infants produce more IFNα than adults. To represent associations between age, viral load, IFNα and the immune signature, we established a network plot of significant correlations (Fig. 2.2E). These data argue against infants being compromised in their response to CHIKV infection; however, we could not determine whether their IFN response was protective. To address this issue and to examine the mechanism of ISG mediated control of CHIKV, we exploited a recently described neonatal mouse model for studying infection (15).

CHIKV infection in neonatal mice results in a robust type I interferon and proinflammatory cytokine response that is critical in controlling infection.

Previously, we reported an age-dependent susceptibility to CHIKV infection in mice. Infection of 6 day old animals resulted in 100% mortality; 9 day old animals developed paralysis, with approximately 50% of the animals succumbing to infection; while by 12 days of age the mice became refractory to symptoms of severe disease and lethality (15). To compare our experimental mouse model of CHIKV infection to the response seen in human infants we assessed the IFN and proinflammatory responses in 8-9 day old mice. We first assessed the induction of the IFN response at the local site of infection by monitoring mRNA levels of IFNβ and selected interferon stimulated genes (ISGs) in the skin. Mice were inoculated with 2 x 10^5 PFU of CHIKV and the injection site was removed between 3–120 hrs post-infection. Increased expression of IFNβ mRNA could be detected as early as 3 hrs post-infection with peak levels being achieved at 16 hrs post-infection (Fig. 2.3A). Similar to IFNβ mRNA induction,

IRF7, Mx1 and ISG15 mRNA levels could also be detected as early as 3 hrs post-infection, with peak levels observed at 16 hrs post-infection (Fig. 2.3A). Thus, at the site of infection, neonatal mice are able to induce IFNβ expression as well as a subset of known ISGs. Of note, IRF7 and Mx1 mRNA expression is indicative of signaling via the type I IFN receptor, suggesting that the production as well as reception of IFNαβ is intact in neonatal mice.

We next assessed the systemic inflammatory response in this model. Similar to our findings in human infants infected with CHIKV, we observed a strong induction of IFNα and IFNγ in infected pups (Fig. 2.3B). Plasma concentration of CCL2, CCL4, CXCL9 and CXCL10 were also elevated, however IL-12p70 was only modestly induced (Fig. 2.3C). Similar to the human data, a mixed Th1, Th2 and Th17 cytokine profile was observed with the induction of IL-12, IL-5, IL-13, IL-15, and IL-17 (Fig. 2.3C). For all analytes, peak levels were seen 16–24h post-infection (Fig. 2.3). Notably, there were some differences seen between the murine neonate and human infant inflammatory profiles. Most interestingly, the mice displayed increased levels of the pyrogenic cytokines, including IL-1β, IL-6 and TNFα, which were not seen in our studies of human infants (Fig. 2.3C). While this may represent differences in pathogenesis, we believe it is more a reflection of the fact that the mice can be assessed within hours of viral inoculation, while the exact timing of the human infection is unknown. Overall, we find that the similarities between the mouse and human responses support the use of neonatal mice to study the response to CHIKV infection, and indicate that induction of IFNs, as well as the triggering of an ISG response, are both rapid and robust.

Next, to confirm that endogenous IFN contributes to the control of CHIKV in neonatal mice, mice lacking subunit 1 of the type I IFN receptor ($IFNAR^{-/-}$) mice were infected with CHIKV at 9 days of age. Consistent with our previous observations in adult mice (15), neonatal

pups lacking IFNAR were highly susceptible to CHIKV infection with 100% of the pups dying by day 2 post-infection (Fig. 2.4A). These pups developed a rapid, disseminated infection. Within 1 day of infection, the IFNAR1$^{-/-}$ mice displayed viral loads at the injection site that were 100-fold higher than that detected in WT controls. We also observed a striking increase in viral titers in the serum and multiple organs, including the brain, liver, and lung (Fig. 2.4B). These data indicate that endogenous IFN, while insufficient to protect mice, plays an important role in limiting CHIKV infection during disease pathogenesis in neonatal animals.

Pre-treatment with Poly I:C prevents clinical disease and CHIKV induced death.

Our results suggest that signaling via the IFNαβ receptor in neonatal mice results in the robust induction of at least a subset of ISGs and interferon-induced serum proteins (Fig 2.3), and that the absence of IFNAR results in exacerbated infection and rapid death (Fig. 2.4). One potential explanation is that neonates possess a developmental delay in their IFN-response that makes them susceptible to infection as compared to adult animals. It was therefore important to determine whether prophylactic innate immune responses could protect neonatal animals from CHIKV infection. To evaluate this question, we injected mice with 25 μg of poly I:C (pIC), a known inducer of type I IFN, and 1 day later mice were challenged with 2 x10^5 PFU of CHIKV. At 7h post treatment with pIC, robust levels of IFNα were detected in the serum of neonatal mice (Fig. 2.5A). Following CHIKV infection, mice were monitored daily for the development of symptoms and followed for lethality. Remarkably, 96% of the pIC treated mice survived, in contrast to only 40% of control mice (Fig 2.5B). Treatment with pIC also prevented CHIKV induced paralysis, with only 7% of the pIC treated mice developing paralysis during the course of the infection, as compared to 84% in the control group (Fig. 2.5C). Independent experiments

were performed using prophylactic treatment with 5000 U IFNβ. At both day 7 and day 11 post-infection, mice receiving recombinant IFNβ displayed less severe disease, as compared to control PBS injected animals (Fig. S2.1), however, we did not see a statistical difference in survival, possibly due to the short half-life of IFNβ. To confirm that the protection induced by pIC was mediated by IFN, we repeated these experiments in IFNAR$^{-/-}$ mice. As seen in Figure 2.5D, treatment of IFNAR$^{-/-}$ mice with pIC resulted in no protection from lethality. These results indicate that the prophylactic engagement of the IFN receptor in neonates is able to induce a protective anti-viral response.

ISG15 plays a significant role in the control of neonatal CHIKV infection.

Interferons mediate their antiviral activity through the induction of ISGs, thus suggesting that investigation of the downstream effector molecules may offer additional insight into how neonates respond to CHIKV infection. The analysis of selected ISGs expressed at the site of infection revealed that ISG15 mRNA was rapidly and strongly induced during CHIKV infection (Fig. 2.3A). ISG15 is an ubiquitin-like molecule that conjugates to both host and viral proteins and has been previously shown to participate in the host response to SINV infection. An evaluation of ISG15 protein expression at the site of infection and within the serum confirmed that ISG15 and ISG15 conjugates were induced during CHIKV infection in WT mice (Fig. 2.6B,C). As we previously described during neonatal SINV infection [45], the expression of ISG15 during CHIKV infection was also dependent upon intact IFN signalling since IFNAR$^{-/-}$ pups infected with CHIKV did not induce detectable levels of ISG15 (Fig. S2.2). To test the hypothesis that ISG15 is important in the control of CHIKV, we infected ISG15$^{-/-}$ neonatal mice, comparing them to weight and age-matched WT control animals. Mice were followed daily for signs of illness and survival. As reported above, infection of 9 day old WT neonatal mice

resulted in 58% lethality, with deaths occurring between days 10-13 post-infection. In contrast, a dramatic increase in lethality was observed in neonatal mice lacking ISG15, with greater than 70% of the ISG15$^{-/-}$ mice succumbing to infection within 3 days, and 100% of the mice dying by day 9 post-infection (Fig. 2.6A).

It has been previously shown that WT mice become resistant to CHIKV induced lethality between 9 to 12 days of age, while mice lacking IFNAR1 remain susceptible to infection even as adults. Since ISG15 is an IFN-induced protein we next determined if its activity was age dependent. We infected either WT or ISG15$^{-/-}$ mice at 11 or 12 days of age, or we infected adult mice between 6-8 weeks of age. By 11 days of age the WT mice had become largely resistant to CHIKV induced lethality with only 15% of the mice succumbing to infection (Fig. S2.3A). In contrast, we observed 100% lethality in the ISG15$^{-/-}$ mice, although the onset of lethality was delayed, with the majority of the mice dying between 10 and 14 days post-infection. By 12 days of age the ISG15$^{-/-}$ mice still showed clinical signs of disease, with a dramatic decrease in weight gain as compared to the WT controls (data not shown), but by this age only 20% of the ISG15$^{-/-}$ mice succumbed to the infection (Fig. S2.3B). Strikingly, adult ISG15$^{-/-}$ mice, similar to WT controls, displayed no lethality and showed no signs of disease following CHIKV infection (Fig. S2.3C). Therefore, we conclude that ISG15 contributes to the control of CHIKV during neonatal infection, but redundant mechanisms are responsible for the control of CHIKV during adult infection.

Since IFNs induce the expression of many ISGs, we next wanted to investigate if ISG15 contributed to the protective anti-viral response established by prophylactic induction of type I IFN. WT or ISG15$^{-/-}$ mice were treated with 10 - 25µg of pIC and 1 day later challenged with 2 x10^5 PFU of CHIKV. Not unexpectedly, pretreatment with pIC offered protection to both WT

and ISG15$^{-/-}$ mice. After pretreatment with 25μg of pIC, 14% of the ISG15$^{-/-}$ mice still succumbed to infection as compared to complete protection seen in the WT mice (Fig. 2.6D). Interestingly, only 50% of the ISG15$^{-/-}$ mice were protected after pretreatment with 10μg pIC, as compared to 85% protection observed in the WT mice (Fig. 2.6E). These data support our observation that ISG15 is induced as part of the IFN response and that it plays an important role during CHIKV infection.

ISG15 controls neonatal CHIKV infection independent of UbE1L mediated conjugation.

We next investigated the mechanism by which ISG15 protects neonatal mice from CHIKV infection. We had previously shown that the conjugation of ISG15 to target proteins is essential for the control of several viral infections (40, 41). UbE1L is the only identified E1 for ISG15, and mice lacking UbE1L express free ISG15, but fail to form ISG15 conjugates (39). To establish a role for ISG15 conjugation, 9 day old UbE1L$^{-/-}$ mice were infected with CHIKV. Surprisingly, UbE1L$^{-/-}$ mice displayed no increase in lethality following CHIKV infection, and instead had a lethality curve similar to that observed in WT mice (Fig. 2.6A). Similarly, pIC treated UbE1L$^{-/-}$ mice were protected to the level of WT controls (Fig. 2.6D, E). Western blot analysis on skin/muscle from the site of infection (Fig. 2.6B), as well as serum (Fig. 2.6C), was used to confirm that UbE1L$^{-/-}$ mice generated no ISG15 conjugates during CHIKV infection, whereas WT mice showed robust conjugate formation. Additional organs (lung and liver) were also examined and no conjugates were detected in UbE1L$^{-/-}$ mice (data not shown). Thus, we demonstrate that the activity of ISG15 during CHIKV infection is UbE1L independent.

In an attempt to provide additional evidence that unconjugated ISG15 was functioning in this model, we generated recombinant double subgenomic CHIK viruses that expressed either

WT ISG15 (CHIK- LRLRGG) or a mutant, non-conjugatable form of ISG15 (CHIK- LRLRAA) (Fig. S2.4A). This strategy was based on our previous report in which recombinant SINV expressing WT ISG15 (LRLRGG) rescued the increased lethality observed in the ISG15$^{-/-}$ mice, while mutant ISG15 (LRLRAA) failed to compensate for the ISG15 deficiency (34, 40). Both CHIK-LRLRGG and CHIK-LRLRAA expressed ISG15 and displayed similar growth kinetics to CHIK-GFP in BHK cells (Fig. S2.4B, 4C). When we infected ISG15$^{-/-}$ mice, however, neither CHIK-LRLRGG nor CHIK-LRLRAA was able to protect ISG15$^{-/-}$ mice (Fig. S2.4D and data not shown). While these results do not allow us to confirm that the activity of ISG15 is independent of conjugation, they do suggest that the mechanism of action of ISG15 during SINV and CHIKV infection are distinct.

To further evaluate the mechanism by which ISG15 functions during neonatal CHIKV infection we examined lymphocyte subsets and viral titers in WT, UbE1L$^{-/-}$ and ISG15$^{-/-}$ mice. We detected no significant differences in the lymphocyte subsets of naïve neonatal WT, UbE1L$^{-/-}$ and ISG15$^{-/-}$ mice (Table S2.2). Similar results have been observed in both naïve and pIC stimulated adult mice (39, 45). These data suggest that differences in starting cell populations do not account for the increase in lethality observed in ISG15$^{-/-}$ mice. We next assessed viral titers on days 1 and 2 post-infection. As expected, UbE1L$^{-/-}$ mice displayed similar viral loads in multiple tissues when compared to WT mice at days 1 and 2 post-infection (Fig. 2.7A and B). Given that the ISG15$^{-/-}$ pups infected at 9 days of age displayed a dramatic increase in lethality, with kinetics similar to that observed in the IFNAR$^{-/-}$ mice, we expected to detect increased viral titers in the ISG15$^{-/-}$ mice. To our surprise, at 1 day post-infection the serum and tissues analyzed from the ISG15$^{-/-}$ mice contained viral titers that were similar to those obtained in both UbE1L$^{-/-}$ and WT mice (Fig. 2.7A). This was in striking contrast to the 2-3 log increase in viral loads

detected in the IFNAR$^{-/-}$ mice 1 day post-infection (Fig. 2.4B). By 2 days post-infection, just prior to when the majority of ISG15$^{-/-}$ mice succumb to infection, we still detected similar viral loads between WT, UbE1L$^{-/-}$ and ISG15$^{-/-}$ mice in the analyzed tissues (Fig. 2.7B). Based on these data we suggest that ISG15 may not be playing a direct anti-viral role, but instead may be acting via an unexpected mechanism of regulating host sensitivity to the viral induced immune response.

Since our evaluation of human infants and neonatal mice demonstrated that CHIKV infection induces a robust proinflammatory cytokine and chemokine response (Fig. 2.1 and 2.3), we investigated the impact of ISG15 deficiency on this host response. IFNβ mRNA levels were induced in the skin of WT, UbE1L$^{-/-}$ and ISG15$^{-/-}$ mice at 24 and 48hrs post infection with no significant differences noted between the three strains of animals (Fig. 2.8A). Serum from WT, UbE1L$^{-/-}$ and ISG15$^{-/-}$ mice collected at 1 or 2 days post-infection were analyzed for IFNα as well as proinflammatory cytokines and chemokines. Analysis of IFNα serum levels also revealed no significant differences between WT, ISG15$^{-/-}$, and UbE1L$^{-/-}$ mice at either 24 or 48 hrs post-infection (Fig. 2.8B). Despite similar viral loads and type I IFN induction, the ISG15$^{-/-}$ mice displayed elevated levels of TNFα, IL-1β and IL-6 as compared to both the WT and UbE1L$^{-/-}$ mice (Fig. 2.8C). Interestingly the levels of these three pyrogenic cytokines in the ISG15$^{-/-}$ mice were comparable to what was observed in the IFNAR$^{-/-}$ pups, despite the latter having significantly higher viral loads. ISG15$^{-/-}$ mice also displayed elevated chemokine levels, including CCL2, CCL3 and CCL5 (Fig. 2.8C). Therefore, although viral titers between ISG15$^{-/-}$, UbE1L$^{-/-}$ and WT mice are similar, ISG15$^{-/-}$ neonates display an exaggerated proinflammatory cytokine response to CHIKV infection. Together, these data indicate that ISG15, independent of

UbE1L mediated conjugation, is contributing to the control of CHIKV infection by blunting potentially pathologic levels of innate effector molecules.

Elevated pro-inflammatory cytokine levels likely contribute to the increased lethality seen in CHIKV infected neonatal ISG15$^{-/-}$ mice.

We hypothesized that the exaggerated cytokine response displayed in ISG15$^{-/-}$ mice during CHIKV infection could contribute to the increased lethality in ISG15$^{-/-}$ compared to WT and UbE1L$^{-/-}$ mice. The levels of TNFα observed were similar to what has been previously reported in adult models of LPS induced septic shock (46, 47) as well as neonatal Sindbis virus infections (48), where mice are thought to die from a cytokine storm. Consistent with a cytokine storm phenotype, no striking differences in histology (H&E) were found between the three genotypes, although necropsy analysis revealed that ISG15$^{-/-}$ had more severe blood vessel and airway injury than WT and UbE1L$^{-/-}$ mice (data not shown). To support our findings, we also performed a blood chemistry analysis on serum collected on day 2 post CHIKV infection from WT, UbE1L$^{-/-}$ and ISG15$^{-/-}$ neonatal mice. Blood chemistry analytes can be used to assess the function of the liver, kidneys, heart, pancreas and other organs. Alteration in blood analyte levels (ALT, AST, BUN and Creatinine) can be an indication of multiple organ dysfunction syndrome (MODS) that can also occur during septic shock (49-51). Preliminary data suggests that WT and UbE1L$^{-/-}$ mice do not display changes in blood analyte levels compared to PBS treated mock controls (Figure S2.5). In contrast, we observed elevated levels of ALT, AST, and BUN in CHIKV infected ISG15$^{-/-}$ mice compared to WT and UbE1L$^{-/-}$ mice (Figure S2.5). We also observed decreased levels of glucose in ISG15$^{-/-}$ mice. No difference was observed in Creatinine levels. This data is consistent with our cytokine data (Figure 2.8C) and suggests that CHIKV infected ISG15$^{-/-}$ may suffer from multiple organ dysfunction. We have also generated

preliminary data that indicates that pre-treating neonatal ISG15-/- mice with a blocking TNFα antibody delays CHIKV induced lethality (data not shown). Altogether, our data supports the hypothesis that elevated cytokine levels contributes to increased lethality in CHIKV infected neonatal ISG15$^{-/-}$ mice.

Discussion

The ongoing epidemic of Chikungunya virus occurring in the Indian Ocean region has highlighted how little we understand about the pathogenesis of this virus. Epidemiological studies have provided the first documentation of vertical transmission, as well as providing detailed information about the severity of disease and long term sequelae (4, 52-54). One important finding from these studies concerns the increased susceptibility of neonates and infants to severe forms of Chikungunya disease (10, 44, 55). In this study, we evaluated the response of infants to CHIKV infection using data from both human samples collected during the La Réunion outbreak, as well as taking advantage of a newly described mouse model of infection. Our results show that human infants and murine neonates mount a robust innate immune response to CHIKV infection, which includes the induction of type I IFNs, several cytokines and chemokines, and the induction of at least a subset of IFN induced genes, including ISG15. We establish a role for ISG15 in the pathogenesis of CHIKV infection with an absolutely essential role in the neonatal response to infection. Moreover, and to our surprise, the reported data suggest that ISG15 acts independently of UbE1L mediated conjugation and rather than exerting a direct anti-viral role, it appears to be implicated in limiting an exaggerated inflammatory response.

In general, neonates are more susceptible to microbial and viral infection. This vulnerability has been explained by two principal mechanisms: broader tropism of the infectious agent or a defective host response. Regarding the latter, many argue that neonatal susceptibility to infection is due to a delayed or weaker immune response (16, 56). Factors contributing to this include delays in immune system maturation, decreased expression of activation receptors, or

distinct regulation of signaling pathways in neonatal vs. adult immune cells. Since the type I IFN response is critical for controlling CHIKV infection (15, 20), we hypothesized that neonates may have a defect in their ability to either produce and/or respond to IFN. Instead, we observed that the production of type I IFN was intact in both human infants and mouse neonates. Furthermore, the relative level of IFN produced in infants was higher than the responses observed in adult human patients, even when viral load was normalized between the two patient groups (Fig. 2.1). These data indicate that neonates do not have a defect in their ability to produce type I IFN during CHIKV infection, and may actually be hyper-responsive. Very little has been reported on the signaling through RLRs or other viral sensors in neonates. Most previous work has supported the notion that signaling through TLR receptors, including TLR4, are diminished in neonates (57, 58). However, one study did find that neonatal mice exhibited increased lethality following LPS treatment, due in part to an exaggerated pro-inflammatory cytokine response as compared to adult mice (59). Future work is needed to characterize differences that may exist between neonatal and adult RLR signaling.

We also demonstrate that neonates can respond to the IFN that is produced. In both human infants and in neonatal mice, several known IFN-induced chemokines and cytokines were upregulated during the course of infection (Fig. 2.1-3). These results suggest that the ability to respond to IFNs was at least partially intact. These observations were confirmed by demonstrating the greater susceptibility of neonatal mice lacking expression of the type I IFN receptor (Fig. 2.4); notably, the kinetics of viral replication and death were massively accelerated as compared to age-matched WT controls. Additionally, we demonstrate that the prophylactic exposure to an interferon-inducing adjuvant protected animals from challenge with lethal doses of CHIKV (Fig. 2.5).

To provide insight into the mechanism by which IFN participates in the host response to CHIKV infection, we evaluated the role of ISG15, an anti-viral host protein that has previously been shown to be important in the control of several viruses, including SINV (34). We found that ISG15$^{-/-}$ mice were more susceptible to CHIKV infection, demonstrating a dramatic increase in lethality as compared to WT mice (Fig. 2.6A). Moreover, ISG15 played a critical role in pIC induced protection of mice in a prophylactic setting (Fig.2.6D, 2.6E). While OAS has previously been shown to inhibit viral replication when over-expressed *in vitro* (60), to our knowledge our data is the first *in vivo* demonstration of an IFN effector molecule having activity against CHIKV.

Most importantly, the results from our current study indicate that ISG15 is regulating CHIKV pathogenesis by a unique mechanism of action. First, we demonstrate that ISG15 regulates CHIKV infection independent of UbE1L mediated conjugation. This is in contrast to both influenza virus and SINV infection, where the anti-viral activity of ISG15 is dependent upon ISG15 conjugation and abrogated in UbE1L$^{-/-}$ animals (40, 41). The protection mediated by ISG15 during pIC prophylaxis also appeared to be UbE1L independent, as UbE1L$^{-/-}$ mice displayed survival curves similar to WT mice (Fig. 2.6D, 2.6E). These results suggest that the non-classical function of ISG15 is at work both during acute viral infection and in the pIC induced protection seen in our mice. UbE1L is the only known E1 for the ISG15 pathway, and our analysis of the UbE1L$^{-/-}$ mice revealed no conjugation activity post-infection (Fig. 2.6 and (39)). Therefore the actions of ISG15 during CHIKV infection are likely to be independent of conjugation, and mediated by free ISG15. One alternative explanation may be the involvement of a second E1, as has been identified for the ubiquitin pathway (61). Second, it appears that during CHIKV infection, ISG15 is not functioning as a direct antiviral molecule. In both the

influenza and SINV models, the increase in lethality was accompanied by a dramatic increase in viral loads (34, 38, 41). In contrast, during CHIKV infection, ISG15$^{-/-}$ mice did not show an increased CHIKV burden (Fig. 2.7). Instead, we noted a significant elevation of several proinflammatory cytokines and chemokines in the ISG15 deficient mice (Fig. 2.8). Therefore, as opposed to having direct antiviral activity, it appears that ISG15 modulates the immune response during CHIKV infection. Finally, in contrast to what was previously reported for control of SINV infection (34), a recombinant CHIKV expressing ISG15 was unable to rescue neonatal ISG15$^{-/-}$ mice from viral induced lethality (Figure S4). The inability to rescue the ISG15$^{-/-}$ phenotype may be due to insufficient expression levels of ISG15; the timing of ISG15 expression may be delayed as compared to WT mice; or may in fact indicate that ISG15 expression is required in an uninfected cell. Since we detect no differences in viral load, and instead observed increased cytokine levels in the ISG15$^{-/-}$ mice, we favor this later possibility. Further analysis into the precise mechanism by which ISG15 regulates the host response to CHIKV should provide additional insight into this issue. Together, our data suggest a novel mechanism for ISG15, which is likely to be independent of conjugation and extrinsic to virally infected cells.

The precise mechanism by which ISG15, independent of UbE1L mediated conjugation, contributes to the control of viral infection is currently unclear. The most intriguing difference we have noted to date is the increased cytokine responses in the mice lacking ISG15 (Fig. 2.8). As noted above, while we cannot formally exclude the possibility of another E1 functioning in this system, it seems most likely that free, unconjugated ISG15 mediates the activity during CHIKV infection. Free ISG15 is found within the cell, but interestingly it may also be secreted by a still undefined mechanism (33). Previous work has shown that unanchored ISG15 can associate non-covalently with proteins (i.e. independent of conjugation). For example, the NS1

protein of influenza B virus can non-covalently bind ISG15, thereby inhibiting its interaction with UbE1L and blocking conjugation of target proteins (24). The over-expression of ISG15 has also been shown to disrupt Nedd4 ligase activity and inhibit Ebola virus VLP release (62, 63). Recent research within the ubiquitin field has described a role for unanchored polyubiquitin chains, shown to regulate TRAF6 function, as well as promote RIG-I dimerization and signaling (64, 65). It is therefore possible that intracellular, unanchored ISG15 interacts non-covalently with members of an innate immune signaling pathway to regulate cytokine and chemokine production or other host response pathways. Alternatively, released ISG15 could be contributing to the phenotype seen during CHIKV infection. Indeed, the 17 kDa form of ISG15 is released into the serum in both WT and UbE1L$^{-/-}$ mice during CHIKV infection (Fig. 2.6). Released ISG15 has been reported to function as an immunomodulatory molecule, increasing NK cell proliferation and lytic activity, acting as a neutrophil chemoattractant, and upregulating E-cadherin expression on dendritic cells (35-37). Released ISG15 could function as in immunomodulatory cytokine by signaling through a receptor to regulate the cytokine response or through its ability to function as a chemoattractant. In order to characterize these effects in greater detail, a receptor for ISG15 must be identified. Future studies evaluating these possibilities will be required in order to further define the mechanism by which ISG15 is contributing to the host response to CHIKV.

Although we do not understand mechanistically why ISG15$^{-/-}$ mice display elevated cytokine levels during CHIKV infection, our data indicates that this cytokine increase is biologically significant. During neonatal Sindbis virus infection, mice are thought to succumb to infection due to a cytokine storm (48). The lack of alterations in major organ histology and the levels of TNFα produced in our CHIKV model are consistent with what has been described for

SINV. We also provide additional evidence that CHIKV infected ISG15$^{-/-}$ mice may suffer from multiple organ dysfunction syndrome (MODS), another readout for septic shock, as indicated by altered blood chemistry levels (Fig. S2.5) (49). Therefore, elevated cytokine production contributes to the increased lethality in ISG15$^{-/-}$ mice. Cytokine production may be a relevant readout for future functional studies to understand the mechanism of ISG15 mediated host regulation.

In conclusion, we have demonstrated that neonates are capable of producing type I interferon in response to CHIKV, which serves to limit viral infection though remains insufficient to clear the virus. We have demonstrated a critical, age-dependent role for ISG15 during neonatal infection. We have also characterized the mechanism of ISG15 activity, revealing a novel mechanism for ISG15, independent of UbE1L mediated conjugation, and functioning as a putative immunomodulator of proinflammatory cytokines. The ability of pIC to protect neonatal mice against CHIKV infection suggests that manipulation of the IFN signaling pathway, and perhaps the induction of ISG15, may be an appropriate therapeutic target for combating CHIKV infection.

Materials and Methods

Ethics Statement

All human studies were approved by the Committee for Clinical Research at the Institut Pasteur, project number RBM 2009-23, on July 9, 2009. Written informed consent was obtained from the study participants or legal guardians. For mouse studies at the Institut Pasteur and at Washington University, the principles of good laboratory animal care were carried out in strict accordance with the recommendations in the Guide for the Care and Use of Laboratory Animals of the National Institutes of Health and following the International Guiding Principles for Biomedical Research Involving Animals. The protocols were approved by the Animal Studies Committee at Washington University (#20090287) and the Institutional Committees on Animal Welfare of the Institut Pasteur (OLAW assurance # A5476-01). All efforts were made to minimize suffering.

Human Study

Retrospective study on patients who presented to the emergency or pediatric service of the Groupe Hospitalier Sud Réunion, Saint Pierre, La Réunion, France from January 2006 through May 2006. Sera samples were collected and stored at -80°C. CHIKV infection was confirmed by RT-PCR. All patients were negative for anti-CHIKV IgG and IgM as assessed by immunocapture Elisa. The control cohort consisted of patients that presented to the orthopedic chirurgy or infant chirurgy service of the Groupe Hospitalier Saint Pierre before the epidemic. These patients were IgG, IgM and RT-PCR negative for CHIKV. Data from adult patients were previously reported (20), but are shown here for comparison to data from infected neonates.

Virus

The preparation of CHIKV from clinical samples has been previously described (66). CHIKV (06.21) strain was isolated during the epidemic in La Réunion and then propagated three time on C6/36 mosquito cells to generate a stock ($6x10^7$ PFU/mL) that was used in all experiments.

Recombinant CHIKV strains. The generation and characterization of a recombinant double subgenomic CHIKV virus expressing GFP, CHIKV-LR 5' GFP, has been previously described (67). Recombinant CHIKV expressing ISG15 were generated as follows.

(i) ISG15 LRLRGG. Nucleotides 1 to 465 of murine ISG15 were PCR amplified using a 5' primer that introduced an AscI restriction site and a 3' primer containing GGT GGG TAA sequence and a PmeI site.

(ii) ISG15 LRLRAA. Nucleotides 1 to 465 of murine ISG15 were PCR amplified using a 5' primer with an AscI restriction site and a 3' primer containing GCG GCG TAA sequence and a PmeI site.

The correct sequence for each virus was confirmed. Generation of recombinant ISG15 viruses was previously described (68). Viral stocks were generated by in vitro transcription of linearized cDNA templates, followed by transfection of the transcripts with Lipofectamine (Invitrogen) into BHK cells. Supernatants were harvested 48 hrs post transfection and viral titers were determined by plaque assay as described below. To examine growth characteristics of the recombinant viruses, BHK cells were infected at a multiplicity of infection (MOI) of 1.0 and viral titers were measured at various times post-infection. To determine the expression of ISG15 from recombinant viruses, BHK cells were infected at an MOI = 1.0 and at various times post-infection total cell lysates were harvested and ISG15 expression was analyzed by Western blot analysis.

Mice

Experiments in mice were carried out at both the Institut Pasteur, Paris, France and at Washington University School of Medicine, St. Louis, Missouri, using the identical CHIKV viral stock described above. Infection of 9 day old pups with 2 x 10^5 PFU subcutaneously (s.c.) resulted in approximately 50-60% lethality in WT mice at both locations. For experiments carried out at the Institut Pasteur, eight day old C57BL/6 litters were obtained from Charles River laboratories (France). For experiments carried out at Washington University, mice were maintained at Washington University School of Medicine in accordance with all federal and University guidelines. ISG15$^{-/-}$ mice were provided by Dr. Ivan Horak and Dr. Klaus-Peter Knobeloch. UbE1L$^{-/-}$ mice were provided by Dr. Dong-Er Zhang. The generation of both the ISG15$^{-/-}$ and UbE1L$^{-/-}$ mice has been previously described (39, 45). C57BL/6, IFNαβ receptor 1 (IFNAR1$^{-/-}$), UbE1L$^{-/-}$ and ISG15$^{-/-}$ mice, all on the C57BL/6 background, were bred and maintained in our mouse colony. Congenic SNP analysis (Taconic laboratories) of UbE1L$^{-/-}$ and ISG15$^{-/-}$ mice confirmed that these mice were fully backcrossed, with 99.93% and 99.72% identity to C57BL/6 mice, respectively. For neonatal experiments mice were infected between 9 and 12 days of age as indicated. Litters were weight matched at the initiation of the experiments. For adult experiments, mice were infected between 6-8 weeks of age and were age and sex matched within experiments.

Viral studies

For neonatal experiments using the clinical isolate of CHIKV, 9 day old pups were infected with 2.0 x 10^5 PFU CHIKV in 20-30 μL of PBS by injection subcutaneously (s.c.) into the right flank.

Infected mice were followed daily for weight gain, signs of disease, and lethality for 21 days post-infection. Paralysis was scored as an inability or long delay (>5s) to return and land on its feet when flipped on its back. For experiments with adult mice, 6-8 week old mice were infected as outlined above and followed for daily weight loss and lethality. For experiments utilizing the recombinant CHIKV clones, 6 day old pups were infected with 3 x 10^5 PFU of the indicated recombinant virus diluted in 30 μL of PBS by s.c. injection into the right flank. Viral titers were determined in organs harvested at the indicated days post-infection. Organs were harvested into 1 ml of DMEM without fetal bovine serum and homogenized with 1.0 mm diameter zirconia-silica beans at 3,200 rpm for 1 minute with a MagnaLyzer prior to plaque assay on BHK cells, protocol modified from (69). Serial dilutions of organ homogenates in DMEM with 1% FBS was added to BHK cells (6x10^5 cells for 6 well plates) and incubated for 1hr at 37°C. An agar overlay was then added to the cells and incubated for 28hrs at 37°C. Plates were fixed with 1% formaldehyde (>30min at room temperature), agar plugs were removed and plaques were visualized using a 1% crystal violet solution.

Poly I:C prophylactic treatment studies

Eight day old mice were injected intraperitoneally (i.p.) with 10-25μg of high molecular weight polyI:C (Invivogen). Twenty-four hours later, mice were challenged with 2 x 10^5 PFU CHIKV s.c. Mice were monitored daily for the development of symptoms and followed for lethality as described above.

Cytokine and blood chemistry analysis

Sera were harvested and conserved at -80ºC for analysis. Human cytokines were measured by Luminex (25 plex kits, Biosource, Invitrogen) following manufacturer's instructions. Human CXCL10 was re-titrated by ELISA (human quantikine ELISA kit, R&D). Mouse sera were obtained after coagulation of blood in T-MG tubes (Terumo). Mouse IFNα levels were quantified by ELISA (PBL biomedical) and other cytokines were measured using Luminex technology with either the 32 plex from Millipore (MPXMCYTO-70X) or by customized 10 plex from Biorad. Blood chemistry analytes were processed by the DCM core facility at Washington University in St. Louis.

qRT-PCR for quantification of viral load and IFN mRNA

For determination of patient viral load, total nucleic acid extraction was performed on sera in a MagNa Pure automate using the Total Nucleic Acid Kit (Roche Diagnostics). CHIKV RNA was detected with specific taqman probes using a one step RT-PCR (Master RNA hybridization probes, Roche) performed on a Chromo 4 machine (Biorad). The 20µL reaction mix contained 2µL of extracted RNA, 7.5µL of LightCycler RNA Master Hyb-Probe, 3.25 mmol/L Mn_2 , 450 nmol/L CHIKV-forward primer, 150 nmol/L CHIKV-reverse primer, 150 nmol/L CHIKV Probe (5 6-carboxyfluorescein-3 TAMRA) (TibMol-Biol). The thermal cycling consisted of a reverse transcription at 61 °C for 20 min followed by 45 cycles at 95 °C for 5 s and 60 °C for 15 s. The fluorescence was measured at 530 nm. CHIKV load is measured using a synthetic RNA calibrator (70). CHIKV-rev CCAAATTGTCCGGGTCCTCCT; CHIKV-forw AAGCTCCGCGTCCTTTACCAAG; Probe: Fam-CCATGTCTTCAGCCTGGACACCTTT-TAMRA.

For mouse studies, skin tissue was harvested at the site of infection on days 1 and 2 post-infection. Tissue was snap frozen in liquid nitrogen and then homogenized in RLT+ with 0.04M DTT, and RNA was extracted with the Qiasymphony robot (Qiagen) with a protease step and a DNase step. The quality and quantity of RNA was evaluated with the Agilent technology, with the RNA integrity number between 8 and 9.5. Reverse transcription was performed with random primers (Roche) using Superscript enzyme (Invivogen). cDNA for murine IFN-β and ISG15 were detected using Applied Biosystem Taqman probes (Mm00439546-s1, Mm01705338-s1). To analyze the relative fold induction of mRNA, GAPD expression levels were determined in parallel for normalization using the CT method.

Western blot analysis

Nine day old mice were infected with $2x10^5$ PFU CHIKV. Tissue homogenates as well as serum samples were subjected to protein electrophoresis on a 12% Tris gel. The gel was transferred to a polyvinylidene fluoride membrane and probed for ISG15 expression using a rabbit anti-ISG15 polyclonal serum (1:5000) as previously described (68). The membrane was then developed with a horseradish peroxidase (HRP)-conjugated goat anti-rabbit antiserum (Jackson Immunoresearch, West Grove, Pennsylvania) diluted 1:200,000. For loading controls, the same blot was re-probed with anti-β-actin mAb (clone AC-74; Sigma) and then developed with a HRP conjugated goat anti-mouse antibody (Jackson Immuno-Research). All blots were developed with chemiluminescent reagent (Millipore).

Flow Cytometry

Spleens were harvested from naïve nine day old WT, UbE1L$^{-/-}$ and ISG15$^{-/-}$ mice (12 mice per strain). Lymphocyte subsets were stained using the following cell surface markers: CD3, CD4, CD8, NK1.1, CD19, F4/80 and Gr1. Data is represented as percent of the total cell population and Kruskal-Wallis test was used to compare the three genotypes.

Statistical analysis

Data were analyzed using the Prism software (Graphpad software). The OMNIVIZ statistical platform (BioWisdom, Cambridge, UK) was used to perform comparisons among data sets using nonparametric tests (Mann-Whitney U-test) and false discovery rate (FDR) procedures, a permutation-based method to correct for the increased probability of obtaining a false positives among all significant tests (71). Differences were considered significant if $p < 0.05$.

List of accession numbers in GenBank

IFNγ: NM_008337, CCL2: NM_011333, CCL4: NM_013652, CXCL9: NM_008599, CXCL10: NM_021274, IL12: NM_008352, IL1Rα: NM_001039701, IL4: NM_021283, IL5: NM_010558, IL13: NM_008355, IL15: NM_008357, IL17: NM_010552, IFNβ: NM_010510, IRF7: NM_016850, Mx1: NM_010846, ISG15: NM_015783, IL1β: NM_008361, IL6: NM_031168, TNFα: NM_013693, IFNAR1: NM_010508, UbE1L: NM_023738.

Acknowledgements

We thank the Centre d'Immunologie Humaine and the CHIKV Task Force from the Institut Pasteur for support of this work and access to critical reagents. We also acknowledge Olivier Schwartz for helpful suggestions and for the careful review of the manuscript.

We thank Kristen Monte and Charlotte Auriau for their outstanding expertise in animal care; and Stéphanie Thomas for support in sample transportation and filing of regulatory procedures. We would also like to thank Suellen Greco for her help with the blood chemistry analysis.

Figure 2.1. Serum concentration of IFN and IFN-induced chemokines is higher in CHIKV infected infants as compared to adults. Patient sera were obtained from acute CHIKV infected adults (age = 16-86 years) and infants (age = 2-5 months). Age matched controls from La Réunion were tested. Chemokines / cytokines were measured using a Luminex assay. **(A)** IFNα and IFNγ levels; **(B)** IFN-induced molecules; and **(C)** Lymphocyte cell derived cytokines are shown. Whisker-box plots are shown (line indicates median; boxes represent first and third quartile; and bars define range). Mann-Whitney U-test was performed using a false discovery rate (FDR) procedure for generating corrected p-values. Comparisons were made between CHIKV patients versus their control cohort (in black); as well as adult versus infant patients (in red). ** indicates $p<0.005$, * indicates $p<0.05$. IFN data from adult patients were previously reported (5), but are shown here for comparison to data from infected neonates.

Figure 2.1

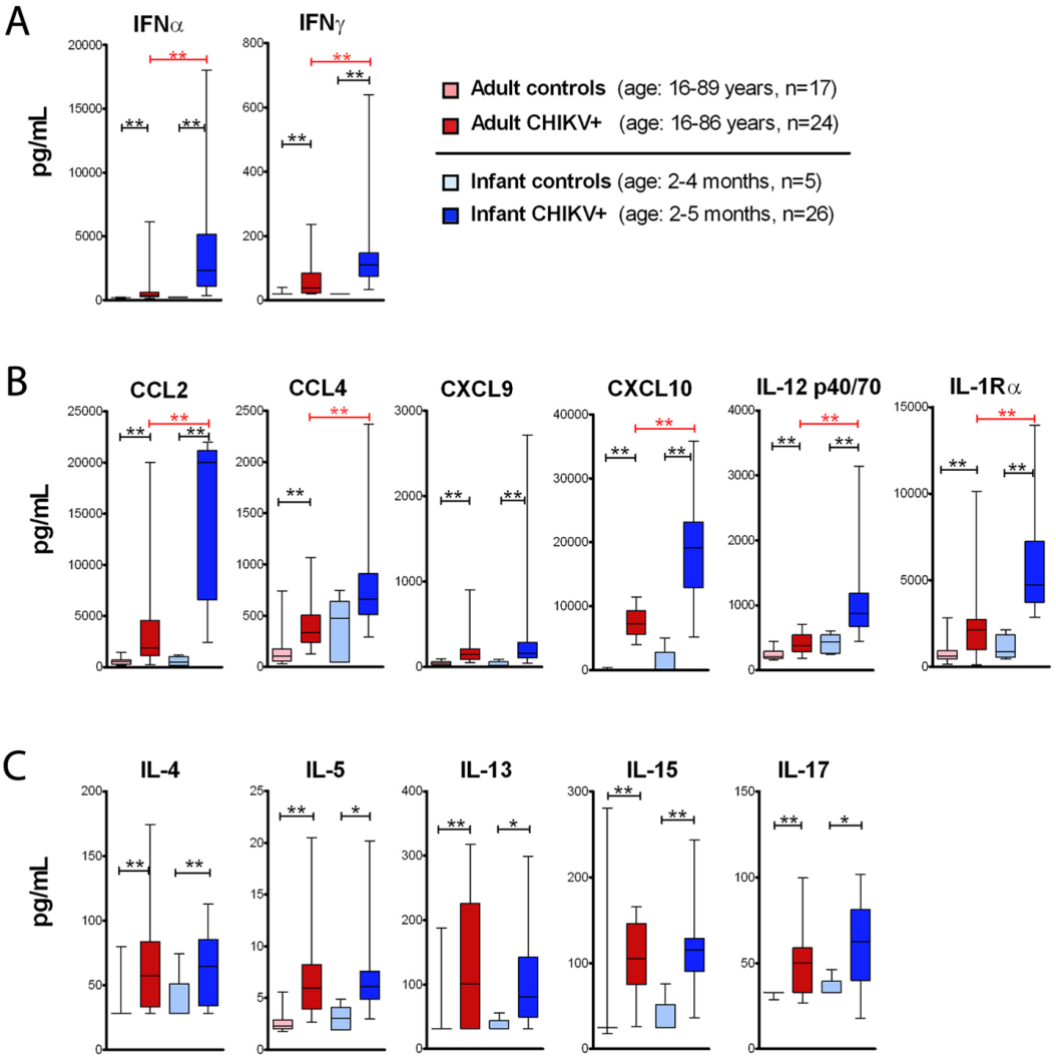
A
IFNα
IFNγ
pg/mL
Adult controls (age: 16-89 years, n=17)
Adult CHIKV+ (age: 16-86 years, n=24)
Infant controls (age: 2-4 months, n=5)
Infant CHIKV+ (age: 2-5 months, n=26)
B
CCL2
CCL4
CXCL9
CXCL10
IL-12 p40/70
IL-1Rα
C
IL-4
IL-5
IL-13
IL-15
IL-17

Figure 2.2. Higher serum IFNα in infants is not explained by differences in viral load. (A-C) Correlations between viral load vs. age; IFNα vs. age; and IFNα vs. viral load were evaluated. CHIKV infected infants are represented by blue squares; CHIKV infected adults are represented by red circles. Lines indicate linear regression and Spearman correlation (r_s) values are shown. **(D)** Each group was divided into two subgroups (<median: low viral load or >median: high viral load; Median = $4.8x10^7$) and statistic are represented (Mann Whitney test) **(E)** For analytes identified in Figure 1 that showed a correlation with viral load, IFN or age are plotted in a network array, illustrating the correlations identified in neonatal *vs.* adult individuals. Connecting lines indicate Spearman correlation (r_s) values; positive correlations in red and negative correlations are depicted in blue. IFN data from adult patients were previously reported (5), but are shown here for comparison to data from infected neonates.

Figure 2.2

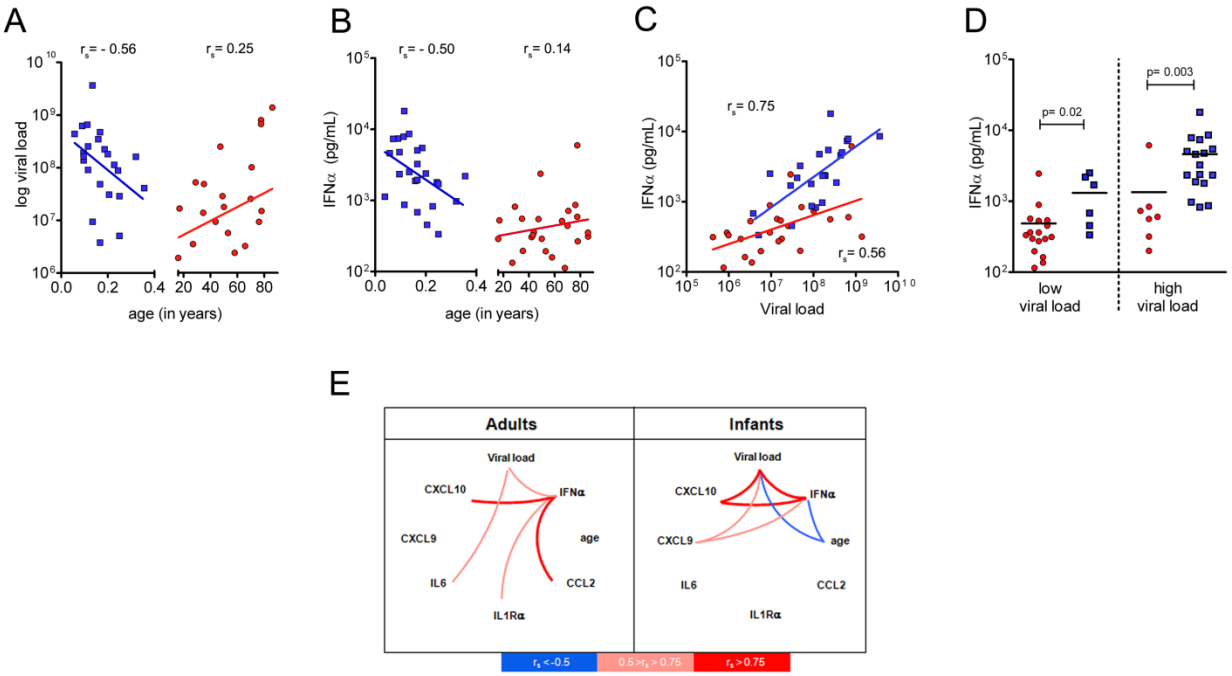
A
r_s= - 0.56
r_s= 0.25
log viral load
age (in years)
B
r_s= - 0.50
r_s= 0.14
IFNα (pg/mL)
age (in years)
C
r_s= 0.75
r_s= 0.56
IFNα (pg/mL)
Viral load
D
p= 0.02
p= 0.003
IFNα (pg/mL)
low viral load
high viral load
E
Adults
Infants
Viral load
CXCL10
IFNα
CXCL9
age
IL6
CCL2
IL1Rα
r_s <-0.5
0.5 >r_s > 0.75
r_s >0.75

Figure 2.3. Neonatal mice mount a robust IFN and pro-inflammatory cytokine/chemokine response following CHIKV infection. Nine day old C57BL/6 mice were injected s.c. in the right flank with CHIKV. **(A)** The skin at the site of infection was harvested at the indicated times post infection and IFNβ, IRF7, Mx1 and ISG15 gene expression was evaluated by qRT-PCR. The ΔCt was calculated using GAPD as a reference gene. At various time points, sera was harvested and tested for **(B)** IFNα by ELISA and IFNγ using Luminex. **(C)** Serum cytokines and chemokines were also analyzed using Luminex. Each graph represents 2-3 independent experiments with 3 mice per experiment.

Figure 2.3

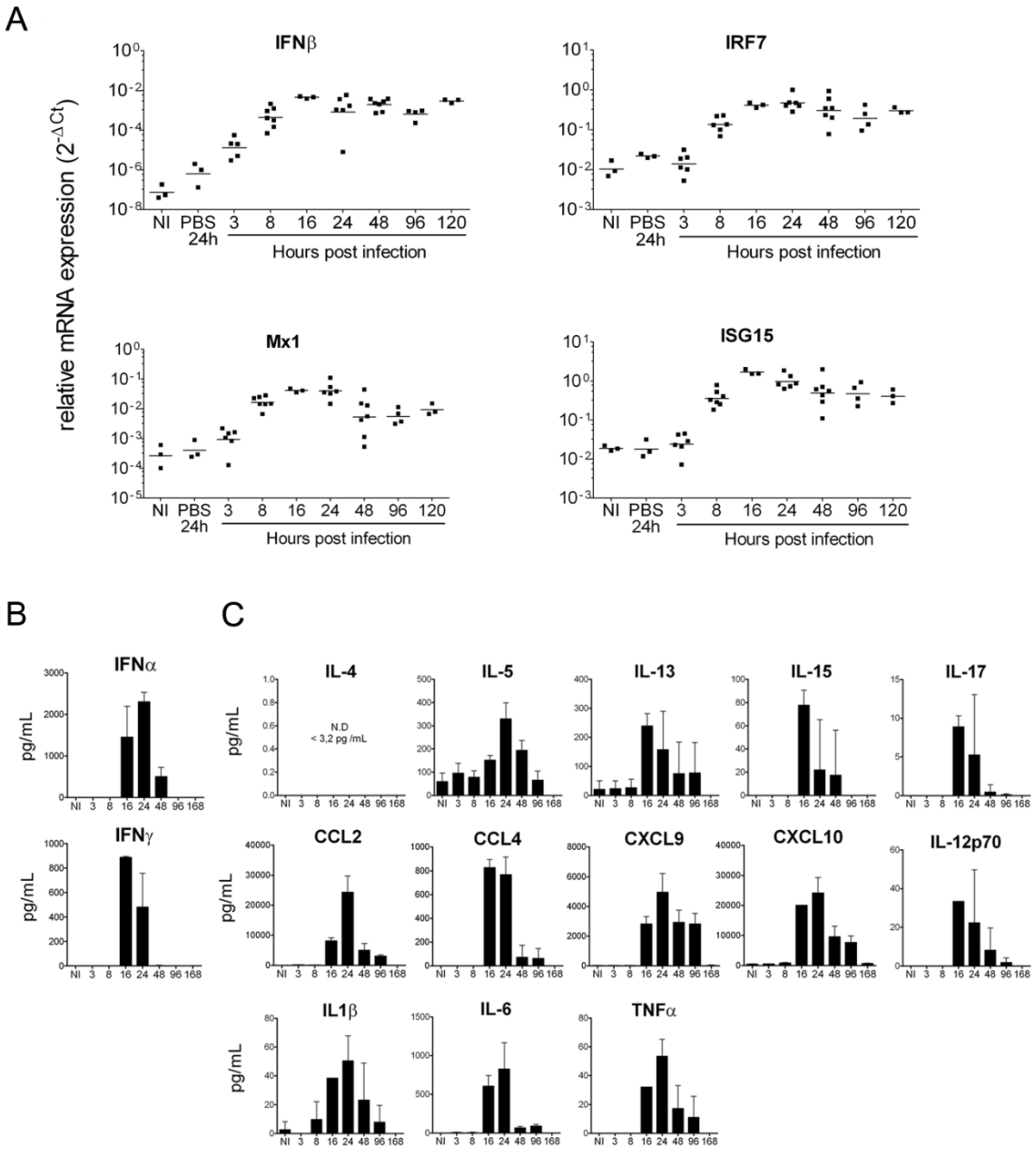
A
IFNβ
IRF7
Mx1
ISG15
relative mRNA expression (2^-ΔCt)
NI PBS 24h 3 8 16 24 48 96 120
Hours post infection
B
IFNα
IFNγ
pg/mL
C
IL-4
N.D
< 3,2 pg /mL
IL-5
IL-13
IL-15
IL-17
CCL2
CCL4
CXCL9
CXCL10
IL-12p70
IL1β
IL-6
TNFα

Figure 2.4. Endogenous Type I IFN is required for the control of neonatal CHIKV infection. WT and IFNAR1$^{-/-}$ mice were infected at 9 days of age with 2x10^5 PFU CHIKV s.c. **(A)** Mice were monitored for lethality for 21 days with data displayed as Kaplan-Meier curves. **(B)** Tissue and sera were collected on day 1 post-infection and viral titers were determined using a standard plaque assay. Mann-Whitney statistical comparison of wild type and IFNAR1$^{-/-}$ viral titers are shown where * indicates $p<0.05$, ** $p<0.005$ and *** $p<0.0005$, and vertical bars represent standard error of the mean.

Figure 2.4

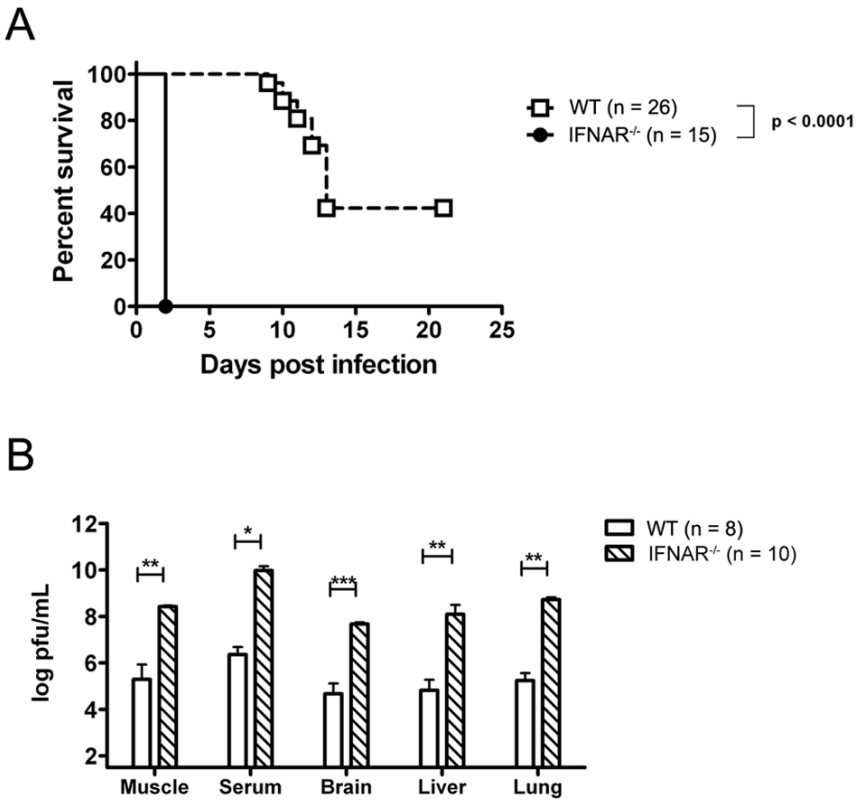
A
Percent survival
100
80
60
40
20
0
0
5
10
15
20
25
Days post infection
WT (n = 26)
IFNAR-/- (n = 15)
p < 0.0001
B
log pfu/mL
12
10
8
6
4
2
**
*
***
**
**
Muscle
Serum
Brain
Liver
Lung
WT (n = 8)
IFNAR-/- (n = 10)

Figure 2.5. Adjuvant induced type I IFN production protects neonates from CHIKV infection. Mice (8 days of age) were injected i.p. with 25 μg of poly (I:C) and 24 hours later mice were infected s.c. in the right flank with CHIKV. **(A)** IFNα levels produced in the serum of neonatal mice 7 hours post injection with 25 μg poly (I:C). **(B)** Survival was monitored daily for four weeks and displayed as Kaplan-Meier survival curves. **(C)** Mice were scored for clinical signs of disease on days 7, 13 and 18 post-infection as discussed in materials and methods. **(D)** $IFNAR1^{-/-}$ mice (8 days of age) were injected i.p. with 25 μg of pIC and 24 hours later mice were infected with CHIKV s.c. Survival was monitored daily.

Figure 2.5

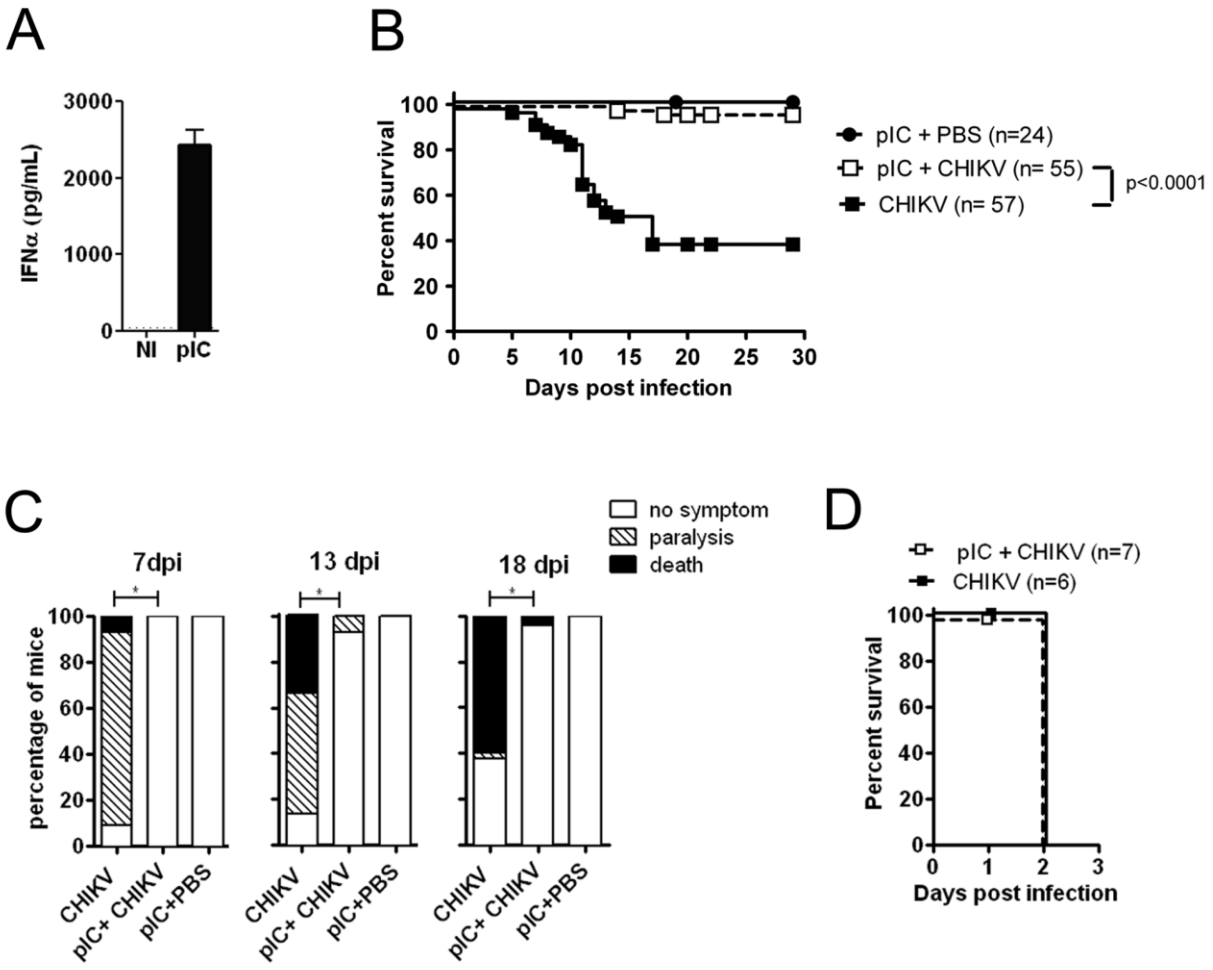
A
IFNα (pg/mL)
3000
2000
1000
0
NI
pIC
B
Percent survival
100
80
60
40
20
0
0 5 10 15 20 25 30
Days post infection
pIC + PBS (n=24)
pIC + CHIKV (n= 55)
CHIKV (n= 57)
p<0.0001
C
no symptom
paralysis
death
7dpi
13 dpi
18 dpi
percentage of mice
CHIKV
pIC+ CHIKV
pIC+PBS
D
pIC + CHIKV (n=7)
CHIKV (n=6)
Percent survival
Days post infection

Figure 2.6. ISG15, independent of UbE1L, plays a critical role during the neonatal response to CHIKV. (A-C) WT, UbE1L$^{-/-}$ and ISG15$^{-/-}$ mice were infected with 2x10^5 PFU CHIKV s.c. at nine days of age. (A) Mice were monitored for lethality for 21 days with data displayed as Kaplan-Meier curves. (B) Skin and muscle homogenates from the site of infection were collected on day 2 post infection and analyzed for ISG15 expression by western blot. (C) Sera collected on days 1, 3 and 6 p.i. and analyzed as in (B). **(D and E)** ISG15$^{-/-}$, UbE1L$^{-/-}$ and WT mice (8 days of age) were injected i.p. with (D) 25 μg or (E) 10 μg of pIC and 24 hours later mice were infected s.c. with 2x10^5 PFU CHIKV. Survival was monitored daily for 21 days and displayed as Kaplan-Meier survival curves. Mice from all three genotypes that were pretreated with 25 μg of poly(I:C) and mock infected with PBS showed no lethality (data not shown).

Figure 2.6

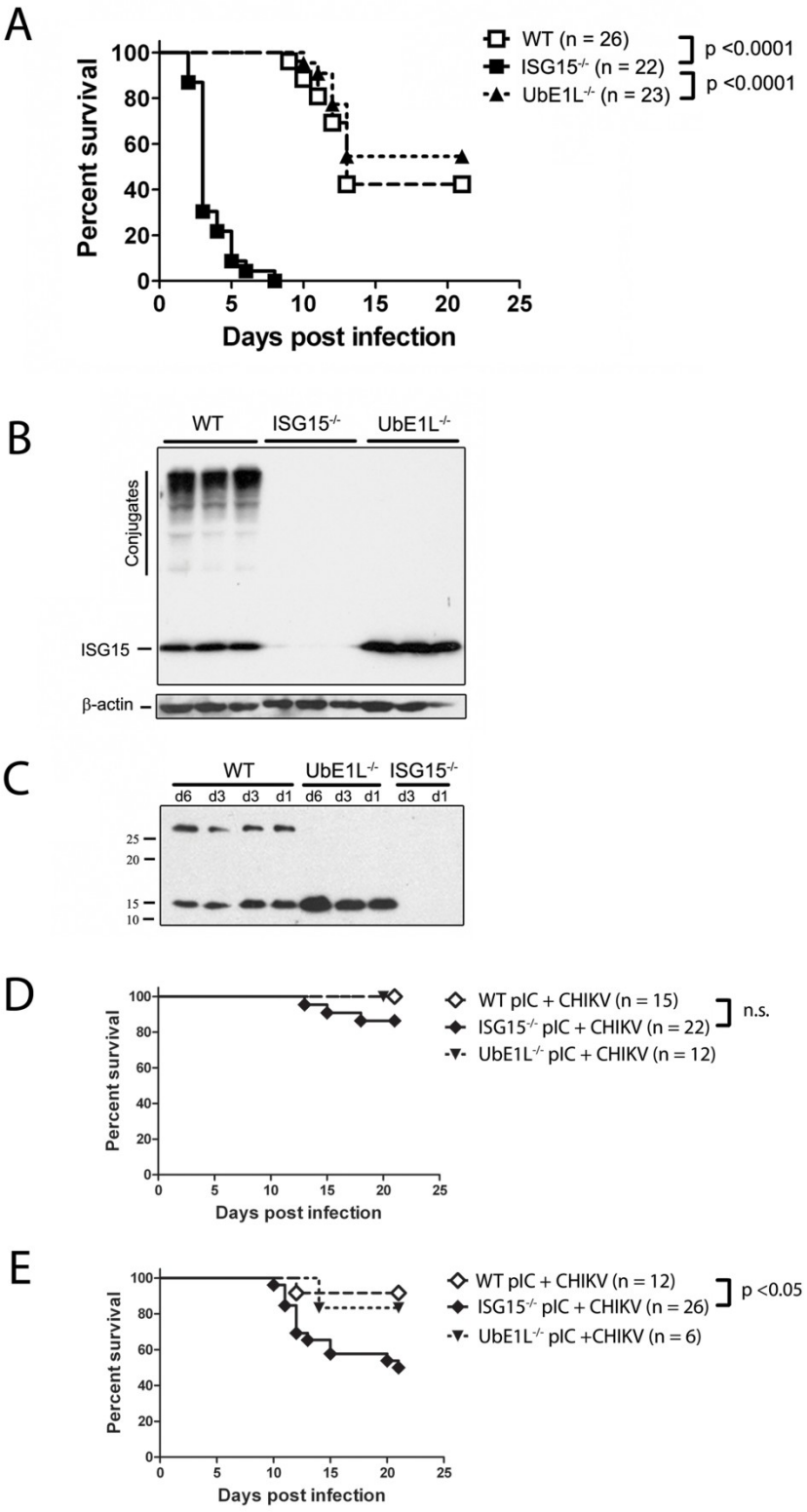
A
Percent survival
Days post infection
WT (n = 26)
ISG15-/- (n = 22)
UbE1L-/- (n = 23)
p <0.0001
p <0.0001
B
WT
ISG15-/-
UbE1L-/-
Conjugates
ISG15
β-actin
C
WT
UbE1L-/-
ISG15-/-
d6 d3 d3 d1 d6 d3 d1 d3 d1
25
20
15
10
D
Percent survival
Days post infection
WT pIC + CHIKV (n = 15)
ISG15-/- pIC + CHIKV (n = 22)
UbE1L-/- pIC + CHIKV (n = 12)
n.s.
E
Percent survival
Days post infection
WT pIC + CHIKV (n = 12)
ISG15-/- pIC + CHIKV (n = 26)
UbE1L-/- pIC +CHIKV (n = 6)
p <0.05

Figure 2.7. ISG15$^{-/-}$ and UbE1L$^{-/-}$ mice display similar viral loads to WT mice. Nine day old WT, UbE1L$^{-/-}$ and ISG15$^{-/-}$ mice were injected with 2x10^5 PFU CHIKV s.c. Tissue and sera were collected on days 1 **(A)** and 2 **(B)** post-infection and viral titers were determined by plaque assay; vertical bars represent standard error of the mean. A three way comparison of the three genotypes performed using a Kruskal-Wallis analysis was not significant except for the lung on day 2 post infection (*, where $p < 0.05$).

Figure 2.7

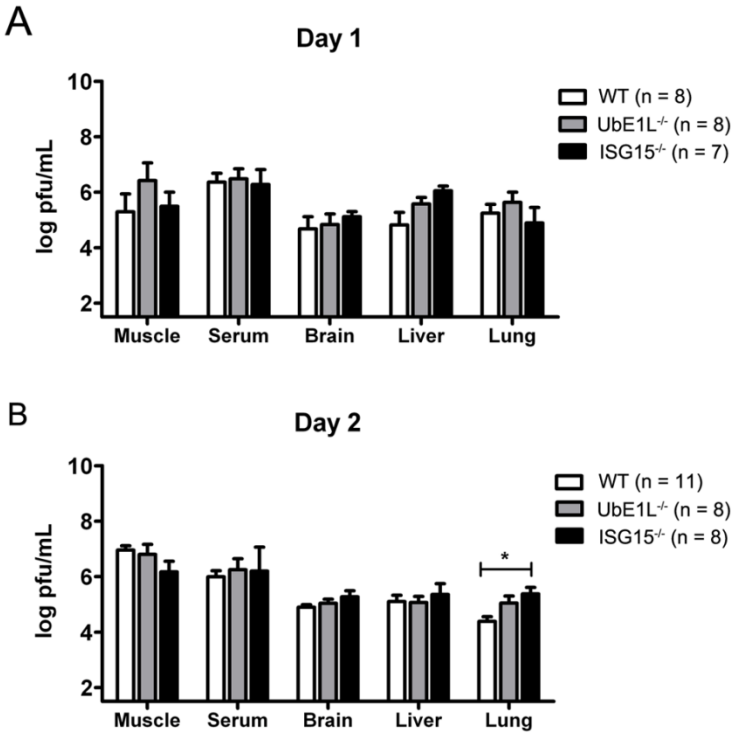
A
Day 1
log pfu/mL
10
8
6
4
2
Muscle
Serum
Brain
Liver
Lung
WT (n = 8)
UbE1L-/- (n = 8)
ISG15-/- (n = 7)
B
Day 2
log pfu/mL
10
8
6
4
2
Muscle
Serum
Brain
Liver
Lung
*
WT (n = 11)
UbE1L-/- (n = 8)
ISG15-/- (n = 8)

Figure 2.8. ISG15$^{-/-}$ neonates display elevated cytokine levels during CHIKV infection. Nine day old WT, IFNAR1$^{-/-}$, UbE1L$^{-/-}$ and ISG15$^{-/-}$ mice were injected with 2x10^5 PFU CHIKV s.c. **(A)** The skin at the site of infection was harvested and the expression of IFNβ mRNA was evaluated by qRT-PCR. Vertical bars represent mean with standard error of the mean. **(B and C)** Serum was collected at the indicated time post-infection. **(B)** IFNα levels were quantified using an ELISA, vertical bars represent mean with standard error of the mean. Statistical comparison between the three genotypes via Mann-Whitney and Kruskal-Wallis test was not significant for both (A) and (B). **(C)** Cytokine and chemokine levels were measured by Bioplex assay (Mann-Whitney * $p < 0.05$, ** $p < 0.005$). Vertical bars represent standard error of the mean.

Figure 2.8

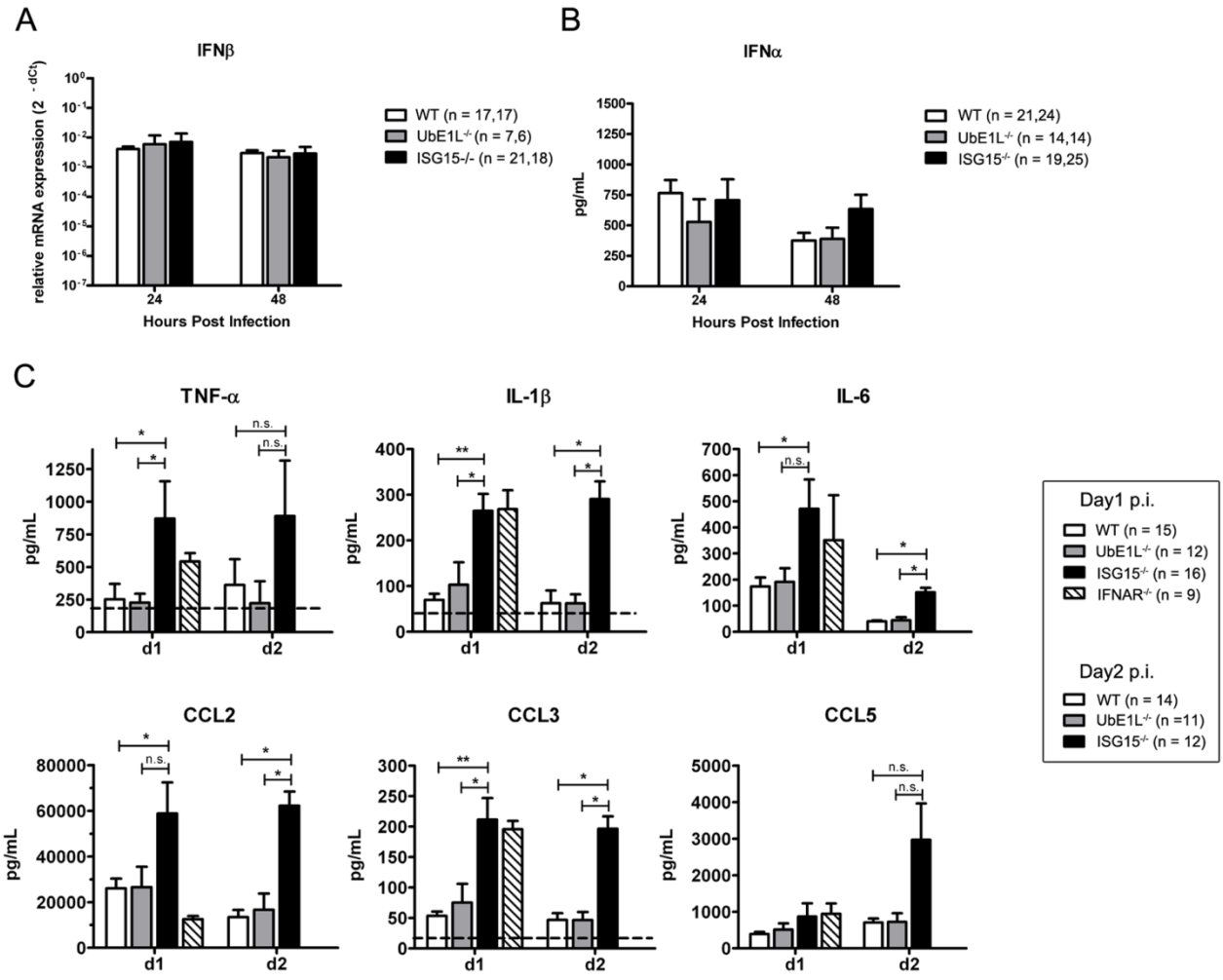
A
IFNβ
relative mRNA expression (2 - dCt)
WT (n = 17,17)
UbE1L-/- (n = 7,6)
ISG15-/- (n = 21,18)
24
48
Hours Post Infection
B
IFNα
pg/mL
WT (n = 21,24)
UbE1L-/- (n = 14,14)
ISG15-/- (n = 19,25)
24
48
Hours Post Infection
C
TNF-α
IL-1β
IL-6
CCL2
CCL3
CCL5
pg/mL
d1
d2
n.s.
Day1 p.i.
WT (n = 15)
UbE1L-/- (n = 12)
ISG15-/- (n = 16)
IFNAR-/- (n = 9)
Day2 p.i.
WT (n = 14)
UbE1L-/- (n =11)
ISG15-/- (n = 12)

Figure S2.1. Pre-treatment with IFNβ improves the outcome of CHIKV infection. Mice 8 days of age were injected i.p. with 5000U of IFNβ and 24 hours later mice were infected s.c. in the right flank with $2x10^5$ PFU CHIKV. Mice were scored for clinical signs of disease on days 7, 11 and 18 post-infection. The ability of the mice to return and land on its feet when flipped over was assessed. Paralysis was defined as the inability or delayed time to return (>5s). 3 independent experiments are compiled.

Figure S2.1

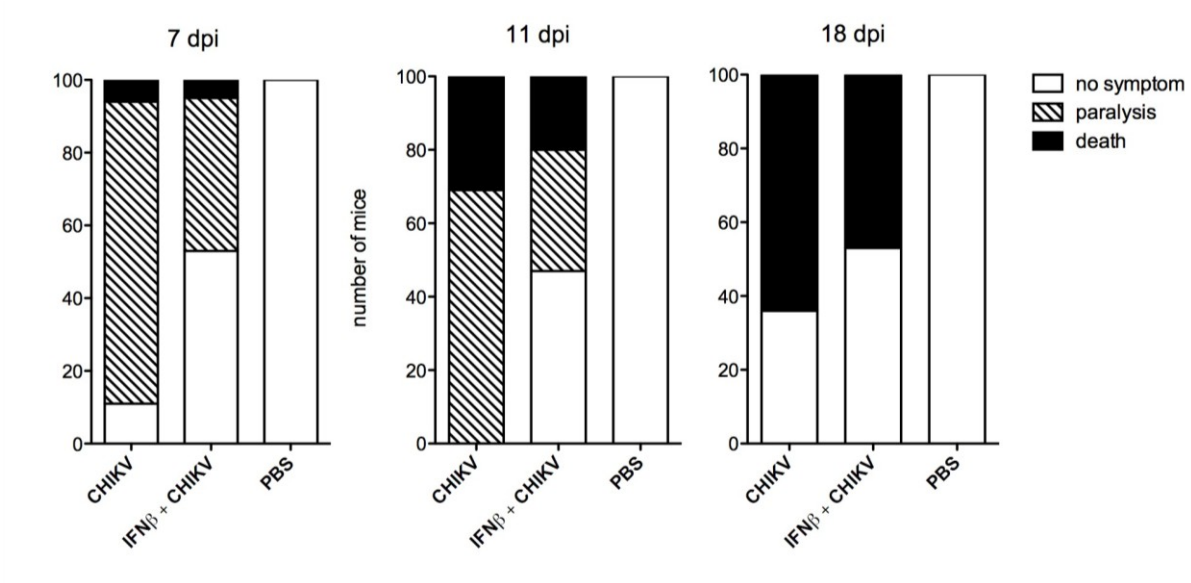
7 dpi
11 dpi
18 dpi
number of mice
100
80
60
40
20
0
CHIKV
IFNβ + CHIKV
PBS
no symptom
paralysis
death

Figure S2.2. Induction of ISG15 during neonatal CHIKV infection is largely dependent upon IFNAR1 signaling. Serum from nine day old WT, UbE1L$^{-/-}$, ISG15$^{-/-}$ and IFNAR$^{-/-}$ mice infected s.c. with 2x10^{5} PFU CHIKV was collected on day 1 post-infection and ISG15 expression was assessed by western blot.

Figure S2.2

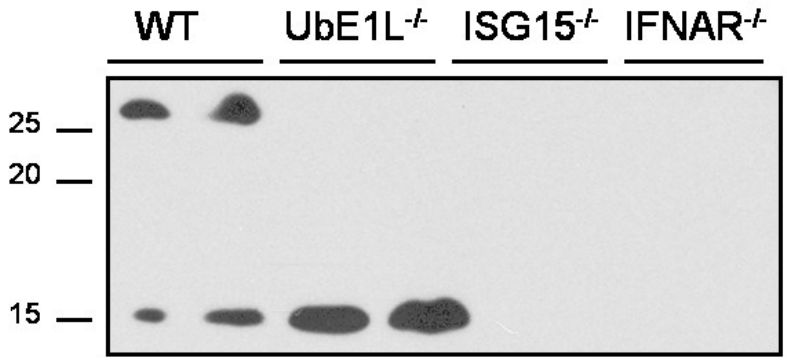

Figure S2.3. The role of ISG15 during CHIKV infection is age dependent. WT, UbE1L$^{-/-}$ and ISG15$^{-/-}$ mice were infected with 2x10^5 PFU CHIKV s.c. at either **(A)** eleven days of age, **(B)** twelve days of age, or **(C)** 6-8 weeks of age and were monitored for survival for 21 days post-infection. Kaplan-Meier survival curves are shown.

Figure S2.3

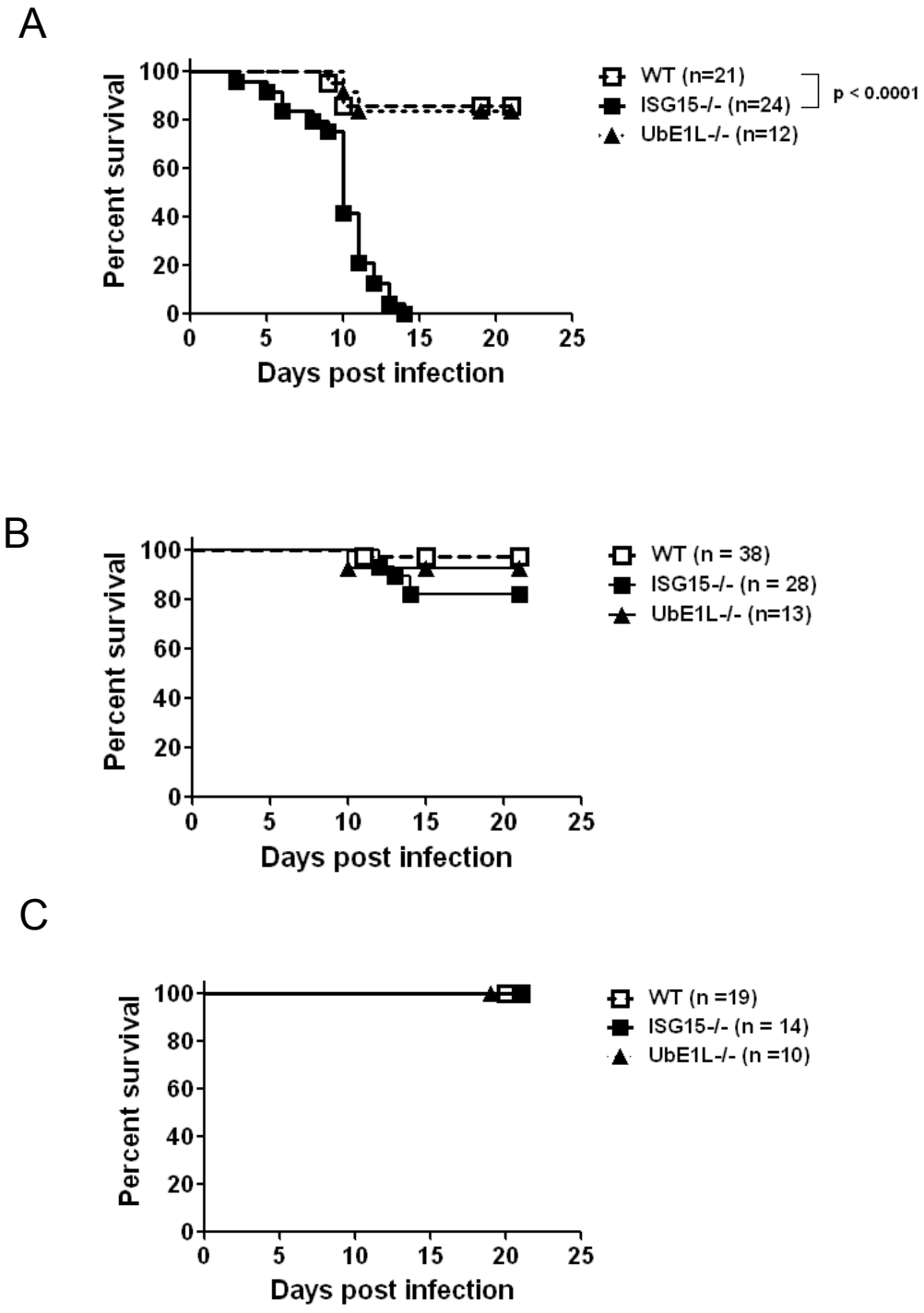
A
Percent survival
Days post infection
WT (n=21)
ISG15-/- (n=24)
UbE1L-/- (n=12)
p < 0.0001
B
Percent survival
Days post infection
WT (n = 38)
ISG15-/- (n = 28)
UbE1L-/- (n=13)
C
Percent survival
Days post infection
WT (n =19)
ISG15-/- (n = 14)
UbE1L-/- (n =10)

Figure S2.4. Recombinant CHIKV viruses expressing WT ISG15 do not rescue ISG15$^{-/-}$ mice. Recombinant CHIK viruses were generated to express the following proteins: wild type ISG15(-LRLRGG), non-conjugatable ISG15(-LRLRAA), and GFP(-GFP). **(A)** Schematic representation of recombinant CHIK clones adapted from Tsetsarkin, et al (2006). **(B and C)** BHK cells were infected with the indicated rCHIK viruses at an MOI=1. (B) Viral titers were measured at 0,6,12,24,48hrs p.i. by plaque assay. (C) Cell lysates were collected at 0,6,12, and 24hrs p.i. and were analyzed for ISG15 expression by western blot. **(D)** Six day old ISG15$^{-/-}$ mice were infected with either CHIK-GFP or CHIK-LRLRGG at $3x10^5$ PFU s.c. Mice were monitored for lethality for 21 days with data displayed as Kaplan-Meier curves.

Figure S2.4

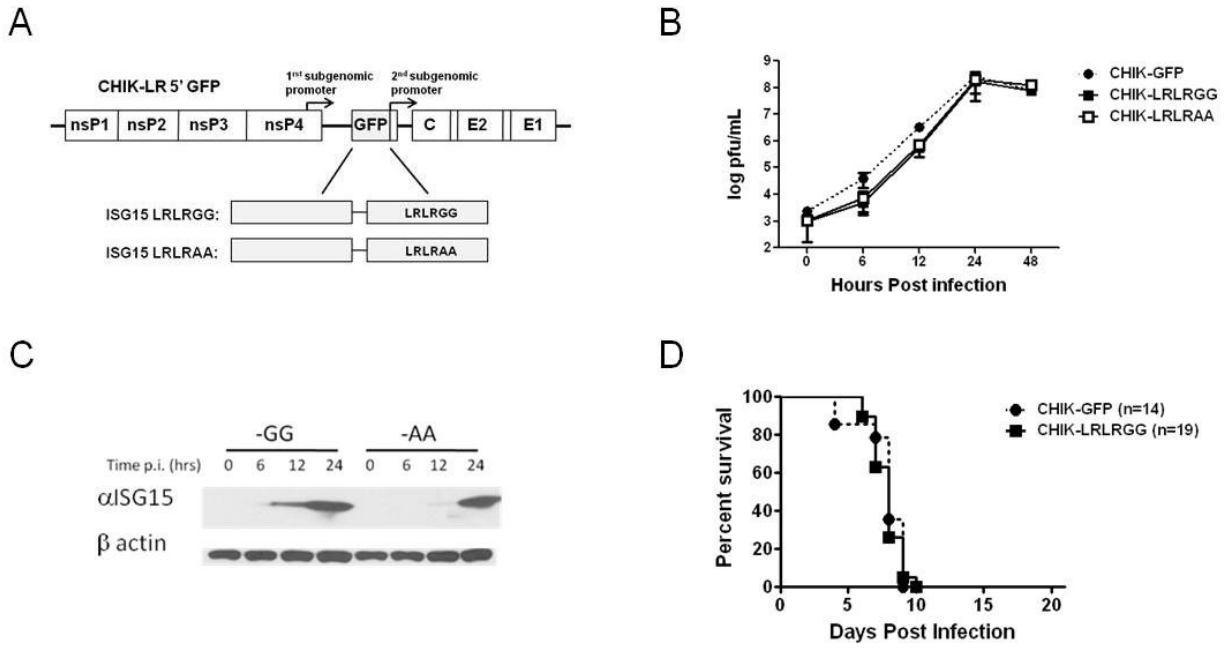
A
CHIK-LR 5' GFP
1st subgenomic promoter
2nd subgenomic promoter
nsP1
nsP2
nsP3
nsP4
GFP
C
E2
E1
ISG15 LRLRGG:
LRLRGG
ISG15 LRLRAA:
LRLRAA
B
log pfu/mL
Hours Post infection
CHIK-GFP
CHIK-LRLRGG
CHIK-LRLRAA
C
-GG
-AA
Time p.i. (hrs)
0 6 12 24 0 6 12 24
αISG15
β actin
D
Percent survival
Days Post Infection
CHIK-GFP (n=14)
CHIK-LRLRGG (n=19)

Figure S2.5. CHIKV infected ISG15$^{-/-}$ mice have increased ALT, AST, BUN serum levels and decreased serum glucose levels compared to WT and UbE1L$^{-/-}$ mice. Nine day old WT, UbE1L$^{-/-}$ and ISG15$^{-/-}$ mice were infected with CHIKV (10^5pfu s.c.). Serum was collected on day 2 p.i. and sent to DCM for blood chemistry analysis. Analyte levels were compared to PBS mock treated WT and ISG15$^{-/-}$ controls. * = $p<0.05$, ** = $p<0.01$

Figure S2.5

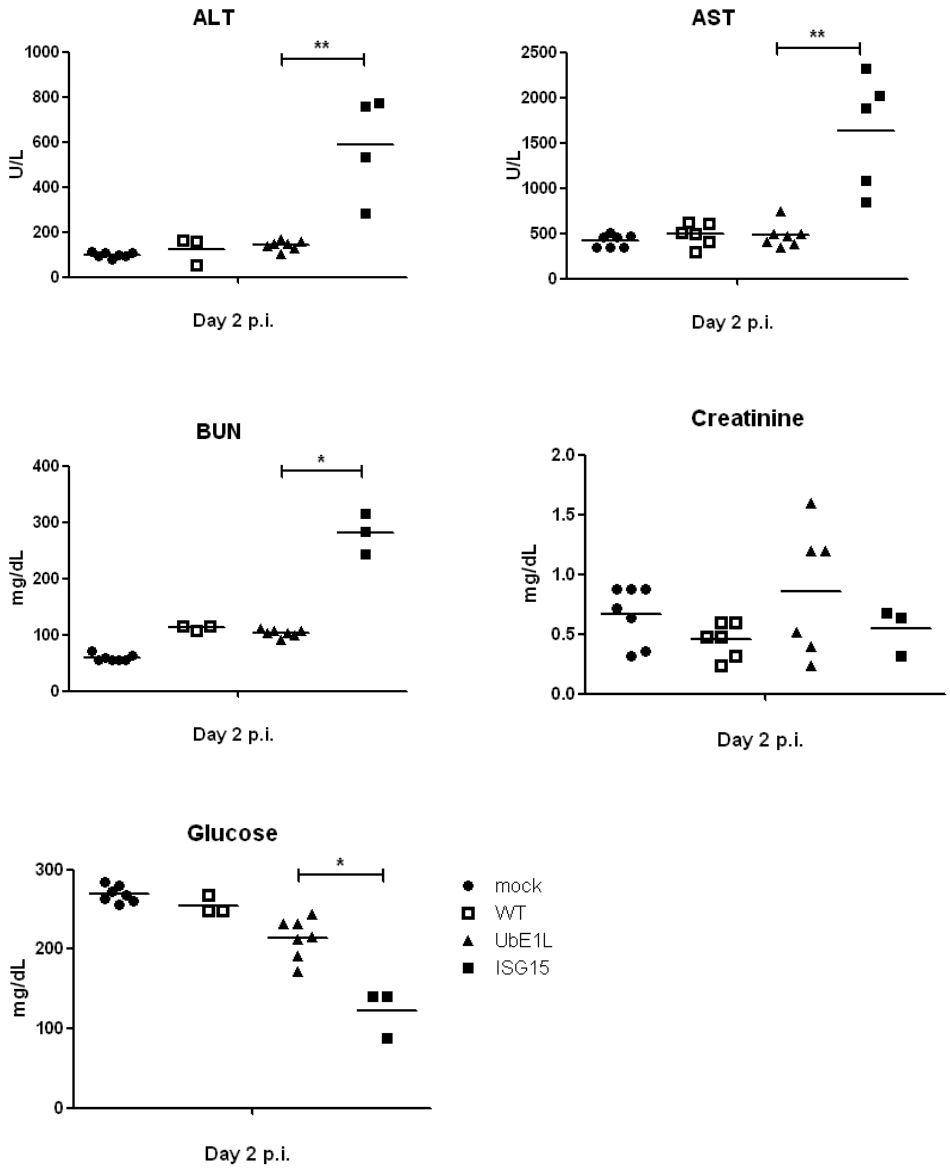
ALT
U/L
1000
800
600
400
200
0
**
Day 2 p.i.
AST
U/L
2500
2000
1500
1000
500
0
**
Day 2 p.i.
BUN
mg/dL
400
300
200
100
0
*
Day 2 p.i.
Creatinine
mg/dL
2.0
1.5
1.0
0.5
0.0
Day 2 p.i.
Glucose
mg/dL
300
200
100
0
*
Day 2 p.i.
mock
WT
UbE1L
ISG15

Table S2.1. Clinical signs in adult and infant cohort.

	Adult	Infant
age	16-86 years	2-5 months
Fever	19/19 (100%)	25/25 (100%)
Arthralgia	16/19 (84 %)	12/25 (50%)
Skin manifestation	10/19 (53 %)	17/25 (68%)
Myalgia	3 /19 (16%)	3 /25 (12%)
Encephalopathy	0	4 /25 (16%)

Table S2.2. Splenic lymphocyte subsets in naïve WT, UbE1L$^{-/-}$ and ISG15$^{-/-}$ neonatal mice (% total cell population, mean ± sem).

Cell Type	WT	ISG15-/-	UbE1L-/-
B cells (CD19+)	9.10 ± 3.0	5.27 ± 2.2	9.08 ± 0.0
NK cells (NK1.1+)	0.43 ± 0.0	0.35 ± 0.0	0.35 ± 0.0
CD4^{+} T cells (CD4+CD3+)	2.85 ± 0.6	2.15 ± 0.5	2.02 ± 0.1
CD8^{+} T cells (CD8+CD3+)	1.52 ± 0.3	1.11 ± 0.2	1.13 ± 0.0
Granulocytes (Gr1^{hi},F4/80^{low})	3.02 ± 0.3	2.58 ± 0.6	2.83 ± 0.0
Monocytes (Gr1^{int},F4/80^{int})	1.38 ± 0.0	1.38 ± 0.1	1.11 ± 0.0

References

1. Borgherini, G., P. Poubeau, F. Staikowsky, M. Lory, N. Le Moullec, J. P. Becquart, C. Wengling, A. Michault, and F. Paganin. 2007. Outbreak of chikungunya on Reunion Island: early clinical and laboratory features in 157 adult patients. *Clin Infect Dis* 44:1401-1407.

2. Lumsden, W. H. 1955. An epidemic of virus disease in Southern Province, Tanganyika Territory, in 1952-53. II. General description and epidemiology. *Trans R Soc Trop Med Hyg* 49:33-57.

3. Gerardin, P., V. Guernier, J. Perrau, A. Fianu, K. Le Roux, P. Grivard, A. Michault, X. de Lamballerie, A. Flahault, and F. Favier. 2008. Estimating Chikungunya prevalence in La Reunion Island outbreak by serosurveys: two methods for two critical times of the epidemic. *BMC Infect Dis* 8:99.

4. Staikowsky, F., K. Le Roux, I. Schuffenecker, P. Laurent, P. Grivard, A. Develay, and A. Michault. 2008. Retrospective survey of Chikungunya disease in Reunion Island hospital staff. *Epidemiol Infect* 136:196-206.

5. Mavalankar, D., P. Shastri, and P. Raman. 2007. Chikungunya epidemic in India: a major public-health disaster. *Lancet Infect Dis* 7:306-307.

6. Her, Z., Y. W. Kam, R. T. Lin, and L. F. Ng. 2009. Chikungunya: a bending reality. *Microbes Infect* 11:1165-1176.

7. Tsetsarkin, K. A., D. L. Vanlandingham, C. E. McGee, and S. Higgs. 2007. A single mutation in chikungunya virus affects vector specificity and epidemic potential. *PLoS Pathog* 3:e201.

8. Angelini, R., A. C. Finarelli, P. Angelini, C. Po, K. Petropulacos, G. Silvi, P. Macini, C. Fortuna, G. Venturi, F. Magurano, C. Fiorentini, A. Marchi, E. Benedetti, P. Bucci, S. Boros, R. Romi, G. Majori, M. G. Ciufolini, L. Nicoletti, G. Rezza, and A. Cassone. 2007. Chikungunya in north-eastern Italy: a summing up of the outbreak. *Euro Surveill* 12:E071122 071122.

9. Gould, E. A., P. Gallian, X. De Lamballerie, and R. N. Charrel. 2010. First cases of autochthonous dengue fever and chikungunya fever in France: from bad dream to reality! *Clin Microbiol Infect* 16:1702-1704.

10. Gerardin, P., G. Barau, A. Michault, M. Bintner, H. Randrianaivo, G. Choker, Y. Lenglet, Y. Touret, A. Bouveret, P. Grivard, K. Le Roux, S. Blanc, I. Schuffenecker, T. Couderc, F. Arenzana-Seisdedos, M. Lecuit, and P. Y. Robillard. 2008. Multidisciplinary prospective study of mother-to-child chikungunya virus infections on the island of La Reunion. *PLoS Med* 5:e60.

11. Seay, A. R., D. E. Griffin, and R. T. Johnson. 1981. Experimental viral polymyositis: age dependency and immune responses to Ross River virus infection in mice. *Neurology* 31:656-660.

12. Fleming, P. 1977. Age-dependent and strain-related differences of virulence of Semliki Forest virus in mice. *J Gen Virol* 37:93-105.

13. Chakravarty, S. K., and J. K. Sarkar. 1969. Susceptibility of new born and adult laboratory animals to Chikungunya virus. *Indian J Med Res* 57:1157-1164.

14. Ziegler, S. A., L. Lu, A. P. da Rosa, S. Y. Xiao, and R. B. Tesh. 2008. An animal model for studying the pathogenesis of chikungunya virus infection. *Am J Trop Med Hyg* 79:133-139.

15. Couderc, T., F. Chretien, C. Schilte, O. Disson, M. Brigitte, F. Guivel-Benhassine, Y. Touret, G. Barau, N. Cayet, I. Schuffenecker, P. Despres, F. Arenzana-Seisdedos, A. Michault, M. L. Albert, and M. Lecuit. 2008. A mouse model for Chikungunya: young age and inefficient type-I interferon signaling are risk factors for severe disease. *PLoS Pathog* 4:e29.

16. Levy, O. 2007. Innate immunity of the newborn: basic mechanisms and clinical correlates. *Nat Rev Immunol* 7:379-390.

17. De Wit, D., V. Olislagers, S. Goriely, F. Vermeulen, H. Wagner, M. Goldman, and F. Willems. 2004. Blood plasmacytoid dendritic cell responses to CpG oligodeoxynucleotides are impaired in human newborns. *Blood* 103:1030-1032.

18. Aksoy, E., V. Albarani, M. Nguyen, J. F. Laes, J. L. Ruelle, D. De Wit, F. Willems, M. Goldman, and S. Goriely. 2007. Interferon regulatory factor 3-dependent responses to lipopolysaccharide are selectively blunted in cord blood cells. *Blood* 109:2887-2893.

19. Marodi, L., K. Goda, A. Palicz, and G. Szabo. 2001. Cytokine receptor signalling in neonatal macrophages: defective STAT-1 phosphorylation in response to stimulation with IFN-gamma. *Clin Exp Immunol* 126:456-460.

20. Schilte, C., T. Couderc, F. Chretien, M. Sourisseau, N. Gangneux, F. Guivel-Benhassine, A. Kraxner, J. Tschopp, S. Higgs, A. Michault, F. Arenzana-Seisdedos, M. Colonna, L. Peduto, O. Schwartz, M. Lecuit, and M. L. Albert. 2010. Type I IFN controls chikungunya virus via its action on nonhematopoietic cells. *J Exp Med* 207:429-442.

21. White, L. K., T. Sali, D. Alvarado, E. Gatti, P. Pierre, D. Streblow, and V. R. Defilippis. 2011. Chikungunya virus induces IPS-1-dependent innate immune activation and protein kinase R-independent translational shutoff. *J Virol* 85:606-620.

22. Sadler, A. J., and B. R. Williams. 2008. Interferon-inducible antiviral effectors. *Nat Rev Immunol* 8:559-568.

23. Narasimhan, J., M. Wang, Z. Fu, J. M. Klein, A. L. Haas, and J. J. Kim. 2005. Crystal structure of the interferon-induced ubiquitin-like protein ISG15. *J Biol Chem* 280:27356-27365.

24. Yuan, W., and R. M. Krug. 2001. Influenza B virus NS1 protein inhibits conjugation of the interferon (IFN)-induced ubiquitin-like ISG15 protein. *EMBO J* 20:362-371.

25. Zhao, C., S. L. Beaudenon, M. L. Kelley, M. B. Waddell, W. Yuan, B. A. Schulman, J. M. Huibregtse, and R. M. Krug. 2004. The UbcH8 ubiquitin E2 enzyme is also the E2 enzyme for ISG15, an IFN-alpha/beta-induced ubiquitin-like protein. *Proc Natl Acad Sci U S A* 101:7578-7582.

26. Kim, K. I., N. V. Giannakopoulos, H. W. Virgin, and D. E. Zhang. 2004. Interferon-inducible ubiquitin E2, Ubc8, is a conjugating enzyme for protein ISGylation. *Mol Cell Biol* 24:9592-9600.

27. Dastur, A., S. Beaudenon, M. Kelley, R. M. Krug, and J. M. Huibregtse. 2006. Herc5, an interferon-induced HECT E3 enzyme, is required for conjugation of ISG15 in human cells. *J Biol Chem* 281:4334-4338.

28. Wong, J. J., Y. F. Pung, N. S. Sze, and K. C. Chin. 2006. HERC5 is an IFN-induced HECT-type E3 protein ligase that mediates type I IFN-induced ISGylation of protein targets. *Proc Natl Acad Sci U S A* 103:10735-10740.

29. Giannakopoulos, N. V., J. K. Luo, V. Papov, W. Zou, D. J. Lenschow, B. S. Jacobs, E. C. Borden, J. Li, H. W. Virgin, and D. E. Zhang. 2005. Proteomic identification of proteins conjugated to ISG15 in mouse and human cells. *Biochem Biophys Res Commun* 336:496-506.

30. Minakawa, M., T. Sone, T. Takeuchi, and H. Yokosawa. 2008. Regulation of the nuclear factor (NF)-kappaB pathway by ISGylation. *Biol Pharm Bull* 31:2223-2227.

31. Jeon, Y. J., J. S. Choi, J. Y. Lee, K. R. Yu, S. M. Kim, S. H. Ka, K. H. Oh, K. I. Kim, D. E. Zhang, O. S. Bang, and C. H. Chung. 2009. ISG15 modification of filamin B negatively regulates the type I interferon-induced JNK signalling pathway. *EMBO Rep* 10:374-380.

32. Okumura, F., W. Zou, and D. E. Zhang. 2007. ISG15 modification of the eIF4E cognate 4EHP enhances cap structure-binding activity of 4EHP. *Genes Dev* 21:255-260.

33. D'Cunha, J., S. Ramanujam, R. J. Wagner, P. L. Witt, E. Knight, Jr., and E. C. Borden. 1996. In vitro and in vivo secretion of human ISG15, an IFN-induced immunomodulatory cytokine. *J Immunol* 157:4100-4108.

34. Lenschow, D. J., C. Lai, N. Frias-Staheli, N. V. Giannakopoulos, A. Lutz, T. Wolff, A. Osiak, B. Levine, R. E. Schmidt, A. Garcia-Sastre, D. A. Leib, A. Pekosz, K. P. Knobeloch, I. Horak, and H. W. t. Virgin. 2007. IFN-stimulated gene 15 functions as a critical antiviral molecule against influenza, herpes, and Sindbis viruses. *Proc Natl Acad Sci U S A* 104:1371-1376.

35. D'Cunha, J., E. Knight, Jr., A. L. Haas, R. L. Truitt, and E. C. Borden. 1996. Immunoregulatory properties of ISG15, an interferon-induced cytokine. *Proc Natl Acad Sci U S A* 93:211-215.

36. Owhashi, M., Y. Taoka, K. Ishii, S. Nakazawa, H. Uemura, and H. Kambara. 2003. Identification of a ubiquitin family protein as a novel neutrophil chemotactic factor. *Biochem Biophys Res Commun* 309:533-539.

37. Padovan, E., L. Terracciano, U. Certa, B. Jacobs, A. Reschner, M. Bolli, G. C. Spagnoli, E. C. Borden, and M. Heberer. 2002. Interferon stimulated gene 15 constitutively produced by melanoma cells induces e-cadherin expression on human dendritic cells. *Cancer Res* 62:3453-3458.

38. Guerra, S., A. Caceres, K. P. Knobeloch, I. Horak, and M. Esteban. 2008. Vaccinia virus E3 protein prevents the antiviral action of ISG15. *PLoS Pathog* 4:e1000096.

39. Kim, K. I., M. Yan, O. Malakhova, J. K. Luo, M. F. Shen, W. Zou, J. C. de la Torre, and D. E. Zhang. 2006. Ube1L and protein ISGylation are not essential for alpha/beta interferon signaling. *Mol Cell Biol* 26:472-479.

40. Giannakopoulos, N. V., E. Arutyunova, C. Lai, D. J. Lenschow, A. L. Haas, and H. W. Virgin. 2009. ISG15 Arg151 and the ISG15-conjugating enzyme UbE1L are important for innate immune control of Sindbis virus. *J Virol* 83:1602-1610.

41. Lai, C., J. J. Struckhoff, J. Schneider, L. Martinez-Sobrido, T. Wolff, A. Garcia-Sastre, D. E. Zhang, and D. J. Lenschow. 2009. Mice lacking the ISG15 E1 enzyme UbE1L demonstrate increased susceptibility to both mouse-adapted and non-mouse-adapted influenza B virus infection. *J Virol* 83:1147-1151.

42. Frias-Staheli, N., N. V. Giannakopoulos, M. Kikkert, S. L. Taylor, A. Bridgen, J. Paragas, J. A. Richt, R. R. Rowland, C. S. Schmaljohn, D. J. Lenschow, E. J. Snijder, A. Garcia-Sastre, and H. W. t. Virgin. 2007. Ovarian tumor domain-containing viral proteases evade ubiquitin- and ISG15-dependent innate immune responses. *Cell Host Microbe* 2:404-416.

43. Lindner, H. A., N. Fotouhi-Ardakani, V. Lytvyn, P. Lachance, T. Sulea, and R. Menard. 2005. The papain-like protease from the severe acute respiratory syndrome coronavirus is a deubiquitinating enzyme. *J Virol* 79:15199-15208.

44. Renault, P., J. L. Solet, D. Sissoko, E. Balleydier, S. Larrieu, L. Filleul, C. Lassalle, J. Thiria, E. Rachou, H. de Valk, D. Ilef, M. Ledrans, I. Quatresous, P. Quenel, and V. Pierre. 2007. A major epidemic of chikungunya virus infection on Reunion Island, France, 2005-2006. *Am J Trop Med Hyg* 77:727-731.

45. Osiak, A., O. Utermohlen, S. Niendorf, I. Horak, and K. P. Knobeloch. 2005. ISG15, an interferon-stimulated ubiquitin-like protein, is not essential for STAT1 signaling and responses against vesicular stomatitis and lymphocytic choriomeningitis virus. *Mol Cell Biol* 25:6338-6345.

46. Mohler, K. M., D. S. Torrance, C. A. Smith, R. G. Goodwin, K. E. Stremler, V. P. Fung, H. Madani, and M. B. Widmer. 1993. Soluble tumor necrosis factor (TNF) receptors are effective therapeutic agents in lethal endotoxemia and function simultaneously as both TNF carriers and TNF antagonists. *J Immunol* 151:1548-1561.

47. Merrill, J. C., J. You, C. Constable, S. E. Leeman, and S. Amar. 2011. Whole-body deletion of LPS-induced TNF-alpha factor (LITAF) markedly improves experimental endotoxic shock and inflammatory arthritis. *Proc Natl Acad Sci U S A* 108:21247-21252.

48. Trgovcich, J., K. Ryman, P. Extrom, J. C. Eldridge, J. F. Aronson, and R. E. Johnston. 1997. Sindbis virus infection of neonatal mice results in a severe stress response. *Virology* 227:234-238.

49. Wang, H., and S. Ma. 2008. The cytokine storm and factors determining the sequence and severity of organ dysfunction in multiple organ dysfunction syndrome. *Am J Emerg Med* 26:711-715.

50. Khadaroo, R. G., and J. C. Marshall. 2002. ARDS and the multiple organ dysfunction syndrome. Common mechanisms of a common systemic process. *Crit Care Clin* 18:127-141.

51. Sun, Y., C. Jin, F. Zhan, X. Wang, M. Liang, Q. Zhang, S. Ding, X. Guan, X. Huo, C. Li, J. Qu, Q. Wang, S. Zhang, Y. Zhang, S. Wang, A. Xu, Z. Bi, and D. Li. 2012. Host cytokine storm is associated with disease severity of severe fever with thrombocytopenia syndrome. *J Infect Dis* 206:1085-1094.

52. Touret, Y., H. Randrianaivo, A. Michault, I. Schuffenecker, E. Kauffmann, Y. Lenglet, G. Barau, and A. Fourmaintraux. 2006. [Early maternal-fetal transmission of the Chikungunya virus]. *Presse Med* 35:1656-1658.

53. Sissoko, D., D. Malvy, K. Ezzedine, P. Renault, F. Moscetti, M. Ledrans, and V. Pierre. 2009. Post-epidemic Chikungunya disease on Reunion Island: course of rheumatic manifestations and associated factors over a 15-month period. *PLoS Negl Trop Dis* 3:e389.

54. Hoarau, J. J., M. C. Jaffar Bandjee, P. Krejbich Trotot, T. Das, G. Li-Pat-Yuen, B. Dassa, M. Denizot, E. Guichard, A. Ribera, T. Henni, F. Tallet, M. P. Moiton, B. A. Gauzere, S. Bruniquet, Z. Jaffar Bandjee, P. Morbidelli, G. Martigny, M. Jolivet, F. Gay, M. Grandadam, H. Tolou, V. Vieillard, P. Debre, B. Autran, and P. Gasque. 2011. Persistent chronic inflammation and infection by Chikungunya arthritogenic alphavirus in spite of a robust host immune response. *J Immunol* 184:5914-5927.

55. Chhabra, M., V. Mittal, D. Bhattacharya, U. Rana, and S. Lal. 2008. Chikungunya fever: a re-emerging viral infection. *Indian J Med Microbiol* 26:5-12.

56. Strunk, T., A. Currie, P. Richmond, K. Simmer, and D. Burgner. 2010. Innate immunity in human newborn infants: prematurity means more than immaturity. *J Matern Fetal Neonatal Med* 24:25-31.

57. De Wit, D., S. Tonon, V. Olislagers, S. Goriely, M. Boutriaux, M. Goldman, and F. Willems. 2003. Impaired responses to toll-like receptor 4 and toll-like receptor 3 ligands in human cord blood. *J Autoimmun* 21:277-281.

58. Belderbos, M. E., G. M. van Bleek, O. Levy, M. O. Blanken, M. L. Houben, L. Schuijff, J. L. Kimpen, and L. Bont. 2009. Skewed pattern of Toll-like receptor 4-mediated cytokine production in human neonatal blood: low LPS-induced IL-12p70 and high IL-10 persist throughout the first month of life. *Clin Immunol* 133:228-237.

59. Zhao, J., K. D. Kim, X. Yang, S. Auh, Y. X. Fu, and H. Tang. 2008. Hyper innate responses in neonates lead to increased morbidity and mortality after infection. *Proc Natl Acad Sci U S A* 105:7528-7533.

60. Brehin, A. C., I. Casademont, M. P. Frenkiel, C. Julier, A. Sakuntabhai, and P. Despres. 2009. The large form of human 2',5'-Oligoadenylate Synthetase (OAS3) exerts antiviral effect against Chikungunya virus. *Virology* 384:216-222.

61. Chiu, Y. H., Q. Sun, and Z. J. Chen. 2007. E1-L2 activates both ubiquitin and FAT10. *Mol Cell* 27:1014-1023.

62. Malakhova, O. A., and D. E. Zhang. 2008. ISG15 inhibits Nedd4 ubiquitin E3 activity and enhances the innate antiviral response. *J Biol Chem* 283:8783-8787.

63. Okumura, A., P. M. Pitha, and R. N. Harty. 2008. ISG15 inhibits Ebola VP40 VLP budding in an L-domain-dependent manner by blocking Nedd4 ligase activity. *Proc Natl Acad Sci U S A* 105:3974-3979.

64. Xia, Z. P., L. Sun, X. Chen, G. Pineda, X. Jiang, A. Adhikari, W. Zeng, and Z. J. Chen. 2009. Direct activation of protein kinases by unanchored polyubiquitin chains. *Nature* 461:114-119.

65. Zeng, W., L. Sun, X. Jiang, X. Chen, F. Hou, A. Adhikari, M. Xu, and Z. J. Chen. 2010. Reconstitution of the RIG-I pathway reveals a signaling role of unanchored polyubiquitin chains in innate immunity. *Cell* 141:315-330.

66. Schuffenecker, I., I. Iteman, A. Michault, S. Murri, L. Frangeul, M. C. Vaney, R. Lavenir, N. Pardigon, J. M. Reynes, F. Pettinelli, L. Biscornet, L. Diancourt, S. Michel, S. Duquerroy, G. Guigon, M. P. Frenkiel, A. C. Brehin, N. Cubito, P. Despres, F. Kunst, F. A. Rey, H. Zeller, and S. Brisse. 2006. Genome microevolution of chikungunya viruses causing the Indian Ocean outbreak. *PLoS Med* 3:e263.

67. Tsetsarkin, K., S. Higgs, C. E. McGee, X. De Lamballerie, R. N. Charrel, and D. L. Vanlandingham. 2006. Infectious clones of Chikungunya virus (La Reunion isolate) for vector competence studies. *Vector Borne Zoonotic Dis* 6:325-337.

68. Lenschow, D. J., N. V. Giannakopoulos, L. J. Gunn, C. Johnston, A. K. O'Guin, R. E. Schmidt, B. Levine, and H. W. t. Virgin. 2005. Identification of interferon-stimulated gene 15 as an antiviral molecule during Sindbis virus infection in vivo. *J Virol* 79:13974-13983.

69. Diamond, M. S., D. Edgil, T. G. Roberts, B. Lu, and E. Harris. 2000. Infection of human cells by dengue virus is modulated by different cell types and viral strains. *J Virol* 74:7814-7823.

70. Laurent, P., K. Le Roux, P. Grivard, G. Bertil, F. Naze, M. Picard, F. Staikowsky, G. Barau, I. Schuffenecker, and A. Michault. 2007. Development of a sensitive real-time reverse transcriptase PCR assay with an internal control to detect and quantify chikungunya virus. *Clin Chem* 53:1408-1414.

71. Brazeau, D. A. 2004. Combining genome-wide and targeted gene expression profiling in drug discovery: microarrays and real-time PCR. *Drug Discov Today* 9:838-845.

CHAPTER 3

Identification of Non-Covalent Binding Partners for ISG15 and Potential Functional Consequences

Abstract

During Chikungunya virus (CHIKV) infection, ISG15 appears to play an immunoregulatory role that is independent of UbE1L mediated conjugation. To understand mechanistically how free ISG15 protects mice from infection, we characterized both intra- and extracellular unconjugated ISG15 using mass spectrometry. By purifying serum ISG15 from pIC stimulated mice, we have identified phosphorylation as a possible post translational modification of extracellular ISG15. We have also identified the previously uncharacterized 30kDa serum ISG15 band as ISG15 conjugated to hemoglobin subunit beta-1. To identify non-covalent binding partners for intracellular ISG15, we pulled down cytosolic proteins from BMM using a tagged ISG15 construct. Using this technique, we were able to identify over 140 unique potential binding partners for free ISG15. To verify the ability of ISG15 to bind to our mass spec hits, we have begun preliminary interaction studies and demonstrate that ISG15 co-ips with MDA5. As a start to functional studies, we also demonstrate that free ISG15 can regulate cytokine production in response to pIC stimulation. Further characterization of both intra- and extracellular ISG15 will hopefully guide future experiments needed to determine ISG15s ability to regulate the host response to viral infection.

Introduction

Since the initial discovery of ubiquitin as a mechanism to target misfolded proteins to the proteasome (1), this field has grown to include a multifaceted role for ubiquitin in a wide array of cellular pathways. Ubiquitin's activity is not limited to K48-conjugated chains, but includes a variety of different linkages, activity for mono- and polyubiquitin, unanchored and conjugated chains (2-7). In addition to its conjugation ability, ubiquitin also mediates non-covalent interactions with proteins that contain Ubiquitin-binding domains(8, 9). We hypothesize that like ubiquitin, ISG15 plays a multi-functional role that is dependent on both covalent modifications and non-covalent interactions. How these interactions provide protection during viral infection is largely unknown.

The mechanism by which ISG15 protects against viral infection is in-part dependent on the type of invading pathogen. Based on our viral models, we have come up with two potential non-mutually exclusive hypotheses on how ISG15 protects against virus infection. During influenza B and Sindbis virus infection (10-12), ISG15 regulates viral loads, suggesting that ISG15 can be directly antiviral. To date, this antiviral activity of ISG15 appears to be conjugation dependent. During Chikungunya (13), influenza A and Sendai virus infections (Dave Morales, unpublished), ISG15 does not regulate viral loads, suggesting an alternative mechanism for ISG15. We hypothesize that ISG15 can also regulate the host response to viral infection and dysregulation of the host response in ISG15$^{-/-}$ mice can lead to lethality. The regulation of host response can either be conjugation dependent (influenza A and Sendai) or conjugation independent (Chikungunya virus).

Our Chikungunya virus model provided a unique opportunity to go after a conjugation independent mechanism for ISG15. Upon further investigation, we have also identified other

alphaviruses where the role of ISG15 appears to be UbE1L independent, including neonatal Ross River Virus and Barmah Forest Virus infections (Fig. S3.1). Based on our CHIKV model, we hypothesized that ISG15 regulates the immune response to viral infection, as we observed increased pro-inflammatory cytokine production in $ISG15^{-/-}$ despite similar viral loads as WT and $UbE1L^{-/-}$ mice (13). Free ISG15 is found both intra- and extracellularly, therefore we have two primary models by which free ISG15 could impact an immune response: (1) Extracellular free ISG15 binds to an unidentified cell surface receptor which then modulates downstream cellular signaling and/or (2) Intracellular free ISG15 binds non-covalently to intracellular molecules, which then leads to altered cell signaling pathways. The key to addressing both of these potential mechanisms is to identify the non-covalent binding partners for free ISG15.

Free ISG15 has been suggested to have cytokine like activity. Non-conjugated ISG15 can be detected in the sera of humans treated with IFNβ as well as mice infected with certain viruses (14). Recombinant ISG15 has been shown to increase NK cell proliferation and lytic activity (15). Extracellular ISG15 has also been shown to act as a neutrophil chemoattractant and can upregulate e-cadherin expression on dendritic cells (16, 17). Recently, recombinant ISG15 in concert with IL-12 stimulation has been shown to upregulate IFNγ (18). The cytokine activity of ISG15 may be biologically significant, as humans with null mutations for ISG15 display Mendelian susceptibility to mycobacterial disease (MSMD), possibly due to lack of ISG15 mediated IFNγ production (18). Although ISG15 appears to have cytokine activity, a receptor for ISG15 has not been identified.

Much less is known about the role of free ISG15 within a cell. During in vivo viral infection, both free ISG15 and ISG15 conjugates can be detected in tissue homogenates (13, 19). The over-expression of ISG15 has also been shown to disrupt Nedd4 ligase activity and inhibit

Ebola virus VLP release, although it is unclear whether or not this activity is conjugation dependent (20-22) . Recent research within the ubiquitin field has described a role for unanchored polyubiquitin chains, shown to regulate TAK1 activation as well as RIG-I and MDA5 signaling (23-25). Unanchored polyubiquitin chains generated by TRAF6 (23) or TRIM5 (26) bind to and activate the TAK1 complex, which influences downstream NF-κB signaling. Unanchored polyubiquitin chains also bind to the CARD domains of RIG-I and MDA5, which allows for oligomerization and optimal IRF3 activation (24, 25). Binding partners for free ISG15 within a cell is largely unknown.

The following describes our initial steps towards identifying mechanisms for both intra and extracellular ISG15. Through mass spectrometry, we have identified phosphorylation as a possible post-translational modification for serum ISG15. We have also identified the 30kDa ISG15 band normally found in the serum of infected mice as ISG15 bound to hemoglobin subunit beta-1. By generating recombinant tagged ISG15, we have identified over 140 potential binding partners for intracellular ISG15 via mass spectrometry. Preliminary experiments have been used to verify ISG15s ability to interact with the proteins identified from our mass spec analysis and we demonstrate that ISG15 can co-immunoprecipitate with MDA5. Finally, we demonstrate that free ISG15 can regulate cytokine production in response to pIC stimulation. Our mass spec analysis of both extra- and intracellular ISG15 will aid future studies in identifying a mechanism of action for free ISG15.

Results

Serum ISG15 may be phosphorylated and the 30kDa ISG15 band is ISG15 conjugated to hemoglobin subunit β-1.

Although ISG15 has been suggested to have cytokine like activity (15-17), a receptor for ISG15 has not been identified. To complement ongoing studies for the ISG15 receptor, we decided to characterize the natural secreted form of ISG15 to identify any post translational modifications that may or may not be required for its binding/activity. In addition, we also hoped to identify the previously unknown 30kDa ISG15 conjugate that is found in the serum of virally infected WT mice (13).

To identify post translational modifications as well as the 30kDa ISG15 conjugate, we purified serum ISG15 and sent isolated bands to the Yale MS & Proteomics facility. Adult WT and ISG15$^{-/-}$ mice were injected with 50ug pIC ip, which is sufficient to induce serum ISG15 expression (data not shown). Serum was harvested on day 2 post treatment and ISG15 was immunoprecipitated. Pulldown of ISG15 was confirmed by western blot analysis and bound proteins were identified by SyproRuby stain (Fig. 3.1). Comparison of WT and ISG15$^{-/-}$ serum allowed for identification of unique bands found only in WT serum, which were excised and sent for mass spec analysis.

Gel bands were digested with trypsin and then analyzed via LC-MS/MS. Phosphopeptides were enriched by passage over a titanium dioxide (TiO2) column. Results were analyzed using the Swissprotein database and the confidence level was set to 95%. Two lower molecular weight bands around 15kDa described as ISG15 lo and ISG15 hi were identified as hemoglobin (alpha (15.1kDa) and beta-1 (15.8kDa) subunits) and ISG15, respectively. Two

phosphorylated peptides were identified from the ISG15 band: a threonine at position 24 (N-terminal domain) and a tyrosine at position 139 (C-terminal domain) (Fig. 3.2 A and B) No other modifications were found, with searches for methylation, acetylation, ubiquitination and sumolyation. Phosphorylation of ISG15, either intra- or extracellular, has not been described and will need to be verified.

Four higher molecular weight bands (between 30-40kDa) were sent for basic protein identification, two from WT serum (W1 and W2) and the corresponding negative control bands from ISG15$^{-/-}$ serum (S1 and S2).The 30kDa ISG15 conjugate (W2) was identified as ISG15 (MW=17.8kDa, 42% coverage) and hemoglobin subunit beta-1 (MW=15.8kDa, 59% coverage). Neither of these proteins were identified in the corresponding ISG15$^{-/-}$ band S2. Numerous unique proteins were identified for the W1 band, which based on our western blot analysis did not appear to be an ISG15 conjugate. Based on the function of the identified proteins, we hypothesized that the most likely candidate is the hemoglobin binding protein haptoglobin (MW=38.7kDa, 5.5% coverage).

In an attempt to confirm that the ISG15 30kDa band is ISG15 conjugated to hemoglobin subunit beta-1, we ran a western on CHIKV infected serum samples as well as our serum ISG15 pulldown and stained with an anti-hemoglobin antibody (Fig. 3.3). From our ISG15 pulldown, we were able to detect the 30kDa band with the hemoglobin antibody. No 30kDa band was detected in CHIKV infected serum, although we observed robust staining for free hemoglobin. We hypothesize that only a small fraction of serum hemoglobin is modified, resulting in our inability to detect the 30kDa band with the hemoglobin antibody in straight serum. A functional role for the 30kDa serum ISG15 conjugate has not been described.

Identification of Intracellular Binding Partners for Free ISG15 using Mass Spectrometry.

We hypothesized that free intracellular ISG15 could have activity within a cell, independent of its ability to conjugate to target proteins, by binding non-covalently to other intracellular proteins. Therefore, we generated recombinant ISG15 for immunoprecipitation studies to identify potential binding partners by mass spectrometry.

ISG15 was cloned into a pfuse-hIgG1e3 Fc2 expression vector that includes a secretion signal and a C-terminal mutant human Fc tag that is unable to bind to FcR. DIII (from WNV) was also cloned to act as a negative control. Recombinant protein expression was confirmed by western blot analysis (Fig. 3.4A). BMM, which produce many of the cytokines that were elevated in our CHIKV model, were chosen as the target cell. Cytosol from IFNβ and pIC stimulated ISG15$^{-/-}$ BMM was mixed with the recombinant protein and ISG15-Fc was immunoprecipitated. Unique bands were identified by comparing ISG15-Fc and DIII-Fc pulldowns and excised for basic protein identification by mass spec (Danforth facility) (Fig. 3.4B). Similar to our serum ISG15 pulldown, gel bands were trypsinized and analyzed using LC-MS/MS. Data was searched against the NCBInr database.

Over 140 proteins were identified by mass spec analysis (after subtracting available negative control hits) (Table 3.1). Proteins identified represent a variety of cellular pathways, including innate immunity, vesicle sorting, cytoskeletal, ribosomal components and heat shock proteins. Priority for studying potential hits was given by the following criteria: (1) interest (i.e. innate immunity), (2) proteins that were also identified in Nadia's Y2H screen (PCBP1 and Clathrin, unpublished), (3) protein size matched the isolated protein band and (4) protein is not found in the negative control band. Based on these criteria, the following proteins were identified for initial follow up studies: MDA5, p62 (sequestosome-1), p40phox (NCF4), STAT1/2, and

poly(C) binding protein 1 (PCBP1). Additional proteins found in Table 3.1 may share equal potential for (1) binding to ISG15 and (2) important biological activity.

Human ISG15 co-precipitates with human MDA5

One of the proteins identified in our mass spec analysis was MDA5, a known intracellular viral RNA sensor. MDA5, in combination with other viral sensors, has been shown to play a role during CHIKV infection (27). Unanchored polyubiquitin chains have also been shown to regulate MDA5 function (25). Therefore, we thought that MDA5 was a good candidate for an ISG15 binding partner.

To confirm MDA5 as a binding partner for free ISG15, we over-expressed flag tagged human MDA5 with either vector alone or with human or mouse ISG15 (without the conjugation system) by transfecting 293T cells. Flag-MDA5 was immunoprecipitated and western blot analysis was used to verify the pulldown (αFlag) and check for the presence of free ISG15 (αISG15). Human ISG15 can be pulled down by anti-Flag human MDA5 immunoprecipitation (Lane 2- Fig. 3.5). Interestingly, mouse ISG15 did not co-ip with human MDA5 (Lane 3), which may suggest a species specific interaction. We also attempted pulldowns with two truncated forms of human MDA5 that were obtained from Michael Gale's lab: MDA5 1-294 (CARD domains) and MDA5 295-1025 (RNA helicase domain) (Lanes 4-7)(28). Human ISG15 could be pulled down by both of these constructs (Lanes 5 & 7), although there appeared to be more ISG15 with MDA5 1-294. We also attempted to pulldown ISG15 with Flag human RIG-I, which was not identified in our mass spec analysis. We saw only a weak band for human ISG15, suggesting weak or no binding, and no bands for mouse ISG15 (Lanes 8-9). Therefore, human ISG15 co-precipitates with human MDA5 but not RIG-I. Preliminary data also suggests that

ISG15 may co-ip with additional binding partners identified via mass spec, including STAT1, p62 and p40phox (NCF4).

ISG15$^{-/-}$ mice and cells have increased IL-6 production in response to pIC stimulation.

If we are able to confirm MDA5 as a binding partner for free ISG15, it will be important to determine if there is a functional consequence for this interaction. The best approach will be to stimulate MDA5 in the presence or absence of ISG15. MDA5 has been shown to be responsible for cytokine production (IFNα, TNFα, MCP-1, IL-6) in response to naked pIC and complexed pIC (transfection) (29). Cytokine production following pIC stimulation is primarily MDA5 dependent, althoughTLR3 can also produce these cytokines in response to pIC (29). We hypothesized that ISG15 regulates cytokine production downstream of MDA5 signaling. Therefore, we investigated the ability of ISG15 to regulate cytokine production in response to pIC.

In order to address whether ISG15 could directly affect cytokine production, we developed an in vitro model to examine ISG15s impact on pIC stimulation. Primary cells (BMM, BMDC, and muscle fibroblasts) were generated from WT, UbE1L$^{-/-}$ and ISG15$^{-/-}$ mice. Cells were pretreated with IFNβ to induce ISG15 (data not shown). 24hrs post IFNβ treatment, cells were then stimulated with pIC (10ug/mL). Cell supernatants were harvested at 4,12 and 24hrs post pIC stimulation. Cytokine production (TNFα, IL-1β, IL-6, IL-10, and various chemokines) were assessed by bioplex.

Production of IL-6 following pIC stimulation appeared to replicate our in vivo CHIKV results: WT and UBE1L$^{-/-}$ cells produce similar levels of IL-6, whereas ISG15$^{-/-}$ cells have increased IL-6 production (at best 2-fold) at 12 and 24hrs post stimulation. This phenotype was

found for BMM (Fig. 3.6A) and primary muscle fibroblasts (Fig. 3.6B). Preliminary data suggests that this same trend was also observed in BMDC, although IL-6 production was much lower than BMM and muscle cells (data not shown). Therefore, under these conditions, free ISG15 appears to act as a negative regulator of IL-6 production following pIC stimulation.

To complement our in vitro findings, we also developed an in vivo model for pIC stimulation. Nine day old WT, UbE1L$^{-/-}$, and ISG15$^{-/-}$ mice were injected with pIC (10ug) s.c. and serum was harvested at 6 and 24hrs post treatment. ISG15 could be found in the serum of pIC stimulated WT and UbE1L$^{-/-}$ mice at both 6 and 24hrs post stimulation (data not shown). Similar to our in vitro findings, ISG15$^{-/-}$ mice display elevated levels of IL-6 production at 6hrs post treatment compared to WT and UbE1L$^{-/-}$ mice (Fig. 3.6C). This data suggests that free ISG15 regulates IL-6 production following pIC stimulation.

Similar to IL-6, production of IL-10 following pIC stimulation in BMM appeared to replicate our in vivo CHIKV phenotype (Table 3.2). ISG15$^{-/-}$ BMM pretreated with pIC produced more IL-10 (at best 2-fold) than WT and UbE1L$^{-/-}$ BMM 12 and 24hrs post stimulation. As IL-6 is a known regulator of IL-10 (30), it is unclear as to whether this phenotype is due to ISG15s ability to directly regulate the IL-10 pathway or simply due to increased levels of IL-6. BMDCs and primary muscle fibroblasts did not produce IL-10 in response to pIC stimulation, suggesting that unlike IL-6, this phenotype is cell type dependent.

The other analytes that we evaluated did not show the same trend as IL-6 and IL-10 production (Table 3.2). WT BMM display increased TNFα production compared to UbE1L$^{-/-}$ and ISG15$^{-/-}$ BMM 4hrs after pIC stimulation. In addition, IL-1β production was not detected and no difference was observed for chemokine levels (MIP-1α, MCP-1 and GM-CSF). In addition, ISG15 mediated regulation appears to be cell type dependent, as different cells produced

different cytokine patterns in response to pIC stimulation. Interestingly, changing the type of TLR stimulation, including LPS (TLR4) or Imiquimod+ATP (inflammasome activation) also produced a different pattern of ISG15 mediated cytokine regulation (Figure S3.2 and Table 3.2). Preliminary data suggests that IL-6 production following LPS stimulation in vitro (Fig. S3.2A) or in vivo (Fig. S3.2B) is positively regulated by ISG15 conjugation. Following inflammasome activation, production of IL-1β appears to be negatively regulated by ISG15 conjugation (Table 3.2)Therefore, free ISG15 does not act as a master regulator for cytokine production and regulation may be dependent on select cytokine signaling pathways, the type of cell as well as the type of stimulation.

Discussion

Free extracellular ISG15 has been described to have cytokine activity, although how ISG15 mediates this activity is unknown (15-17). Even less has been reported for the activity of free intracellular ISG15 (20-22). However, our CHIKV model, as well as recent reports that confirm earlier cytokine studies (18), suggest that free ISG15 has an important role in the immune response to both viral and bacterial pathogens. To setup future mechanistic studies, we have characterized both free forms of ISG15, intra- and extracellular, using mass spectrometry. Our results show that serum ISG15 may be modified by phosphorylation, which may or may not be necessary for ISG15 function. In addition, we identify the 30kDa ISG15 conjugate commonly found in virally infected WT mice as ISG15 conjugated to hemoglobin subunit beta-1. For intracellular ISG15, we have identified 146 potential binding partners that are involved in multiple cellular pathways. Preliminary co-ip data confirms that at least some of these hits may be valid, as ISG15 can co-ip with MDA5. We also demonstrate that ISG15 can regulate cytokine production in response to pIC stimulation, although it is unclear if this is dependent on ISG15s interaction with MDA5.

Recombinant ISG15 has been shown to regulate innate immune cell responses, affecting the activity of monocytes, neutrophils and NK cells. To fully understand how extracellular ISG15 mediates its activity, a receptor for serum ISG15 must be identified. As a requisite step in identifying an ISG15 receptor, we have identified phosphorylation as a potential post-translational modification of 15kDa serum ISG15 (Fig. 3.1 and 3.2). Interestingly, we identified two phosphopeptides for ISG15, each corresponding to one of the two ubiquitin domains of ISG15: Thr^{24} N-terminus and Y^{139} C-terminus. Mutagenesis of these two sites will help confirm whether ISG15 is phosphorylated and may aid in future functional studies. The consequences of

ISG15 phosphorylation are unknown. It is unclear if phosphorylation affects the secretion or activity of ISG15, if intracellular ISG15 is also modified, and what percentage of total ISG15 gets modified. Generation of recombinant ISG15 in the literature was not described as being phosphorylated and yet activity was still reported, so it is unclear if phosphorylation will affect the activity of secreted ISG15.

We have also identified the 30kDa serum ISG15 conjugate as ISG15 bound to hemoglobin subunit beta-1 (Fig. 3.1 and 3.3). To our knowledge, the role of the 30kDa conjugate has not been investigated and its function is unknown. Its role outside of the cell may have an important biological function or it may be a byproduct of red blood cell lysis. Intracellular ISGylated hemoglobin may also have an important function that remains to be investigated. Although hemoglobin expression is predominantly found in red blood cells, it can also be expressed in additional cell types, including alveolar cell lines, activated macrophages from adult mice and embryonic neurons (31-33). We hypothesize that identification of hemoglobin as the ISG15 lo band may result from degradation of the 30kDa ISG15 band or may result from non-covalent association with the ISG15 or hemoglobin portion of the 30kDa band. Indeed, it is known that hemoglobin beta and alpha subunits form a tetramer complex. We suspect that the unique higher molecular weight band W1 is likely haptoglobin. Haptoglobin, which binds to and sequesters serum hemoglobin, may be coming down in our ISG15 ip due to its interaction with the hemoglobin subunit beta (34). However, this also remains to be verified. Identification of the ISGylated hemoglobin subunit beta-1 residue (via mass spec (diglycine shift) or Lysine mutagenesis) may aid in the discovery of a functional role for the 30kDa ISG15 conjugate.

Most importantly, we have shown that free ISG15 has the capacity to bind to many different intracellular proteins, independent of its conjugation activity (Fig. 3.4). Most of these

potential binding targets remain to be verified and may be either direct or indirect ISG15 binding partners. We recognize that ISG15 may be binding to only a select few of these potential targets and a large number of hits that we have generated may result from the formation of protein complexes that are not dependent on direct ISG15 binding. Nonetheless, these mass spectrometry hits will allow us to focus on different cellular pathways that free ISG15 may be involved in, including innate immune signaling and vesicle sorting pathways. Our mass spec hits are specific for IFNβ/pIC stimulated BMM, therefore may not represent additional binding partners in different cells or in response to other forms of stimulation (TLR4, inflammasome, etc).

The results that we have generated from our non-covalent pulldown have directed our attention to cellular pathways that ISG15 may be involved in. We note that ISG15 associates with several ribosomal components and proteins associated with protein translation. We hypothesize that this association may be linked to the conjugation activity of Herc5, the main E3 ligase for ISG15 that also associates with ribosomal subunits (35). Several proteins involved in vesicular transport were also identified, including the retrograde transport proteins SNX1 and SNX2. As ISG15 lacks a signal peptide necessary for classical protein secretion, we hypothesize that ISG15s ability to interact with vesicular proteins may lead to discovery of the secretion mechanism for ISG15. Alternatively, ISG15s ability to interact with the vesicular transport pathway may be a way to regulate cell responsiveness by retrograde transport of cell surface receptors (36) or may reflect previously reported data where ISG15 impacts VLP release via the ESCRT pathway (22). Perhaps unexpectedly, we also identified several proteasome regulatory subunits, as a role for ISG15 in proteasome mediated degradation has not been described. Lastly, as ISG15 plays a vital role during viral infection, we hypothesize that the proteins that we have identified as innate immune proteins may represent important binding interactions for ISG15.

Indeed, we have identified the PRRs MDA5, LGP2, and DAI as well as additional proteins known to play a role in cytokine production, such as FLN29 and BCAP1 (37, 38). In Chapter 4, we briefly discuss the importance of some of the proteins that we have identified for use in future functional studies.

In an attempt to verify targets of our intracellular ISG15 analysis, we demonstrate that ISG15 co-ips with MDA5 (Fig. 3.5). The ability of ISG15 to directly bind MDA5 has not been demonstrated and will require further study. MDA5 is an exciting potential target for ISG15 as it is a known sensor for CHIKV, plays a role in cytokine production, and is also known to be regulated by unanchored ubiquitin chains (25, 27, 39). Unanchored polyubiquitin chains bind to the Card domains of both MDA5 and RIG-I, which allows for oligomerization and full activation of downstream signaling (25). One hypothesis that could explain our observations is that free ISG15 disrupts the binding of unanchored ubiquitin chains to MDA5, resulting in down-regulation of this signaling pathway. Therefore, when ISG15 is absent, the MDA5 signaling pathway will remain active, resulting in increased cytokine production observed in $ISG15^{-/-}$. Interestingly, RIG-I was not identified in our mass spec analysis and ISG15 did not co-ip with RIG-I in our overexpression studies, suggesting that ISG15s ability to co-ip with MDA5 may result from a specific interaction.

In an attempt to show that there is a functional consequence for ISG15s interaction with MDA5, we also stimulated cells and mice with the MDA5/TLR3 agonist pIC (29). We were encouraged to find that IL-6 production following pIC stimulation in vitro and in vivo gave similar results to our CHIKV model (Fig. 3.6). Preliminary data generated by infecting primary muscle fibroblasts with CHIKV suggested that IL-6 production did mirror our in vivo findings, although the levels of IL-6 produced were significantly lower than following pIC stimulation

(data not shown). We hypothesize that this may be due to CHIKVs ability to interfere with transcription and translation (40). Although we were able to demonstrate a role for ISG15 in cytokine production, we were unable to generate an in vitro model that completely replicates our in vivo CHIKV phenotype. This may be due to our inability to generate the complex cellular and tissue interactions found in vivo or due to using pIC stimulation instead of CHIKV infection.

We hypothesize that ISG15 may regulate MDA5 mediated signaling, however, we cannot rule out a contribution of TLR3 in our pIC stimulation studies. We also cannot explain why only some and not all cytokines appear to be regulated by free ISG15. If our hypothesis that ISG15 can directly regulate PRR signaling was correct, we would hypothesize that more cytokines would be dependent on free ISG15 (which we observe from our in vivo model but not in vitro). An alternative hypothesis may be that ISG15 regulates PRR cytokine production farther downstream of the initial PRR signaling pathway, which could allow for individual cytokine regulation.

In summary, we have begun preliminary functional studies to identify a mechanism of action for free ISG15. We have characterized the natural secreted forms of ISG15, identifying phosphorylation as a potential post translational modification and identifying the 30kDa conjugate as ISG15 bound to hemoglobin subunit beta-1. We have also identified many different potential binding partners for free intracellular ISG15 and have verified ISG15s ability to co-ip with MDA5. We demonstrate that ISG15 regulates cytokine production following PRR activation and show that ISG15$^{-/-}$ have elevated IL-6 levels following pIC stimulation. Free ISG15s ability to form non-covalent interactions with other proteins represents an exciting opportunity to identify a conjugation independent mechanism for ISG15.

Materials and Methods

Mice

Mouse studies were performed at Washington University in St. Louis in accordance with the recommendations in the Guide for the Care and Use of Laboratory Animals of the National Institutes of Health and following the International Guiding Principles for Biomedical Research Involving Animals. The protocols were approved by the Animal Studies Committee at Washington University (#20090287). The generation of both the ISG15$^{-/-}$ and UbE1L$^{-/-}$ mice has been previously described (41, 42). Congenic SNP analysis (Taconic laboratories) of UbE1L$^{-/-}$ and ISG15$^{-/-}$ mice confirmed that these mice were fully backcrossed, with 99.93% and 99.72% identity to C57BL/6 mice, respectively. For serum ISG15, adult 6-8week old WT and ISG15$^{-/-}$ mice were injected with 50ug pIC i.p. and serum was harvested 48hrs post-treatment. For in vivo pIC stimulation, 9 day old WT, UbE1L$^{-/-}$ and ISG15$^{-/-}$ pups were injected with 10ug pIC s.c.

Purification of Serum ISG15

Serum from pIC treated WT and ISG15$^{-/-}$ adult mice was incubated with monoclonal 3C2 anti ISG15 coupled beads, washed with PBS and eluted using a glycine buffer (0.1M, pH 2.5). Pulldown of ISG15 was confirmed using western blot analysis by running proteins on a 12% Tris gel, transferring to a polyvinylidene fluoride membrane, and blotting with a rabbit anti-ISG15 polyclonal serum (1:5000) as previously described (19). Bound proteins were run on a precast 12% Tris gel and identified using SyproRuby stain. Unique bands were excised and sent for identification of post-translational modifications and basic protein identification by mass spectrometry.

Generation of tagged ISG15 for Non-covalent pulldowns

Mouse ISG15 and the WNV domain DIII were cloned into the expression vector pfuse-hIgG1e3 Fc2 (invivogen), which includes a signal peptide for secretion and a C-terminal Fc tag. Generation of Fc tagged constructs was confirmed by transfecting 293T cells using Lipofectamine and harvesting supernatant and cell lysate 48hrs post transfection. Proteins were run on a 12% Tris gel and transferred to a polyvinylidene fluoride membrane for western blot analysis. Anti-human Fc (Goat anti-human Fc-HRP: Jackson Immunoresearch 109-035-098) was used for detection. The membrane was incubated in 5-10% milk 1:15000 antibody dilution for 1-2hrs,washed 4x with PBS-Tween and resolved with Chemiluminescent HRP substrate (Millipore Immobilon Western: WBKLS0500).

Mass production of Fc-tagged proteins was performed by transfecting 293 suspension cells (293F cells) provided by Dr. Daved Fremont. Cells were grown in serum free media (Gibco FreeStyle 293 media; cat no: 12338-018) at 37C, 8% CO2 in a ThermoScientific 500mL flask (4115-0500 PETG flask with vented closure). Cells were seeded at $0.5x10^6$ cells/mL in 100mL the day before transfection of the Fc constructs using PEI (1ug DNA/mL). Supernatant was harvested every three days. Fc constructs were purified from supernatant using Protein A beads and dialyzed against PBS using Slide-A-Lyzer Dialysis Cassettes (ThermoScientific). Purification was confirmed using western blot analysis described above and SyproRuby staining.

For identification of binding partners, purified Fc constructs was mixed with cytosol from bone marrow macrophages (BMM). Generation of BMM is previously described. $ISG15^{-/-}$ BMM were lysed with digitonin buffer and the cytosol enriched fraction was incubated with the Fc constructs overnight. Fc proteins along with binding partners were purified using Protein A

beads. Bound proteins were run on a precast 12% Tris gel and identified using SyproRuby stain. Unique bands were excised and sent for protein identification by mass spectrometry.

Mass Spectrometry

Unique bands for the serum ISG15 pulldown were sent to the MS & Proteomics WM Keck Foundation Biotechnology Resource Laboratory at Yale University. Analysis was led by Dr. Kathryn Stone and Jean Kanyo. Gel bands were digested with trypsin and then peptides were separated on a Waters nanoACQUITY (75 μm x 250 mm eluted at 300nl/min.) with MS analysis on a LTQ Orbitrap mass spectrometer. ISG15 lo and hi gel bands were also passed over a titanium dioxide column to enrich for phosphopeptides. The LC-MS/MS results were searched using the SwissProt database. Mascot distiller and the Mascot search algorithm were used for database searches. Unique bands for the Fc-ISG15 pulldown were sent to the Donald Danforth Plant Science Center Proteomics and Mass Spectrometry Facility in St. Louis with analysis by Dr. Sophie Alvarez. As described above, gel bands were digested with trypsin for LC-MS/MS analysis. Confidence level for all hits was set at 95%.

Co-immunoprecipitations

293T cells were transfected (Lipofectamine) with human or mouse ISG15 alone or in combination with Flag tagged target constructs. Human MDA5 and RIG-I constructs were obtained from Dr. Michael Gale's lab and are previously described (28). 24hrs post transfection, cells were lysed with digitonin and cell lysate was incubated with anti-Flag beads. Pulldown of Flag and/or ISG15 constructs was confirmed via western blot analysis, as described above. Anti-Flag and rabbit anti-ISG15 polyclonal sera was used for protein detection.

TLR Stimulation and Cytokine Analysis

For in vitro stimulation, primary bone marrow derived macrophages, bone marrow derived dendritic cells and primary muscle fibroblasts were generated. Cells were pretreated with 10U/mL IFNβ. 24hrs post IFN treatment, cells were stimulated with pIC (10ug/mL), LPS (10ng/mL) or imiquimod pulsed with ATP (43). Cell supernatants were harvested at 4, 12, and 24hrs post treatment. For in vivo stimulation, 9 day old mice were treated with pIC (10ug) s.c. and serum was harvested 6 and 24hrs post stimulation. Cytokines were measured using Luminex technology with a customized 6plex from Biorad.

Figure 3.1. Mass spectrometry analysis of serum ISG15 indicates that free ISG15 (ISG15 Hi) may be phosphorylated and the 30kDa band (W2) is ISG15 conjugated to hemoglobin subunit beta-1. WT and ISG15$^{-/-}$ adult mice were injected with 50ug pIC i.p. and serum was harvested on day 2 post treatment. Serum ISG15 was pulled down with aISG15 coupled beads (mouse monoclonal). **(A)** Western blot was used to confirm pulldown of ISG15 (rabbit polyclonal). **(B)** ISG15 and associated bands were identified by Syproruby stain. Bands sent off for mass spec (Yale) are highlighted in red.

Figure 3.1

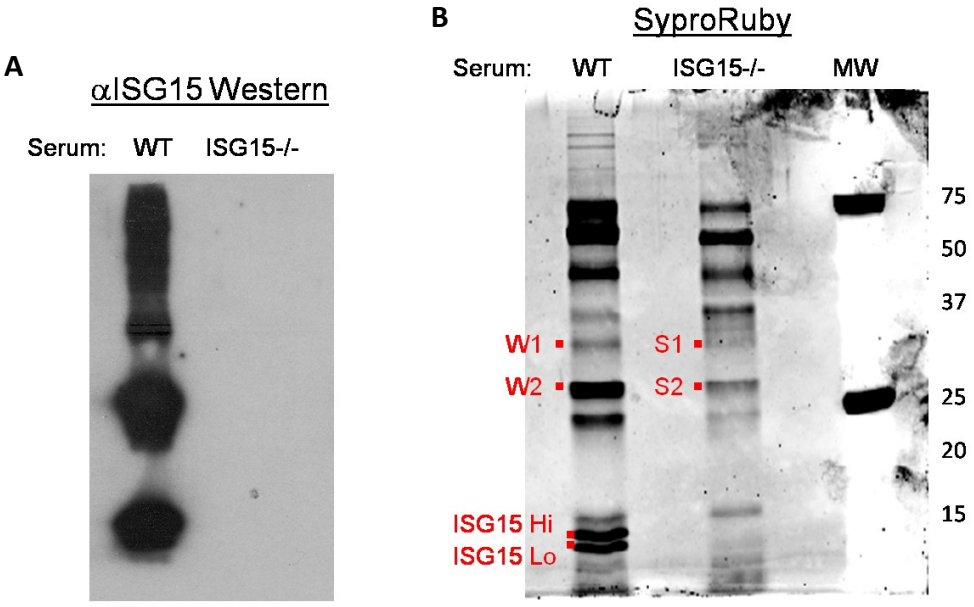
A
αISG15 Western
Serum: WT ISG15-/-
B
SyproRuby
Serum: WT ISG15-/- MW
75
50
37
25
20
15
W1
W2
S1
S2
ISG15 Hi
ISG15 Lo

Figure 3.2. Thr^{24} and Tyr^{139} were identified as potential phosphorylation sites for serum ISG15. WT and $ISG15^{-/-}$ adult mice were injected with 50ug pIC i.p. and serum was harvested on day 2 post treatment. Serum ISG15 was pulled down with aISG15 coupled beads (mouse monoclonal). Purified protein was digested with trypsin and phosphopeptides were enriched using a TiO2 column for mass spec analysis at the Yale MS & Proteomics facility. Phosphorylated residues (red) from their respective peptides (black) are represented in the context of the mouse ISG15 amino acid sequence (processed)(grey).

Figure 3.2

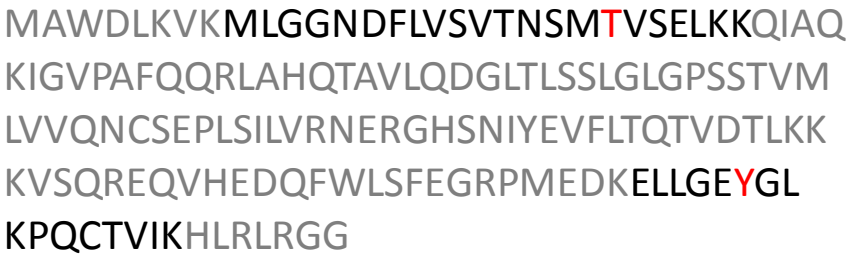
MAWDLKVKMLGGNDFLVSVTNSMTVSELKKQIAQ
KIGVPAFQQRLAHQTAVLQDGLTLSSLGLGPSSTVM
LVVQNCSEPLSILVRNERGHSNIYEVFLTQTVDTLKK
KVSQREQVHEDQFWLSFEGRPMEDKELLGEYGL
KPQCTVIKHLRLRGG

Figure 3.3. The 30kDa ISG15 band appears to be ISG15 conjugated to hemoglobin subunit beta-1 (preliminary data). (A) Serum ISG15 from pIC stimulated adult mice was pulled down with aISG15 coupled beads and blotted for aISG15 and αHemoglobin β (αHgbβ) **(B)** Nine day old WT, UbE1L$^{-/-}$ and ISG15$^{-/-}$ neonates were infected with CHIKV (10^5pfu s.c.). Serum was harvested on day 2 post infection and blotted for aISG15 and αHgbβ.

Figure 3.3

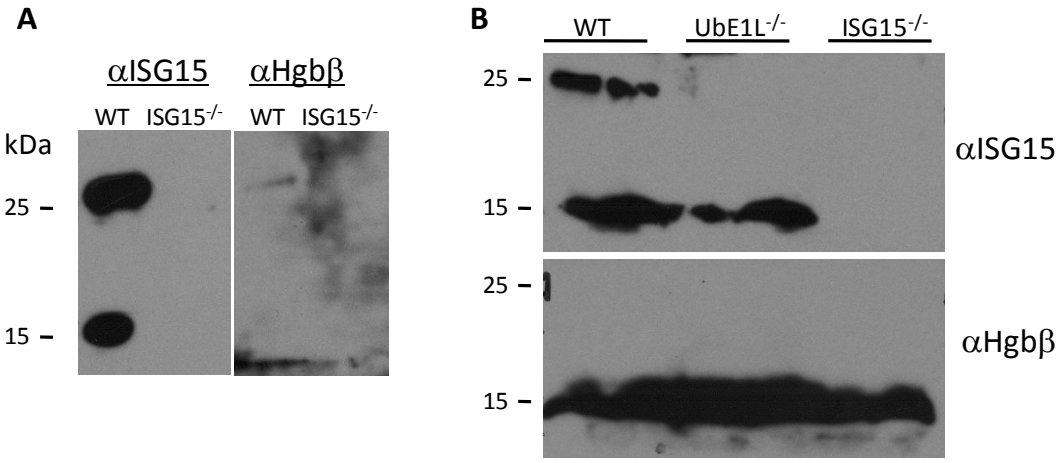
A
αISG15
αHgbβ
WT ISG15-/-
WT ISG15-/-
kDa
25
15
B
WT
UbE1L-/-
ISG15-/-
25
15
αISG15
25
15
αHgbβ

Figure 3.4. Generation of recombinant ISG15-Fc and identification of non-covalent binding partners. ISG15 and DIII (WNV) were cloned into an expression vector that includes a secretion signal and a C-terminal mutated human Fc tag that is unable to bind to FcR. 293S cells were transfected and Fc tagged proteins were purified from supernatant with Protein A beads. Bound Fc proteins were eluted with glycine, collected in Tris and dialyzed in PBS. **(A)** Anti-Fc western blot was used to confirm the presence of both proteins after the purification process. The lower MW band in the ISG15-Fc fraction appears to be a cleaved Fc contaminant. **(B)** Purified proteins were then mixed with cytosol from IFNβ/pIC stimulated ISG15$^{-/-}$ BMM. ISG15-Fc was pulled down with Protein A beads along with bound proteins. Unique bands were sent for mass spec protein id (Danforth). Excised bands are indicated on the right insert (ISG15-Fc bands in blue, control bands in green).

Figure 3.4

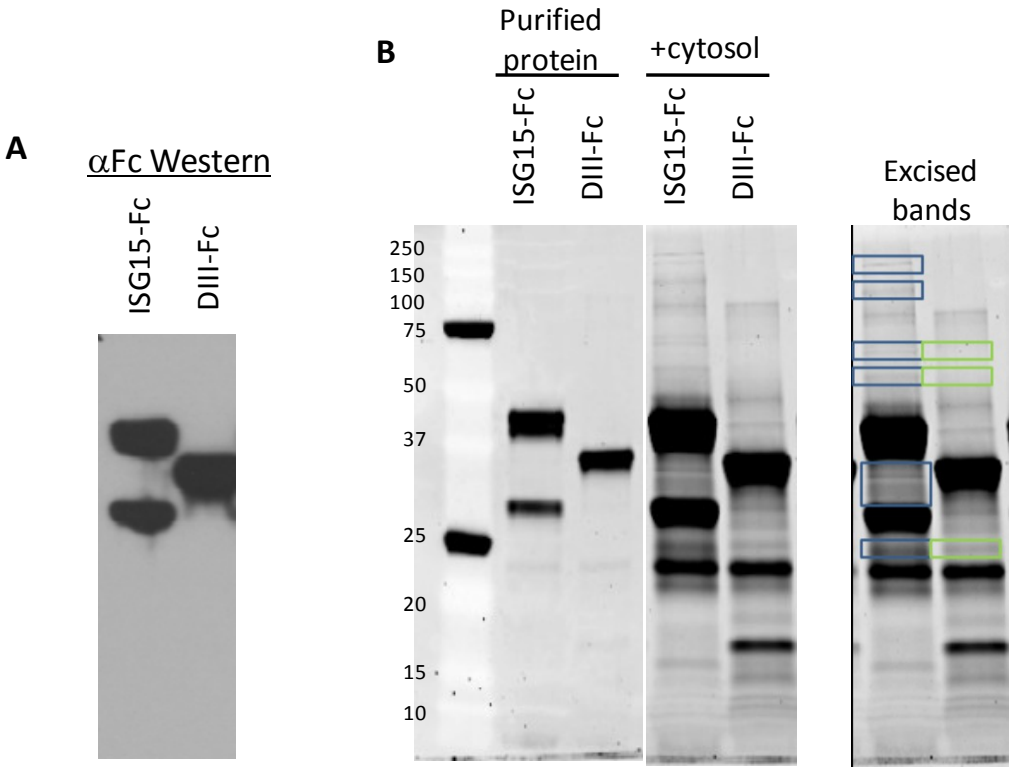
A
αFc Western
ISG15-Fc
DIII-Fc
B
Purified protein
+cytosol
ISG15-Fc
DIII-Fc
ISG15-Fc
DIII-Fc
Excised bands
250
150
100
75
50
37
25
20
15
10

Figure 3.5. Human ISG15 interacts with human MDA5 by co-ip. Flag tagged hMDA5 (or hRIG-I) was coexpressed with untagged hISG15 (1:1 ratio) in 293T cells. Cells were lysed with Digitonin and Flag proteins were immunoprecipitated. Western blot was used to confirm protein expression in bound **(A)** and unbound **(B)** fractions.

Figure 3.5

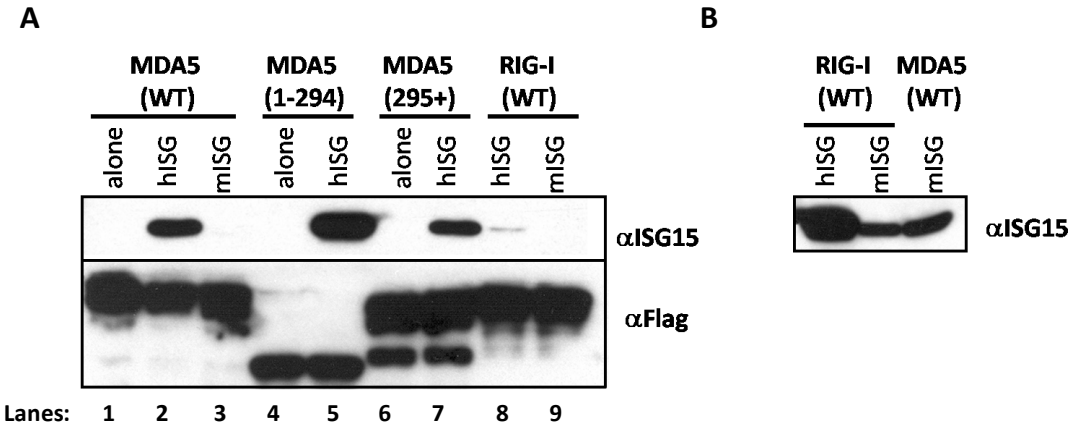
A
MDA5 (WT)
MDA5 (1-294)
MDA5 (295+)
RIG-I (WT)
alone
hISG
mISG
alone
hISG
alone
hISG
hISG
mISG
αISG15
αFlag
Lanes: 1 2 3 4 5 6 7 8 9
B
RIG-I (WT)
MDA5 (WT)
hISG
mISG
mISG
αISG15

Figure 3.6. ISG15$^{-/-}$ cells and mice produce more IL-6 than both WT and UbE1L$^{-/-}$ following pIC stimulation. Bone marrow macrophages (BMM) **(A)** and primary muscle fibroblasts **(B)** were pretreated with IFNb for 24hrs and then stimulated with pIC (10ug/mL). **(C)** WT, UbE1L$^{-/-}$ and ISG15$^{-/-}$ mice were injected with 10ug pIC s.c. (A-C) Supernatant and serum was harvested at the indicated timepoints and IL-6 levels were measured by bioplex.

Figure 3.6

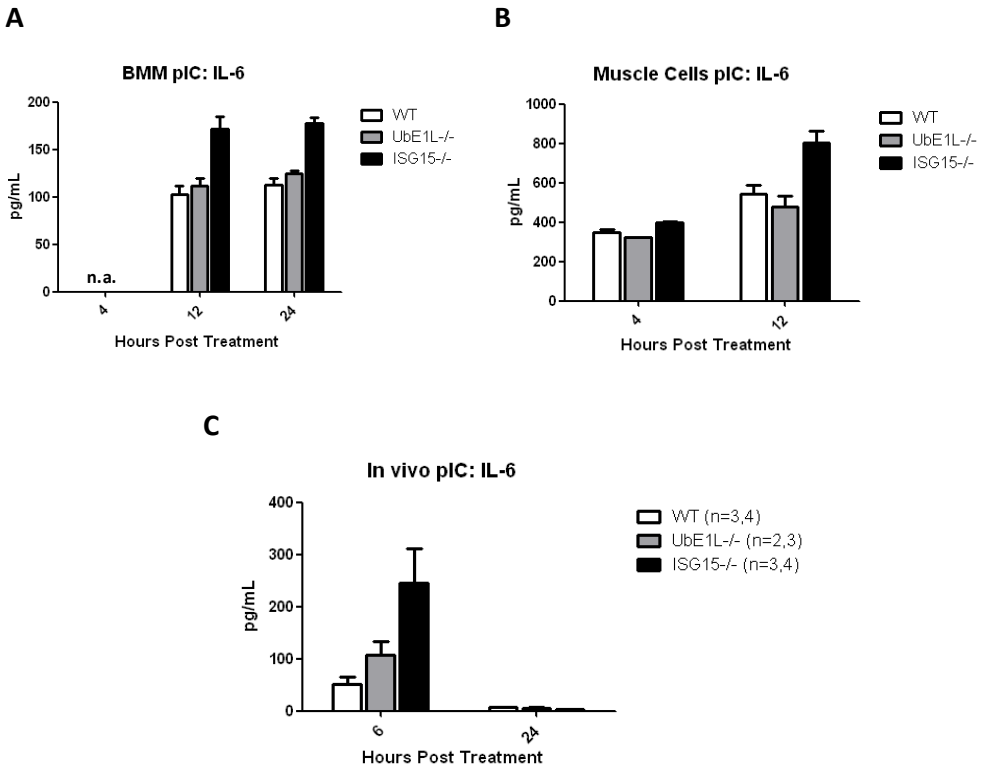
A
BMM pIC: IL-6
pg/mL
200
150
100
50
0
n.a.
4
12
24
Hours Post Treatment
WT
UbE1L-/-
ISG15-/-
B
Muscle Cells pIC: IL-6
pg/mL
1000
800
600
400
200
0
4
12
Hours Post Treatment
WT
UbE1L-/-
ISG15-/-
C
In vivo pIC: IL-6
pg/mL
400
300
200
100
0
6
24
Hours Post Treatment
WT (n=3,4)
UbE1L-/- (n=2,3)
ISG15-/- (n=3,4)

Figure S3.1. ISG15, independent of UbE1L, plays a critical role during the neonatal response to certain alphavirus infections. WT, UbE1L$^{-/-}$ and ISG15$^{-/-}$ mice were infected with **(A)** 10^3pfu RRV s.c. at 14 days of age, **(B)** 10^5pfu VEEV TC-83 s.c. at 9 days of age, **(C)** 10^6pfu Barmah Forest Virus s.c. at 9 days of age, **(D)** 10^5pfu Bebaru s.c. at 9 days of age. Mice were monitored for lethality for 21 days with data displayed as Kaplan-Meier curves. Similar survival for Bebaru was observed at 100pfu. No lethality was observed in adult ISG15$^{-/-}$ mice infected with TC-83 (10^4pfu i.c.) or Bebaru (10^6pfu s.c.).

Figure S3.1

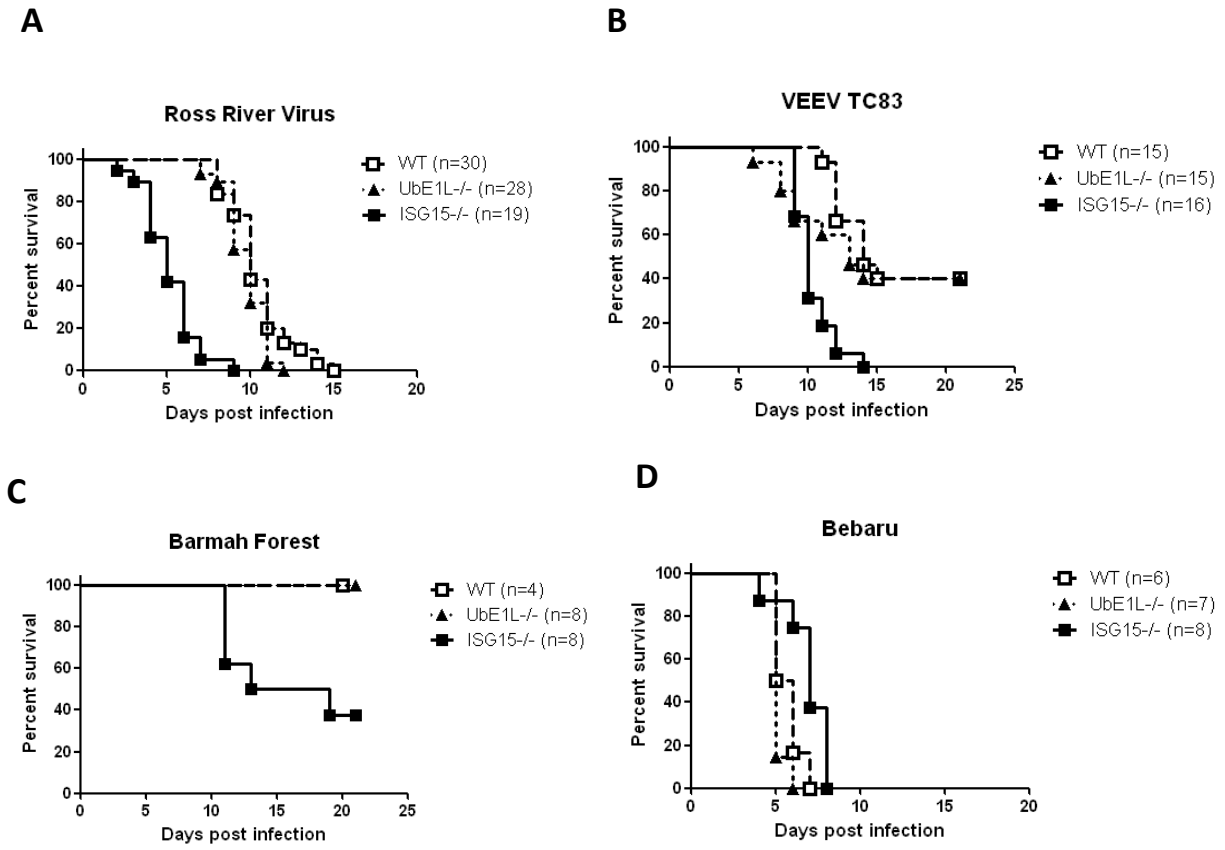
A
Ross River Virus
Percent survival
Days post infection
WT (n=30)
UbE1L-/- (n=28)
ISG15-/- (n=19)
B
VEEV TC83
Percent survival
Days post infection
WT (n=15)
UbE1L-/- (n=15)
ISG15-/- (n=16)
C
Barmah Forest
Percent survival
Days post infection
WT (n=4)
UbE1L-/- (n=8)
ISG15-/- (n=8)
D
Bebaru
Percent survival
Days post infection
WT (n=6)
UbE1L-/- (n=7)
ISG15-/- (n=8)

Figure S3.2. ISG15$^{-/-}$ and UbE1L$^{-/-}$ mice and cells produce less IL-6 in response to LPS compared to WT mice/cells (preliminary data). (A) WT, UbE1L$^{-/-}$ and ISG15$^{-/-}$ BMM were pretreated with 10U IFNb 24hrs before stimulation with LPS. Supernatants were collected at 4 and 12hrs post LPS treatment. IL-6 levels were measured by bioplex. **(B)** Nine day old WT and ISG15$^{-/-}$ mice were treated with LPS i.p. and serum was harvested 6 and 24hrs post treatment. IL-6 levels were measured by bioplex.

Figure S3.2

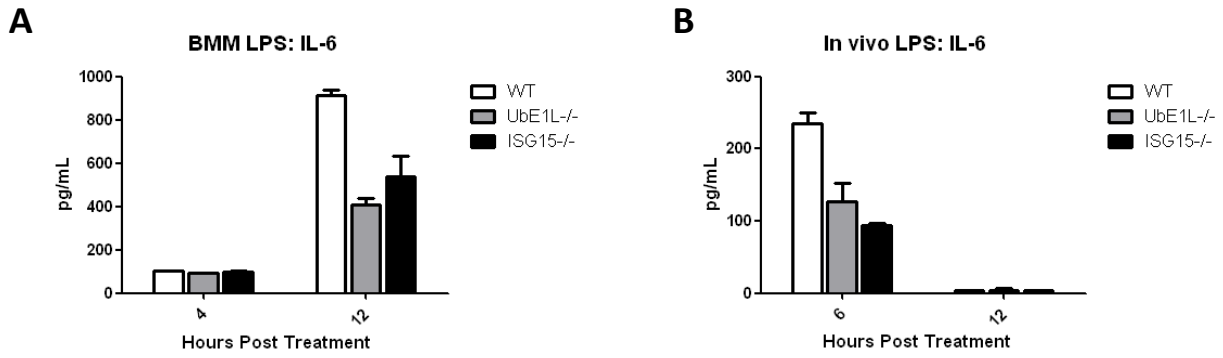
A
BMM LPS: IL-6
pg/mL
1000
800
600
400
200
0
4
12
Hours Post Treatment
WT
UbE1L-/-
ISG15-/-
B
In vivo LPS: IL-6
pg/mL
300
200
100
0
6
12
Hours Post Treatment
WT
UbE1L-/-
ISG15-/-

Table 3.1 Potential Non-Covalent Binding partners for free ISG15 identified via mass spec (ISG15-Fc pulldown with IFNβ/pIC stimulated ISG15$^{-/-}$ BMM).

Biological Process	NCBI Accession Number	Gene Name	Protein Name	#U pep
Signaling	13959396	Iqgap1	Ras GTPase-activating-like protein IQGAP1	15
	148668602	Ap3bp1	AP-3 complex subunit beta-1	6
	114326482	Stat1	Signal transducer and activator of transcription 1	7
	13633965	Stat2	Signal transducer and activator of transcription 2	8
	187471159	Hmha1	Minor histocompatibility protein HA-1	6
	170172575	Inppl1	Phosphatidylinositol 3,4,5-trisphosphate 5-phosphatase 2	7
	148701340	Fermt3	Fermitin family homolog 3	7
	168983832	Anxa2	Annexin A2	6
	46559406	Pak2	Serine/threonine-protein kinase PAK 2	4
	124517663	Anxa1	Annexin A1	4
	157951604	Cap1	Adenylyl cyclase-associated protein 1	3
	13096922	Arhgap17	Rho GTPase-activating protein 17	2
	13878195	Pik3ap1	Phosphoinositide 3-kinase adapter protein 1	3
	11528490	Flii	Protein flightless-1 homolog	4
	123701966	Kctd12	BTB/POZ domain-containing protein KCTD12	4
	24025665	Plekho2	Pleckstrin homology domain-containing family O member 2	4
	123241346	Sh3bp1	SH3 domain-binding protein 1	3
	1209068	Inpp5d	Phosphatidylinositol 3,4,5-trisphosphate 5-phosphatase 1 (Ship1)	3
	15489209	Themis2	THEMIS2 (Icb1)	2
	123227481	Ybx1	Y box protein 1	2
	124248570	G3bp2	GTPase activating protein (SH3 domain) binding protein 2	2
	225543183	Vwa5a	von Willebrand factor A domain-containing protein 5A (Loh11cr2a)	3
	20138411	Ptk2b	Protein-tyrosine kinase 2-beta	3
	1915913	Dpysl2	Dihydropyrimidinase-related protein 2	3
	192657	Ppp3ca	Serine/threonine-protein phosphatase 2B catalytic subunit alpha isoform	2
	255003810	Rab3gap2	Rab3 GTPase-activating protein non-catalytic subunit	2
	37590218	Abr	Active breakpoint cluster region-related protein	2
	45597447	Sod1	Superoxide dismutase [Cu-Zn]	2
	40675709	Syk	Tyrosine-protein kinase (Syk)	2
	309255	Gnai2	Guanine nucleotide-binding protein G(i) subunit alpha-2	2
	19852058	Dscaml1	Down syndrome cell adhesion molecule-like protein	2
	6644338	Prdx5	Peroxiredoxin-5	2
Innate Immunity	6754954	Sqstm1	Sequestosome 1 (p62)	6

	91064876	Gbp5	Guanylate binding protein 5	7
	132252411	Ifih1	Melanoma differentiation-associated protein 5 (MDA5)	7
	160333495	Gm14446	Gm14446 protein	8
	213418055	Samhd1	SAM domain and HD domain-containing protein 1 (Mg11)	5
	15030162	Gbp2	Interferon-induced guanylate-binding protein 2	6
	51702775	PPIA	Peptidyl-prolyl cis-trans isomerase A (Cyclophilin A)	4
	115270958	Gvin1	Interferon-induced very large GTPase 1	2
	70608133	Dhx58	Probable ATP-dependent RNA helicase DHX58 (LGP2)	4
	14861844	D1Pas1	Putative ATP-dependent RNA helicase Pl10	4
	15489209	Themis2	THEMIS2 (Icb1)	2
	23468336	Trafd1	FLN29 (TRAF-type zinc finger domain-containing protein 1)	3
	6754994	Pcbp1	poly(rC)-binding protein 1	3
	18044838	Zbp1	Z-DNA-binding protein 1	2
	26326901	Ripk1	Receptor-interacting serine/threonine-protein kinase 1	2
	1698556	Ncf4	Neutrophil cytosol factor 4 (p40phox)	2
	287323109	Hck	Tyrosine-protein kinase HCK	2
	114326482	Stat1	Signal transducer and activator of transcription 1	7
	13633965	Stat2	Signal transducer and activator of transcription 2	8
Vesicle Transport/ Phagocytosis	15341745	Ehd4	EH-domain containing 4	15
	13385878	Snx2	Sorting nexin 2	11
	31543349	Nsf	Vesicle-fusing ATPase	8
	12248793	Snx1	Sorting nexin 1	7
	51491845	Cltc	Clathrin heavy chain 1	3
	227116320	Fkbp15	FK506-binding protein 15	4
	83649760	Wash1	WAS protein family homolog 1	3
	22122347	Gga1	ADP-ribosylation factor-binding protein GGA1	2
	23956096	Uso1	General vesicular transport factor p115	2
	22477515	Ehd1	EH-domain containing 1	2
Protein Translation	26354649	Pabp1	Polyadenylate binding protein 1	13
	13278382	Eef1a1	Elongation factor 1-alpha1	8
	12963511	Rps19	40S ribosomal protein S19	9
	200796	Rps16	40S ribosomal protein S16	10
	3097244	Rps14	Ribosomal protein S14	7
	6677775	Rpl22	60S ribosomal protein L22	5
	1083569	Hnrnpk	Heterogeneous nuclear ribonucleoprotein K	6
	116517301	Ptbp1	Polypyrimidine tract binding protein 1	2
	127798883	Cyfip1	Cytoplasmic FMR1-interacting protein 1	4
	127799069	Syncrip	Heterogeneous nuclear ribonucleoprotein Q (hnRNP Q)	4
	9506571	Eif2s1	Eukaryotic translation initiation factor 2 subunit 1	4

	118344452	Srp72	Srp72	2
	11527388	Qki	Protein quaking	3
	13905140	Farsa	Phenylalanine--tRNA ligase alpha subunit	3
	118600514	Fam129a	Niban	2
	123235430	Srp14	Srp14	2
Cytoskeletal	61743961	Ahnak	AHNAK nucleoprotein isoform 1	37
	114326446	Myh9	Myosin-9	28
	227116327	Tln1	Talin 1	7
	125347376	Flna	Filamin A	12
	7106439	Tubb5	Tubulin beta-5 chain	4
	33620739	Myl6	Myosin light polypeptide 6	8
	134288917	Dync1h1	Cytoplasmic dynein 1 heavy chain	12
	148747189	Map4	Microtubule-associated protein 4	4
	47124599	Diap1	Diap1 protein	5
	149263685	Ahnak2	AHNAK2	2
	127798883	Cyfip1	Cytoplasmic FMR1-interacting protein 1	4
	118136288	Fmnl1	Formin-like protein 1	3
	255069756	Myo1f	Myosin IF	3
	123207565	Dync1i2	Dynein cytoplasmic 1 intermediate chain 2	3
	110625624	Tcp1	T-complex protein 1 subunit alpha	3
	161086971	Capza1	F-actin-capping protein subunit alpha-1	2
	6756085	Zyx	Zyxin	2
	148708988	Dsp	Desmoplakin	2
	22122795	Dync1li1	Dynein cytoplasmic 1 light intermediate chain 1	2
	21594742	Elmo1	Engulfment and cell motility protein 1	2
	125987599	Cd2ap	CD2-associated protein	2
Ubiquitin/UBL	7710044	Keap1	Kelch-like ECH-associated protein 1	9
	237820660	Ubr4	E3 ubiquitin-protein ligase UBR4	12
	127139140	Trim21	E3 ubiquitin-protein ligase TRIM21	5
	123264882	Rnf213	Ring finger protein 213	6
	116283726	Psmd1	Psmd1 protein	5
	6679501	Psmc1	26S protease regulatory subunit 4	4
	15823094	Ubl4	Housekeeping protein DXS254E	4
	31980712	Usp25	Ubiquitin carboxyl-terminal hydrolase 25	2
	4507793	UBE2N	ubiquitin-conjugating enzyme E2 N	3
	257153392	Ufd1l	Ubiquitin fusion degradation protein 1 homolog	3
	6754724	Psmd7	26S proteasome non-ATPase regulatory subunit 7	2
	5031981	Psmd14	26S proteasome non-ATPase regulatory subunit 14	2
	19705424	Psmd3	26S proteasome non-ATPase regulatory subunit 3	2
	5353754	Ddb1	DNA damage-binding protein 1	2
Protein Folding/ Stress Response	118490060	Hspa1a	Inducible heat shock protein 70	8
	118142832	Hsp90aa	Hsp90aa protein	6
	126723461	Cct8	T-complex protein 1 subunit theta	3
	62948125	Cct6a	Chaperonin containing Tcp1, subunit 6a (Zeta)	3

	110625624	Tcp1	T-complex protein 1 subunit alpha	3
	238814391	Cct7	Chaperonin subunit 7 (Eta), isoform CRA_a	2
	5353754	Ddb1	DNA damage-binding protein 1	2
Metabolism	1674501	Anpep	Aminopeptidase N	3
	1405933	Pkm	Pyruvate kinase isozymes M1/M2	5
	109734501	Hk3	Hk3 protein (hexokinase 3)	2
	19527028	Hdlbp	High density lipoprotein-binding protein (Vigilin)	4
	13529599	Ldha	L-lactate dehydrogenase	3
	110590524	Nampt	Nicotinamide phosphoribosyltransferase	2
	14250204	Mthfd1	C-1-tetrahydrofolate synthase, cytoplasmic	2
	26347093	Pfkp	6-phosphofructokinase type C	2
	52353955	Phgdh	D-3-phosphoglycerate dehydrogenase	2
Other	7242171	Pcna	Proliferating cell nuclear antigen	2
	27371140	Bag6	Bat3 protein	2
	15079335	Snrpd3	Small nuclear ribonucleoprotein D3	2

Resources: NCBI protein: http://www.ncbi.nlm.nih.gov
UniProtKB: http://www.uniprot.org/uniprot

Table 3.2. Regulation of BMM cytokine production by ISG15 in response to TLR stimulation. (negative or positive regulation, free or conjugation dependent)

TLR Stimulation	IL-6	IL-10	TNFα	IL-1β	chemokine
pIC	neg/Free	neg/Free	pos/Conj	n.d.	No diff
LPS	pos/Conj	neg/Conj	No diff	No diff	No diff
Imiq+ATP	n.d.	n.d.	n.d.	neg/Conj	n.d.

References

1. Glickman, M. H., and A. Ciechanover. 2002. The ubiquitin-proteasome proteolytic pathway: destruction for the sake of construction. *Physiol Rev* 82:373-428.

2. Welchman, R. L., C. Gordon, and R. J. Mayer. 2005. Ubiquitin and ubiquitin-like proteins as multifunctional signals. *Nat Rev Mol Cell Biol* 6:599-609.

3. Hochstrasser, M. 2000. Evolution and function of ubiquitin-like protein-conjugation systems. *Nat Cell Biol* 2:E153-157.

4. Hicke, L. 2001. Protein regulation by monoubiquitin. *Nat Rev Mol Cell Biol* 2:195-201.
5. Huang, T. T., and A. D. D'Andrea. 2006. Regulation of DNA repair by ubiquitylation. *Nat Rev Mol Cell Biol* 7:323-334.

6. Jesenberger, V., and S. Jentsch. 2002. Deadly encounter: ubiquitin meets apoptosis. *Nat Rev Mol Cell Biol* 3:112-121.

7. Muratani, M., and W. P. Tansey. 2003. How the ubiquitin-proteasome system controls transcription. *Nat Rev Mol Cell Biol* 4:192-201.

8. Hicke, L., H. L. Schubert, and C. P. Hill. 2005. Ubiquitin-binding domains. *Nat Rev Mol Cell Biol* 6:610-621.

9. Hurley, J. H., S. Lee, and G. Prag. 2006. Ubiquitin-binding domains. *Biochem J* 399:361-372.

10. Lenschow, D. J., C. Lai, N. Frias-Staheli, N. V. Giannakopoulos, A. Lutz, T. Wolff, A. Osiak, B. Levine, R. E. Schmidt, A. Garcia-Sastre, D. A. Leib, A. Pekosz, K. P. Knobeloch, I. Horak, and H. W. t. Virgin. 2007. IFN-stimulated gene 15 functions as a critical antiviral molecule against influenza, herpes, and Sindbis viruses. *Proc Natl Acad Sci U S A* 104:1371-1376.

11. Giannakopoulos, N. V., E. Arutyunova, C. Lai, D. J. Lenschow, A. L. Haas, and H. W. Virgin. 2009. ISG15 Arg151 and the ISG15-conjugating enzyme UbE1L are important for innate immune control of Sindbis virus. *J Virol* 83:1602-1610.

12. Lai, C., J. J. Struckhoff, J. Schneider, L. Martinez-Sobrido, T. Wolff, A. Garcia-Sastre, D. E. Zhang, and D. J. Lenschow. 2009. Mice lacking the ISG15 E1 enzyme UbE1L demonstrate increased susceptibility to both mouse-adapted and non-mouse-adapted influenza B virus infection. *J Virol* 83:1147-1151.

13. Werneke, S. W., C. Schilte, A. Rohatgi, K. J. Monte, A. Michault, F. Arenzana-Seisdedos, D. L. Vanlandingham, S. Higgs, A. Fontanet, M. L. Albert, and D. J.

Lenschow. 2011. ISG15 is critical in the control of Chikungunya virus infection independent of UbE1L mediated conjugation. *PLoS Pathog* 7:e1002322.

14. D'Cunha, J., S. Ramanujam, R. J. Wagner, P. L. Witt, E. Knight, Jr., and E. C. Borden. 1996. In vitro and in vivo secretion of human ISG15, an IFN-induced immunomodulatory cytokine. *J Immunol* 157:4100-4108.

15. D'Cunha, J., E. Knight, Jr., A. L. Haas, R. L. Truitt, and E. C. Borden. 1996. Immunoregulatory properties of ISG15, an interferon-induced cytokine. *Proc Natl Acad Sci U S A* 93:211-215.

16. Owhashi, M., Y. Taoka, K. Ishii, S. Nakazawa, H. Uemura, and H. Kambara. 2003. Identification of a ubiquitin family protein as a novel neutrophil chemotactic factor. *Biochem Biophys Res Commun* 309:533-539.

17. Padovan, E., L. Terracciano, U. Certa, B. Jacobs, A. Reschner, M. Bolli, G. C. Spagnoli, E. C. Borden, and M. Heberer. 2002. Interferon stimulated gene 15 constitutively produced by melanoma cells induces e-cadherin expression on human dendritic cells. *Cancer Res* 62:3453-3458.

18. Bogunovic, D., M. Byun, L. A. Durfee, A. Abhyankar, O. Sanal, D. Mansouri, S. Salem, I. Radovanovic, A. V. Grant, P. Adimi, N. Mansouri, S. Okada, V. L. Bryant, X. F. Kong, A. Kreins, M. M. Velez, B. Boisson, S. Khalilzadeh, U. Ozcelik, I. A. Darazam, J. W. Schoggins, C. M. Rice, S. Al-Muhsen, M. Behr, G. Vogt, A. Puel, J. Bustamante, P. Gros, J. M. Huibregtse, L. Abel, S. Boisson-Dupuis, and J. L. Casanova. 2012. Mycobacterial disease and impaired IFN-gamma immunity in humans with inherited ISG15 deficiency. *Science* 337:1684-1688.

19. Lenschow, D. J., N. V. Giannakopoulos, L. J. Gunn, C. Johnston, A. K. O'Guin, R. E. Schmidt, B. Levine, and H. W. t. Virgin. 2005. Identification of interferon-stimulated gene 15 as an antiviral molecule during Sindbis virus infection in vivo. *J Virol* 79:13974-13983.

20. Malakhova, O. A., and D. E. Zhang. 2008. ISG15 inhibits Nedd4 ubiquitin E3 activity and enhances the innate antiviral response. *J Biol Chem* 283:8783-8787.

21. Okumura, A., P. M. Pitha, and R. N. Harty. 2008. ISG15 inhibits Ebola VP40 VLP budding in an L-domain-dependent manner by blocking Nedd4 ligase activity. *Proc Natl Acad Sci U S A* 105:3974-3979.

22. Pincetic, A., Z. Kuang, E. J. Seo, and J. Leis. 2010. The interferon-induced gene ISG15 blocks retrovirus release from cells late in the budding process. *J Virol* 84:4725-4736.

23. Xia, Z. P., L. Sun, X. Chen, G. Pineda, X. Jiang, A. Adhikari, W. Zeng, and Z. J. Chen. 2009. Direct activation of protein kinases by unanchored polyubiquitin chains. *Nature* 461:114-119.

24. Zeng, W., L. Sun, X. Jiang, X. Chen, F. Hou, A. Adhikari, M. Xu, and Z. J. Chen. 2010. Reconstitution of the RIG-I pathway reveals a signaling role of unanchored polyubiquitin chains in innate immunity. *Cell* 141:315-330.

25. Jiang, X., L. N. Kinch, C. A. Brautigam, X. Chen, F. Du, N. V. Grishin, and Z. J. Chen. 2012. Ubiquitin-induced oligomerization of the RNA sensors RIG-I and MDA5 activates antiviral innate immune response. *Immunity* 36:959-973.

26. Pertel, T., S. Hausmann, D. Morger, S. Zuger, J. Guerra, J. Lascano, C. Reinhard, F. A. Santoni, P. D. Uchil, L. Chatel, A. Bisiaux, M. L. Albert, C. Strambio-De-Castillia, W. Mothes, M. Pizzato, M. G. Grutter, and J. Luban. 2011. TRIM5 is an innate immune sensor for the retrovirus capsid lattice. *Nature* 472:361-365.

27. Schilte, C., T. Couderc, F. Chretien, M. Sourisseau, N. Gangneux, F. Guivel-Benhassine, A. Kraxner, J. Tschopp, S. Higgs, A. Michault, F. Arenzana-Seisdedos, M. Colonna, L. Peduto, O. Schwartz, M. Lecuit, and M. L. Albert. 2010. Type I IFN controls chikungunya virus via its action on nonhematopoietic cells. *J Exp Med* 207:429-442.

28. Saito, T., R. Hirai, Y. M. Loo, D. Owen, C. L. Johnson, S. C. Sinha, S. Akira, T. Fujita, and M. Gale, Jr. 2007. Regulation of innate antiviral defenses through a shared repressor domain in RIG-I and LGP2. *Proc Natl Acad Sci U S A* 104:582-587.

29. Gitlin, L., W. Barchet, S. Gilfillan, M. Cella, B. Beutler, R. A. Flavell, M. S. Diamond, and M. Colonna. 2006. Essential role of mda-5 in type I IFN responses to polyriboinosinic:polyribocytidylic acid and encephalomyocarditis picornavirus. *Proc Natl Acad Sci U S A* 103:8459-8464.

30. Saraiva, M., and A. O'Garra. 2010. The regulation of IL-10 production by immune cells. *Nat Rev Immunol* 10:170-181.

31. Grek, C. L., D. A. Newton, D. D. Spyropoulos, and J. E. Baatz. 2011. Hypoxia up-regulates expression of hemoglobin in alveolar epithelial cells. *Am J Respir Cell Mol Biol* 44:439-447.

32. Liu, L., M. Zeng, and J. S. Stamler. 1999. Hemoglobin induction in mouse macrophages. *Proc Natl Acad Sci U S A* 96:6643-6647.

33. Ohyagi, Y., T. Yamada, and I. Goto. 1994. Hemoglobin as a novel protein developmentally regulated in neurons. *Brain Res* 635:323-327.

34. Greer, J., W. D. Liao, and W. E. Brown. 1981. Haptoglobin-hemoglobin complex. Subunit interaction probed by cross-linking. *J Biol Chem* 256:8771-8774.

35. Durfee, L. A., N. Lyon, K. Seo, and J. M. Huibregtse. 2010. The ISG15 conjugation system broadly targets newly synthesized proteins: implications for the antiviral function of ISG15. *Mol Cell* 38:722-732.

36. Cullen, P. J., and H. C. Korswagen. 2012. Sorting nexins provide diversity for retromer-dependent trafficking events. *Nat Cell Biol* 14:29-37.

37. Sanada, T., G. Takaesu, R. Mashima, R. Yoshida, T. Kobayashi, and A. Yoshimura. 2008. FLN29 deficiency reveals its negative regulatory role in the Toll-like receptor (TLR) and retinoic acid-inducible gene I (RIG-I)-like helicase signaling pathway. *J Biol Chem* 283:33858-33864.

38. Matsumura, T., M. Oyama, H. Kozuka-Hata, K. Ishikawa, T. Inoue, T. Muta, K. Semba, and J. Inoue. 2010. Identification of BCAP-(L) as a negative regulator of the TLR signaling-induced production of IL-6 and IL-10 in macrophages by tyrosine phosphoproteomics. *Biochem Biophys Res Commun* 400:265-270.

39. Takeuchi, O., and S. Akira. 2008. MDA5/RIG-I and virus recognition. *Curr Opin Immunol* 20:17-22.

40. White, L. K., T. Sali, D. Alvarado, E. Gatti, P. Pierre, D. Streblow, and V. R. Defilippis. 2011. Chikungunya virus induces IPS-1-dependent innate immune activation and protein kinase R-independent translational shutoff. *J Virol* 85:606-620.

41. Kim, K. I., M. Yan, O. Malakhova, J. K. Luo, M. F. Shen, W. Zou, J. C. de la Torre, and D. E. Zhang. 2006. Ube1L and protein ISGylation are not essential for alpha/beta interferon signaling. *Mol Cell Biol* 26:472-479.

42. Osiak, A., O. Utermohlen, S. Niendorf, I. Horak, and K. P. Knobeloch. 2005. ISG15, an interferon-stimulated ubiquitin-like protein, is not essential for STAT1 signaling and responses against vesicular stomatitis and lymphocytic choriomeningitis virus. *Mol Cell Biol* 25:6338-6345.

43. Kanneganti, T. D., N. Ozoren, M. Body-Malapel, A. Amer, J. H. Park, L. Franchi, J. Whitfield, W. Barchet, M. Colonna, P. Vandenabeele, J. Bertin, A. Coyle, E. P. Grant, S. Akira, and G. Nunez. 2006. Bacterial RNA and small antiviral compounds activate caspase-1 through cryopyrin/Nalp3. *Nature* 440:233-236.

CHAPTER 4

Summary and Future Directions

The following chapter contains an excerpt from the following publication:

Joubert, P. E., **S. W. Werneke**, C. de la Calle, F. Guivel-Benhassine, A. Giodini, L. Peduto, B. Levine, O. Schwartz, D. J. Lenschow, and M. L. Albert. 2012. Chikungunya virus-induced autophagy delays caspase-dependent cell death. *J Exp Med* 209:1029-1047.

Summary

Although Chikungunya Virus was first described in 1952, very little was known about CHIKV until recently, due to increased attention brought about by the 2005 La Reunion outbreak (1, 2). During this outbreak, in addition to the classical symptoms of rash, joint pain and fever, novel symptoms were also reported, with increased severity in infants, elderly and the immune compromised (3-6). As the CHIKV epidemic grew, scientists recognized the need to learn more about the life cycle and host response to CHIKV, in the hopes of alleviating or preventing future CHIKV outbreaks. Our collaborators at the Pasteur Institute successfully developed a mouse model for CHIKV, allowing for initial studies on CHKV pathogenesis (7). As with other viruses, type I interferons (IFN) were shown to be vital for the control of CHIKV infection (7, 8). Type I IFN mediates antiviral protection through the upregulation of hundreds of IFN stimulated genes (ISGs) (9). However, the role of ISGs during CHIKV infection was largely unknown. In this thesis, we focused our efforts on learning more about CHIKV pathogenesis, in part by describing a role for the interferon stimulated gene ISG15.

Due to increased severity of disease symptoms in infants, we focused our attention on a neonatal model of CHIKV infection. Interestingly, although infants show increased severity, this is not due to a lack of a robust immune response. In Chapter 2, we demonstrate that both human infants and neonatal mice generate a robust type I IFN response during CHIKV infection. Signaling through the type I IFN receptor is at least partially intact, as we were able to detect IRF7, Mx1 and ISG15 mRNA induction at the site of infection in neonatal mice. In order to understand mechanistically how type I IFNs protect neonates from CHIK induced lethality, we evaluated a role for ISG15.

A role for ISG15 in viral infection has been previously described. During Influenza B and Sindbis virus infections, ISG15 mediates protection through conjugation. ISG15$^{-/-}$ mice and mice that lack the ability to form ISG15 conjugates, UbE1L$^{-/-}$, phenocopy each other and show increased viral loads compared to WT mice. During CHIKV infection, we also show that ISG15$^{-/-}$ mice have increased susceptibility to viral induced lethality. We were surprised to find, however, that UbE1L$^{-/-}$ mice phenocopy WT mice during CHIKV infection. We also found that ISG15$^{-/-}$ mice did not have increased viral loads compared to WT mice. Instead, we observed an increase in pro-inflammatory cytokines and chemokines in ISG15$^{-/-}$ mice. Altogether, this data suggested that the mechanism by which ISG15 protects against CHIKV infection is different from the antiviral role described for ISG15 during both influenza B and Sindbis virus models. UbE1L is the only identified E1 for ISG15 and we were unable to detect ISG15 conjugates in CHIKV infected UbE1L$^{-/-}$ mice. Therefore, we hypothesized that the role of ISG15 during CHIKV infection is conjugation independent and occurs through the regulation of the host response to viral infection.

To provide additional support for a role for unconjugated ISG15 during CHIKV infection, we generated recombinant Chikungunya viruses that expressed wild type or conjugation deficient ISG15, where the C-terminal LRLRGG motif necessary for conjugation has been mutated to LRLRAA (CHIK-GG and CHIK-AA, respectively). This strategy was previously employed during Sindbis virus infection, where a LRLRGG expressing recombinant Sindbis virus could rescue ISG15$^{-/-}$ from lethality, whereas conjugation deficient ISG15 expressing Sindbis could not (10, 11). Once again we were surprised by our results, as we could not rescue ISG15$^{-/-}$ mice with the CHIK-GG expressing virus. There several possibilities as to why we were unable to provide protection, including insufficient levels of ISG15 expression or

ISG15 may not be stably expressed. Our data may also suggest that ISG15 is not expressed in the right cell type or the expression of ISG15 is required in an uninfected cell. Although there are several possibilities as to why our wild type ISG15 recombinant virus was unable to rescue $ISG15^{-/-}$ mice, we hypothesize that this also hints at a novel mechanism for ISG15.

Taken together, our data indicates that ISG15 functions by a previously unidentified mechanism to control the host response to CHIKV. Free ISG15, not the conjugated form, appears to be necessary for protection. We also hypothesize from our recombinant CHIKV model that ISG15 functions in an uninfected cell. Unlike previous models (10, 12), ISG15 is not directly antiviral, but instead regulates the host immune response.

Unanchored ISG15 can be found within a cell and can also be detected in the serum of infected mice. In order to determine how ISG15 protects against CHIKV infection, we decided to characterize both intra- and extracellular free ISG15. Cytokine activity for extracellular ISG15 has been reported and unanchored polyubiquitin chains regulate signaling within cells (13-18). In Chapter 3, we identify phosphorylation as a possible post-translational modification for serum ISG15. We also identify the 30kDa ISG15 serum band as ISG15 bound to hemoglobin subunit beta 1. The consequences of phosphorylation and the functional role of the 30kDa conjugate are unknown. We hypothesize that for either form of serum ISG15 to have activity, they must signal through an unidentified ISG15 cell surface receptor.

To identify non-covalent binding partners for ISG15, we used a recombinant tagged ISG15 construct for immunoprecipitation studies. Through mass spectrometry, we were able to identify over 140 potential binding partners for intracellular ISG15. Similar to ISGylation, non-covalent binding partners for ISG15 appear to be involved in multiple cellular pathways, including innate immunity, stress response, vesicle sorting, cytoskeletal and cell signaling. We

compared conjugation targets to free ISG15 targets and identified some proteins that did overlap (STAT1, Annexin) (19, 20). However, for the most part, the proteins that we identified represented novel targets. We found two proteins that were also identified in a Y2H screen performed by Nadia Giannakopoulos: PCBP1 (poly(C) binding protein 1) and Clathrin (unpublished data), which may be promising targets. The hits that we have identified need to be verified, although we have begun this process by demonstrating that ISG15 can co-ip with MDA5.

One of the mechanistic clues that we gained from our CHIKV model was the increased pro-inflammatory cytokine production in ISG15$^{-/-}$ mice. Therefore, we began preliminary investigations into ISG15s ability to regulate cytokine production. We demonstrate that ISG15 has the ability to regulate cytokine production following TLR stimulation and show that free ISG15 can regulate IL-6 production in response to pIC. We noted that both pIC and CHIKV can signal through MDA5, a potential non-covalent partner for ISG15. Whether increased cytokine production in response to pIC is due to ISG15s participation in the MDA5 pathway remains to be determined. We found that ISG15s ability to regulate cytokine production is complex, as the cytokine profile produced was dependent on both the type of stimulation and the type of cell.

Altogether, our most significant finding is that ISG15 regulates CHIKV infection independent of UbE1L mediated conjugation. This provides a unique opportunity to identify a mechanism of action for free ISG15. To meet this end, we have characterized both intra- and extracellular ISG15 and have begun functional studies relative to our mass spec results and our CHIKV model. It is our hope that our findings will not be specific to CHIKV, but will aid our overall understanding of ISG15s activity as an important effector of the type I IFN response.

Future Directions

Although we and others have taken important steps to characterize ISG15, the mechanism(s) by which ISG15 protects against viral infection is still largely unknown. Below we discuss future experiments that may aid in this discovery.

Is there a cell surface receptor for ISG15?

Extracellular ISG15 is found in the serum of virally infected mice and has been reported to have cytokine like activity. Stimulation with recombinant ISG15 results in NK cell proliferation, neutrophil recruitment, and dendritic cell maturation (13-15). Importantly, a recent report identifying ISG15 null mutations in humans has shown that recombinant ISG15 has the ability to regulate cell mediated IFNγ production in concert with IL-12 (16). How ISG15 mediates these activities is not understood, although we hypothesize that it is dependent on ISG15s ability to bind to an unidentified cell surface receptor.

Jessea Campbell has initiated preliminary investigations into identifying a receptor for ISG15. Our main goal is to generate recombinant ISG15, identify cells that can bind ISG15, and then generate a cDNA expression library to search for a possible receptor. We started by staining splenocytes from pIC stimulated mice with Fc-tagged mISG15 (Fc empty vector and DIII-Fc as negative controls). Unfortunately, results using Fc tagged versions of ISG15 were inconclusive. Innate immune cells, possibly neutrophils or CD8 dendritic cells, stained positive for ISG15, whereas B and T cells were negative. Primary BMM and BMDCs as well as the macrophage RAW cell line also bound ISG15-Fc (data not shown). Fc empty vector showed no binding and DIII Fc binding was lower than ISG15-Fc. Interestingly, pretreatment of RAW cells increased

the amount of ISG15-Fc binding. We hypothesize that, similar to the ISG15 conjugation cascade, the ISG15 receptor may be induced. However, when we generated a mutant Fc that could not bind Fc receptor, ISG15 binding was lost. This data suggests that our initial findings were dependent on Fc binding, although it is unclear why there remained a difference between non-mutant DIII and ISG15 constructs. As an alternative approach, we have generated BirA tagged ISG15 for the generation of ISG15 tetramers for use in similar experiments.

We hypothesize that innate hematopoietic cells are likely candidates for expression of an ISG15 receptor, as ISG15s activity has been reported for these cells in the literature and they play an important role in the initial response to viral infection when ISG15 is first expressed. Although we have not determined whether ISG15 mediated protection during CHIKV infection is dependent on intra- or extracellular ISG15, we propose that resident non-hematopoietic cells (i.e. muscle fibroblasts) should also be investigated, as Schlite et al has demonstrated that IFN mediated control of CHIKV infection is dependent on non-hematopoietic cells (8).

Generation of recombinant ISG15- mutant Fc for our intracellular mass spec studies as well as our cell surface staining provided a potential useful tool for investigating the functional consequences of extracellular ISG15 stimulation. To investigate a role for extracellular ISG15, we pre and/or post treated ISG15$^{-/-}$ primary BMM and muscle fibroblasts with recombinant ISG15 and then stimulated with pIC. Supernatant was collected and assayed for cytokine production via bioplex. Unfortunately, the conditions used to generate the recombinant protein included a contaminant that led to non-specific activation of BMM, masking any potential ISG15 activity (data not shown). Interestingly, primary muscle fibroblasts did not have non-specific activation and we observed that pretreatment of these cells dramatically decreased the amount of IL-6 produced in response to pIC (Fig. 4.1). These results were dependent on high concentrations

of ISG15, therefore it is unclear whether our results are physiologically relevant. However, this data may suggest that (1) primary muscle fibroblasts can respond to extracellular ISG15 and (2) extracellular ISG15 may negatively regulate IL-6 production.

To verify functional readouts for ISG15, data would be strengthened by having the ability to block extracellular ISG15 activity. We have attempted to block extracellular ISG15 activity in WT neonates during CHIKV infection by administering a rabbit anti-ISG15 polyclonal antibody 24hrs prior to infection. Unfortunately, our antibody pretreatment did not impact the survival, viral loads, or cytokine production in WT mice (Fig 4.2). There are many potential explanations for why our αISG15 antibody could not protect, such as inability of the antibody to block activity, insufficient amount to block activity, or maybe blocking was successful, but extracellular ISG15 is not essential during CHIKV infection. To verify the ability of our ISG15 antibody to block extracellular ISG15 activity, we must first establish a functional readout (preferably in vitro) for recombinant ISG15 stimulation.

Many additional questions need to be addressed to confirm an activity for extracellular ISG15. We do not know how much ISG15 is released following IFN stimulation or viral infection. We also do not know whether release of ISG15 is an active process or due to release from dead or dying cells. If ISG15 secretion is active, what cells are responsible for release of ISG15 during in vivo viral infection? Interestingly, during influenza B chimeric bone marrow studies, ISG15 was found in the serum of WT > $ISG15^{-/-}$ infected mice but not $ISG15^{-/-}$ > WT mice by western blot analysis, suggesting that (1) ISG15 release is an active process and (2) ISG15 may be secreted from hematopoietic cells (data not shown).

In summary, finding an activity for extracellular ISG15 is dependent on further characterization of serum ISG15 (post translational modifications (Chapter 3), mechanism of

secretion, physiological levels) as well as identification of an ISG15 receptor. Once these parameters have been established, functional relevance may be derived by identifying ISG15-ISG15 receptor binding interactions and potential downstream signaling consequences.

Confirmation of non-covalent binding partners for intracellular ISG15

We believe that our identification of non-covalent binding partners for intracellular ISG15 is a promising start to finding mechanisms for both free and conjugated ISG15. We recognize, however, that many of the proteins that we have identified using mass spectrometry may not directly bind ISG15. To confirm binding partners for ISG15, we have begun initial overexpression co-ip studies using a 293 transfection system. If proteins can be verified via overexpression, similar co-ip studies can be used to establish endogenous interactions. Additional mutagenesis analysis will allow for identification of domains and/or residues that are responsible for ISG15 binding, which may aid in future functional studies. Strength and kinetics of binding may also be evaluated using recombinant proteins and such techniques as Surface Plasma Resonance (SPR).

We note that we did not identify any transmembrane proteins from our mass spec analysis. It is possible that the conditions that we used to generate cytosol from BMM did not allow for isolation of transmembrane proteins. We also note that our mass spec hits are specific for IFNβ/pIC stimulated BMM, therefore may not represent additional binding partners in different cells or in response to other forms of stimulation (TLR4, inflammasome, etc). Therefore, our results most likely do not represent the full repertoire of ISG15 binding partners but may be used to direct attention to certain cell signaling pathways.

We hypothesize that like ubiquitin, non-covalent ISG15 may be recognized by proteins that contain an unknown "ISG15 binding domain" (ISGBD). This ISGBD may contain sequence similarities with ubiquitin binding domains (21, 22). We also hypothesize that ISG15 can compete with ubiquitin for binding to known ubiquitin binding domains. Therefore, we searched our non-covalent mass spec results (Table 3.1) for conserved protein binding domains. Interestingly, so far we have only identified three ubiquitin binding domains that unfortunately, are not shared by any of our other mass spec hits: UBA (p62), VHS (Gga1) and UIM (Usp25). Blast searches of portions of these ubiquitin binding domains within functional categories did not reveal a conserved amino acid sequence shared between mass spec hits. These results are preliminary and may improve by decreasing the stringency of our Blast searches or by eliminating proteins on our mass spec list that do not bind ISG15. We suggest that mutagenesis of a known ISG15 interacting partner may be the best approach for identifying an ISG15 binding domain.

What are the functional consequences for intracellular ISG15s non-covalent interactions?

From our mass spec analysis, we have identified proteins involved in many different intracellular pathways, including innate immunity, vesicle sorting, protein translation, cell metabolism and cell signaling pathways. If we are able to confirm ISG15 binding, we will need to demonstrate the functional consequences of this interaction. In Chapters 3, we have highlighted MDA5, a known ubiquitin binding protein, as a promising candidate for ISG15 binding activity. Below we briefly examine a few other candidates that may relate to our observations during CHIKV infection.

NCF4 (neutrophil cytosolic factor 4), also known as p40phox, is a member of the NADPH oxidase. The NADPH oxidase is responsible for the generation of reactive oxygen species (ROS) that play an important role in macrophage activation and inflammation (23). p40phox is one of six subunits that makes up the NADPH oxidase and is known to regulate NADPH oxidase activity in vivo (23). To our knowledge, the contribution of ISG15 to ROS generation has not been evaluated. Our ability to generate primary knockout cells may allow for the development of an in vitro model to assess whether or not ISG15 can influence ROS production.

Poly (C) binding protein 1 (PCBP1) was one of the few mass spec hits that was also identified in Nadia's Y2H screen. Poly (C) binding proteins represent a family of RNA-binding proteins with high affinity and sequence specific interaction with poly(C) (24). PCBPs are involved in multiple cellular processes and have been shown to regulate mRNA stability, transcription and translation. Importantly, PCBP1 and PCBP2 have been shown to mediate the degradation of MAVs through the recruitment of the E3 ubiquitin ligase AIP4 (25, 26). To assess a role for PCBP1, we may evaluate ISG15s ability to regulate MAVs degradation or MAVs downstream signaling.

We have also identified several proteins involved in vesicle sorting, including Sorting Nexins 1 and 2 (Snx1/2), general vesicular transport factor p115 (Uso1), and clathrin heavy chain 1. The mechanism by which ISG15 is secreted is unknown, therefore we hypothesize that ISG15s ability to interact with members of vesicular transport may reveal how ISG15 is released. Knockdown of these sorting proteins may be used to evaluate the importance of these proteins in ISG15 secretion. We recognize that vesicular sorting proteins play additional roles besides protein secretion, including membrane remodeling, cell surface receptor recycling and retrograde

transport from endosomes to the Trans Golgi network (TGN) (27, 28). A potential role for ISG15 in these pathways is unclear.

Another protein that we have identified, p62, also has the capability to bind to both mono and polyubiquitin. As we have generated preliminary data examining a role for ISG15 in autophagy and apoptosis, we will discuss these pathways in more detail in the following section.

A quick look at ISG15 and Autophagy/Apoptosis (includes excerpt from Joubert et al 2012).

Past research has shown that both apoptosis and autophagy are induced during Sindbis virus infection and manipulation of either of these cellular pathways can alter Sindbis disease progression (29-31). Our collaborators at the Pasteur Institute demonstrate that autophagy is induced during CHIKV infection and acts in part by limiting apoptosis induction (32). We also demonstrate that autophagy is necessary for in vivo protection against CHIKV induced lethality. To analyze the potential role of autophagy in CHIKV pathogenesis we used Atg16L hypomorphic mice (Atg16LHM) in which *Atg16L1* gene has been modified by gene trap mutagenesis. These mice display hypomorphic expression of Atg16L protein and reduced autophagy (not depicted; (33)). 9-d-old WT and Atg16LHM mice were infected with CHIKV and followed for lethality (Fig. 4.3A). Although only 60% of WT mice succumbed to CHIKV, we observed an increase in lethality in Atg16LHM mice. These data indicate that autophagy has a pro-survival function during CHIKV infection and limits disease pathogenesis. To understand how autophagy enhances survival, we analyzed viral load in infected tissues in WT and Atg16LHM mice (Fig. 4.3B). Viral load in skin muscle and serum, important targets of CHIKV infection, were similar in WT and Atg16LHM mice, suggesting that autophagy did not

significantly affect in vivo viral infection. Similar results were obtained by analyzing the viral load in lung, liver, brain, and spleen (unpublished data). Interestingly, the one observed difference concerned a delayed clearance of CHIKV in the muscle at day 9 after infection. Joubert et al go on to show that CHIKV Atg16LHM mice display increased levels of caspase 3 activation compared to WT mice despite similar viral loads (data not shown)(32). Our data indicates that autophagy limits apoptotic induction of CHIKV infected tissues and delays lethality of mice.

The ability of ISG15 to regulate autophagy and/or apoptosis is unknown, although we hypothesize that if ISG15 can regulate autophagy/apoptosis, then increased lethality observed in $ISG15^{-/-}$ mice during CHIKV infection may result from altered regulation of these two pathways. Analysis of LC3 and p62 conversion following autophagy induction in vitro did not reveal a role for ISG15 (Fig. 4.4). WT, $UbE1L^{-/-}$ and $ISG15^{-/-}$ MEFs and BMM were treated with EBSS (serum starvation) or Rapamycin/Chloroquine to induce autophagy (33, 34), with or without IFNβ pretreatment. Autophagy induction was assessed by examining LC3-II and p62 accumulation in cell lysates 1-9hrs post stimulation via western blot analysis. Baseline levels of LC3-II and p62 were equivalent between untreated WT, $UbE1L^{-/-}$ and $ISG15^{-/-}$ MEFs. IFNβ pretreatment only slightly increased observed levels of LC3-II and p62 above baseline. Treatment with rapamycin and chloroquine post IFNβ treatment greatly increased the amount of LC3-II and p62 above baseline, however there was no difference between the three genotypes (Fig. 4.4A). BMM behaved similarly to MEFs (Fig. 4.4B). ISG15 expression in IFNβ stimulated cells was also confirmed by western blot analysis. Under these conditions, we were unable to describe a role for ISG15 in autophagy. We hypothesize that ISG15 may not regulate overall

autophagy protein levels, but may impact the delivery of cellular components to the autophagosome.

Although a role for ISG15 in apoptosis/autophagy has not been described, ubiquitin is known to play an important role in both of these pathways. Both mono-ubiquitin and polyubiquitin chains are important molecular tags for targeting intracellular protein aggregates, organelles as well as intracellular pathogens for autophagy (35). Ubiquitinated targets are recognized by autophagy adaptor proteins, primarily p62 and NBR1, which deliver their ubiquitinated targets to the autophagosome. These autophagy adaptor proteins have been termed SLRs (sequestosome 1/p62-like receptors) and represent a newly recognized class of pattern recognition receptors that link autophagy to inflammation and other innate immune pathways (35). From our mass spec analysis, we have identified p62 as a potential binding partner for ISG15 (Chapter 3). Therefore, we hypothesize that, similar to ubiquitin, ISGylated proteins can be recognized by p62 and somehow influence the autophagy pathway. Alternatively, free ISG15 may bind to p62 and inhibit its ability of p62 to bind ubiquitinated cargo. The consequences of ISG15s binding to p62 remains to be investigated, but represents an exciting opportunity for identifying a novel function for ISG15. Through mass spec, we have also identified the p62 interacting protein Keap1 (36, 37), which may also warrant future study.

Ubiquitin has also been shown to play a role in apoptosis, although its role is primarily dependent on ubiquitylation of target proteins for the proteasome (38). We have also begun preliminary investigations into ISG15 and apoptosis. No difference in cell viability have been observed under normal growth conditions for WT, UbE1L$^{-/-}$ and ISG15$^{-/-}$ primary cells (BMM, BMDC, MEFs, muscle fibroblasts) in vitro. Altering the conditions of in vitro cell growth, by treatment with IFNβ, pIC or viral infection has also not generated a difference in cell viability,

although these results have not been closely quantitated or documented. To assess a role for ISG15 in apoptosis during CHIKV infection, we stained CHIKV infected skin and muscle tissue from WT, UbE1L$^{-/-}$, and ISG15$^{-/-}$ neonates with anti-caspase 3 antibody ((Fig. 4.5), staining and analysis done with the help of Pierre-Emmanuel Joubert). Strikingly, ISG15$^{-/-}$ show increased levels of caspase 3 staining during CHIKV infection compared to WT and UbE1L$^{-/-}$ mice. We have previously demonstrated that WT, UbE1L$^{-/-}$ and ISG15$^{-/-}$ mice do not display differences in skin/muscle viral titers. This suggests that the increase in apoptosis is not due to increased viral burden in ISG15$^{-/-}$ mice, however this was not directly shown for the caspase3 samples as anti-CHIK staining was unsuccessful. Future studies are necessary to establish a role for ISG15 in apoptosis.

Alphaviruses and ISG15: To conjugate or not to conjugate?

Sindbis virus (SINV) is an alphavirus that is closely related to CHIKV. Like CHIKV, SINV is an Old World alphavirus that is arthogenic, although neuroadapted strains of SINV have been described (39). As the role of ISG15 during SINV infection is conjugation dependent (11), we were surprised when we discovered that ISG15s role during CHIKV infection was not mediated by UbE1L. This UbE1L independent mechanism of ISG15 was not specific to CHIKV, as we demonstrated a similar phenotype for additional alphaviruses: RRV and BFV. We do not understand why ISG15 mediated restriction of some viruses is conjugation dependent while for others, it appears to be conjugation independent. We hypothesize that viral determinants may dictate how ISG15 mediates its protective effects. The similarities between SINV and CHIKV may provide a unique opportunity to identify which viral proteins influence ISG15 restriction, if this is indeed the case. The generation of chimeric viruses is a common vaccine strategy, and has

been demonstrated with CHIKV using TC-83 and Sindbis virus backbones (40). Therefore, we propose domain swap studies between SINV and CHIKV to determine if ISG15s conjugation restriction can be tied to an individual or set of viral proteins.

What is the role for ISG15 in cytokine production? Does ISG15 regulate cytokine production in response to other stimuli?

Type I IFNs impact the function of both innate and adaptive immunity. IFN production leads to activation of DCs and NK cells and also promotes the survival and effector function of B and T cells (9). It is thought that one of the mechanisms by which IFN alters an immune response is through the regulation of cytokine production. Indeed, IFNs anti-inflammatory properties have been used therapeutically for autoimmune or inflammatory disorders, including multiple sclerosis (MS) (41). Recent research suggests that type I IFN inhibits IL-1β production and inflammasome activation (42). Although IFN has been suggested to regulate cytokine production, the mechanism of action is still largely unknown. Due to our CHIKV phenotype, we hypothesized that ISG15 may be a downstream effector of IFN mediated cytokine regulation.

ISG15$^{-/-}$ mice during CHIKV infection display elevated proinflammatory cytokine levels compared to UbE1L$^{-/-}$ and WT mice. The levels of TNFα observed were similar to that observed in some adult models of LPS induced septic shock (43, 44) as well as neonatal Sindbis virus infections (45), where mice are thought to die from a cytokine storm. Necropsy analysis revealed that ISG15$^{-/-}$ mice had more severe blood vessel and airway injury than WT and UbE1L$^{-/-}$ mice. ISG15$^{-/-}$ mice also had altered blood chemistry, which may indicate multiple organ dysfunction, another potential readout for septic shock (Fig S2.5). We hypothesize that the cytokine increase in vivo may contribute to the increased lethality observed in ISG15$^{-/-}$ mice during CHIKV

infection and suggest that ISG15s ability to regulate cytokine production is biologically significant.

As ISG15 appears to impact cytokine production during CHIKV infection, we investigated cytokine production in ISG15$^{-/-}$ in response to other stimuli. Our lab has previously shown that the role of ISG15 during influenza B virus infection is conjugation dependent. ISG15s action is also directly antiviral, as UbE1L$^{-/-}$ and ISG15$^{-/-}$ mice show elevated influenza B titers compared to WT mice (Fig 4.6A)(12). Interestingly, although conjugation appears to be essential for protection against influenza B, analysis of cytokines produced indicates a mechanism of action for free ISG15 during influenza B infection. UbE1L$^{-/-}$ and ISG15$^{-/-}$ mice have equivalent viral loads during influenza B infection, however, as with CHIKV, ISG15$^{-/-}$ mice display a marked increase in pro-inflammatory cytokine production (Fig 4.6B). We suggest that although this cytokine increase does not appear to contribute to the lethality of ISG15$^{-/-}$ mice, the mechanism of free ISG15 mediated cytokine regulation is still conserved in this influenza B model. We note that one of the key differences between our influenza B and CHIKV models is the age of the mice: CHIKV is neonates and influenza B is adults. We speculate that adult mice are more resistant to cytokine increases, therefore influenza B infected ISG15$^{-/-}$ mice do not show an increase in lethality compared to UbE1L$^{-/-}$ mice. Indeed, our CHIKV model is also age dependent, as older ISG15$^{-/-}$ mice are considerably more resistant to CHIK induced lethality compared to our 9day old model.

In Chapter 3, we demonstrate that ISG15 can regulate cytokine production in response to pIC stimulation. Interestingly, unlike pIC stimulation or CHIKV infection, LPS treatment leads to a different pattern of cytokine production (Table 3.2). Following LPS treatment, ISG15$^{-/-}$ mice and cells show a decrease in IL-6 production. In addition to pIC and LPS, we also tried

inflammasome activation to evaluate IL-1β production. Although preliminary, our data might suggest that inflammasome mediated IL-1β production is regulated by ISG15 conjugation. Altogether, regulation of cytokine production by ISG15 is complex and appears to be dependent on the type of PRR stimulation.

Bridging Free and Conjugated ISG15: The Molecular Tag Hypothesis.

Although the focus of this thesis has been on free ISG15, we hypothesize that the non-covalent binding properties of free ISG15 may be necessary for the function(s) of conjugated ISG15. From western blot analysis, we normally observe that only a small percentage of a target proteins become ISGylated. One of the underlying questions in the field of ISG15 is if only a small percentage of protein gets modified, how can this have a functional consequence? A theory has been proposed by (46) based on their observation that the primary E3 for ISG15, Herc5, associates with ribosomes. They hypothesize that ISG15 non-discriminately labels newly translated proteins and modification of host proteins is "collateral damage." Viral proteins are proposed to be the actual targets of ISGylation and modification of structural proteins inhibits the ability of a virus to form a mature virion due to steric hindrance, thus inhibiting viral replication. This would require that only a fraction of viral proteins gets modified, consistent with most observations.

We wish to extend this theory and propose that ISG15 tags viral proteins for identification by host proteins. During viral assembly, we hypothesize that ISGylated viral proteins are recruited to the viral replication complex. Host proteins can then bind and recognize ISGylated proteins via non-covalent interactions or a hypothetical ISG15 binding domain. This allows for recruitment of host proteins to the viral replication complex and requires that only a

small number of viral proteins become modified. For example, we hypothesize that p62 (one of our mass spec hits) recognizes and binds to ISGylated proteins and targets them for destruction. P62 is recruited to the viral replication complex, allowing for autophagosome formation around the viral replicon for targeted destruction. We hypothesize that other host proteins may also be recruited via a similar mechanism. Another similar theory is that mature virions may be ISGylated, allowing for recognition by the unidentified ISG15 receptor and internalization/destruction of the released virus. Although we hypothesize that the "collateral damage" theory may be valid, we also recognize the potential of ISG15 to serve as an adaptor between host proteins. Therefore, ISG15 regulation of viral replication may be dependent on (1) ISG15 conjugation and (2) recognition of ISGylated proteins via ISG15 binding proteins. Future studies are required to establish a relationship between free and conjugated ISG15.

Figure 4.1. Pretreating ISG15$^{-/-}$ muscle fibroblasts with recombinant ISG15 results in decreased IL-6 production. ISG15$^{-/-}$ primary muscle fibroblasts were pretreated with 1-5 ug/mL recombinant ISG15 -mutant Fc or DIII –mutant Fc protein. 24hrs after ISG15 pretreatment, cells were stimulated with 10ug pIC along with (prepost) or without (pre) 1-5ug ISG15. Cell supernatants were harvested 18hrs post treatment and IL-6 was measured via Bioplex. Representative of two different experiments (N=2).

Figure 4.1

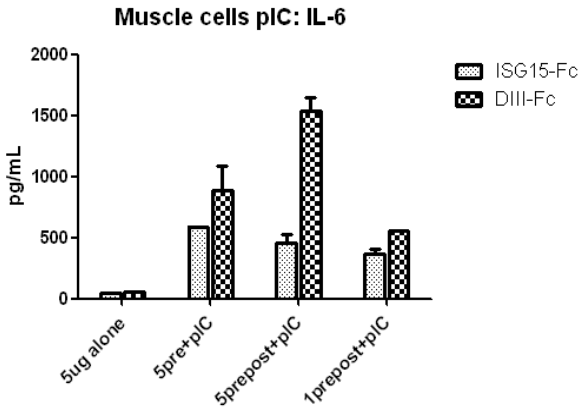
Muscle cells pIC: IL-6
pg/mL
2000
1500
1000
500
0
ISG15-Fc
DIII-Fc
5ug alone
5pre+pIC
5prepost+pIC
1prepost+pIC

Figure 4.2. Pretreatment of WT mice with a polyclonal anti-ISG15 antibody did not impact survival, viral titers or cytokine production during CHIKV infection. (A) Nine day old WT mice were pretreated with 30uL of anti-ISG15 rabbit polyclonal sera (1552) 24hrs before infection with 10^5 PFU CHIKV s.c. Survival was followed for 21 days and compared to untreated WT mice. (B and C) In a separate experiment, WT mice were pretreated with anti-ISG15 or a non-specific antibody (1781) 24hrs before CHIKV infection. Skin/muscle from the site of infection as well as serum was collected on days 1 and 2 post infection. Viral titers were determined by plaque assay and serum cytokine levels were measured via bioplex.

Figure 4.2

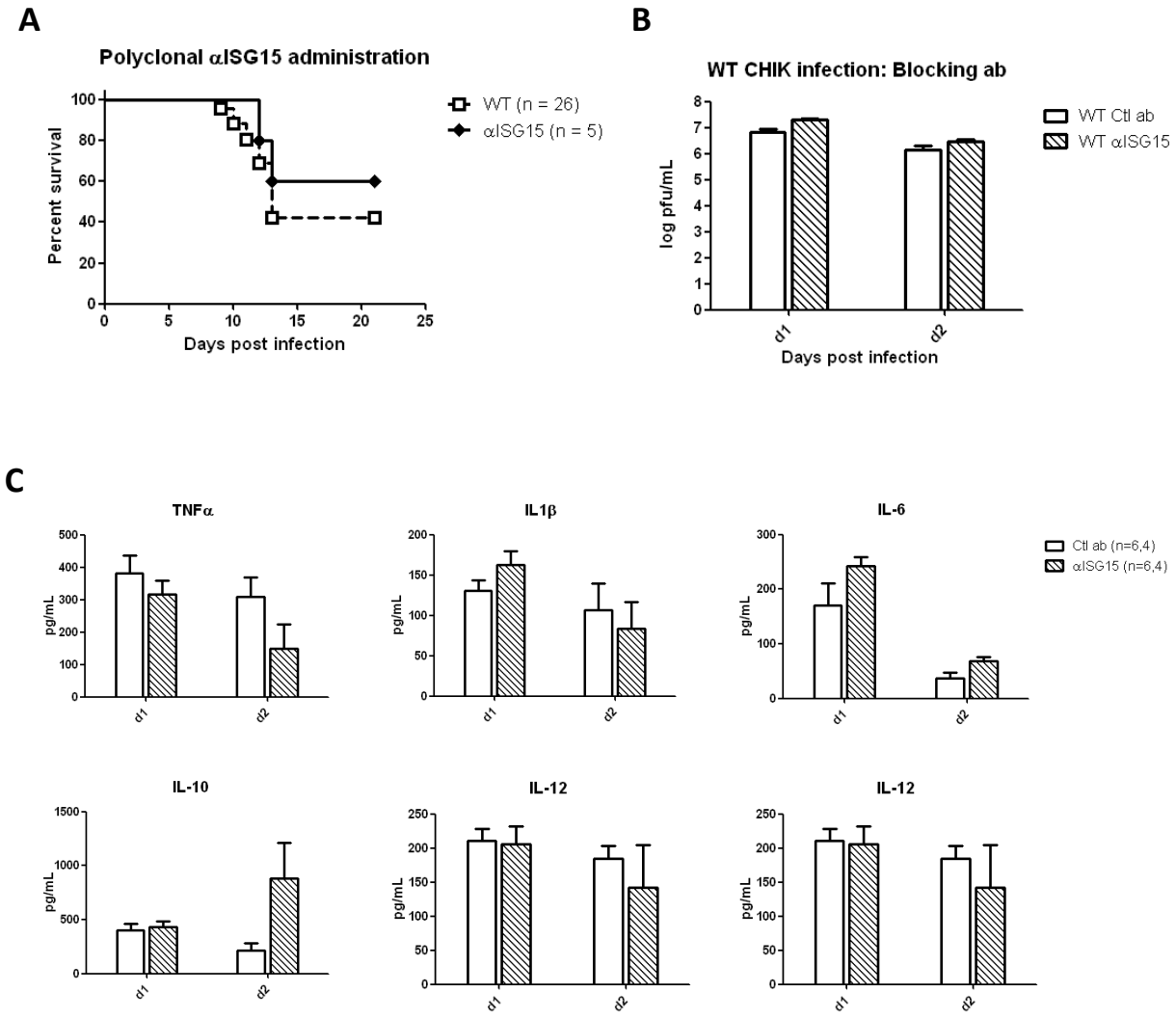
A
Polyclonal αISG15 administration
Percent survival
Days post infection
WT (n = 26)
αISG15 (n = 5)
B
WT CHIK infection: Blocking ab
log pfu/mL
Days post infection
WT Ctl ab
WT αISG15
C
TNFα
IL1β
IL-6
IL-10
IL-12
IL-12
pg/mL
d1
d2
Ctl ab (n=6,4)
αISG15 (n=6,4)

Figure 4.3. Autophagy limits apoptotic induction in CHIKV infected tissues and delays lethality of mice (Joubert et al 2012). (A&B) WT (n = 43) and Atg16L^{HM} mice (n = 34) were infected at 9 d of age with 4×10^5 PFU CHIKV subcutaneously. (A) Mice were monitored for lethality for 21 d with data displayed as Kaplan-Meier curves. (B) Skin, muscle, and serum were collected after days 1, 2, 5, and 9 of infection, homogenized, and viral titers were determined by standard plaque assay. Median values for WT (black bars) or Atg16L^{HM} (blue bars) mice are depicted.

Figure 4.3

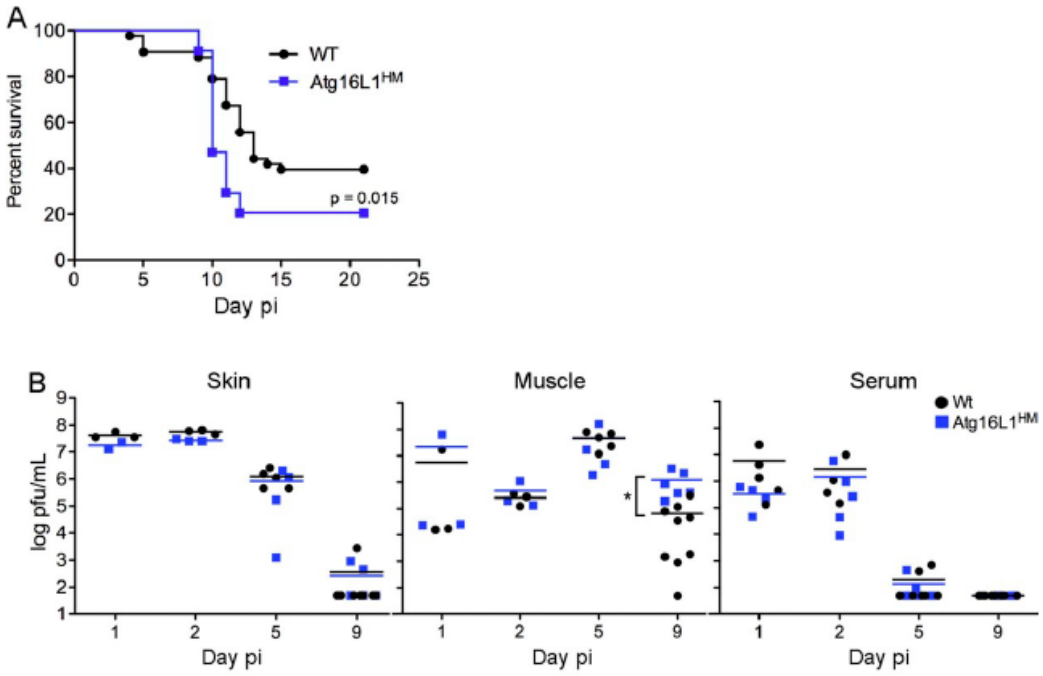
A
Percent survival
Day pi
WT
Atg16L1HM
p = 0.015
B
Skin
Muscle
Serum
log pfu/mL
Day pi
Wt
Atg16L1HM
*

Figure 4.4. ISG15 does not appear to regulate total p62 and LC3-II levels following autophagy induction (preliminary data). (A) WT, UbE1L$^{-/-}$ and ISG15$^{-/-}$ MEFs were pretreated with IFNβ and then stimulated with rapamycin and chloroquine (RC). LC3-II, p62, and ISG15 expression 8hrs post RC stimulation were identified by western blot analysis. **(B)** Activated WT, UbE1L$^{-/-}$ and ISG15$^{-/-}$ primary BMM were treated with EBSS or RC. LC3-II and ISG15 expression 9hrs post autophagy induction were identified by western blot analysis (p62 was not detected). Similar results were obtained for earlier timepoints (2-6hrs) for both BMM and MEFs.

Figure 4.4

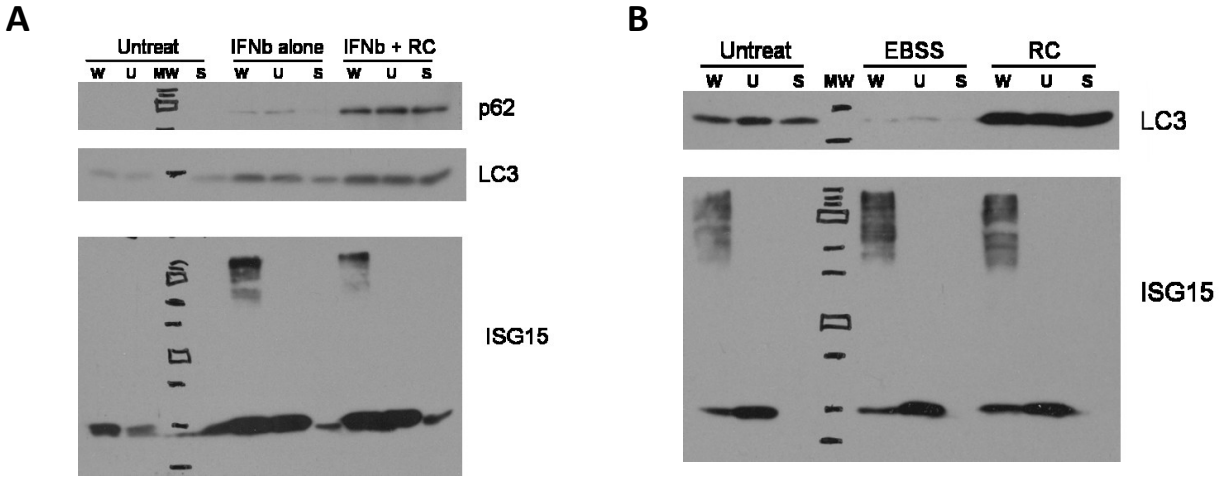
A
Untreat
IFNb alone
IFNb + RC
W U MW S W U S W U S
p62
LC3
ISG15
B
Untreat
EBSS
RC
W U S MW W U S W U S
LC3
ISG15

Figure 4.5 CHIKV infected ISG15$^{-/-}$ mice may have elevated levels of apoptosis at the site of infection compared to WT and UbE1L$^{-/-}$ mice (preliminary data in collaboration with Pierre-Emmanuel Joubert). Nine day old WT, UbE1L$^{-/-}$ and ISG15$^{-/-}$ mice were infected at with 4×10^5 PFU CHIKV s.c. Skin/muscle from the site of infection was collected on day 2 p.i. Tissue was fixed in PFA, frozen in OCT blocks, and stained for cleaved capsase-3. Each bar represents an individual mouse. Number of caspase 3 positive cells was counted from three separate sections for each mouse.

Figure 4.5

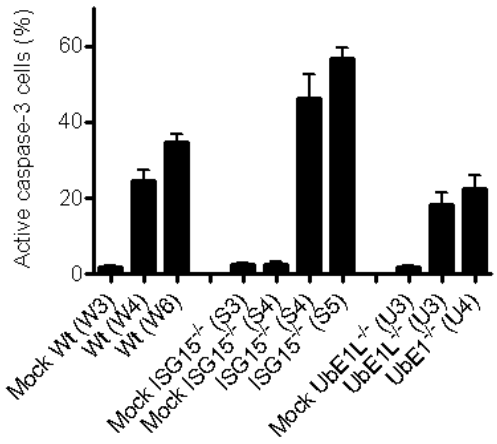
Active caspase-3 cells (%)
60
40
20
0
Mock Wt (W3)
Wt (W4)
Wt (W6)
Mock ISG15-/- (S3)
Mock ISG15-/- (S4)
ISG15-/- (S4)
ISG15-/- (S5)
Mock UbE1L-/- (U3)
UbE1L-/- (U3)
UbE1-/- (U4)

Figure 4.6. Influenza B infected ISG15$^{-/-}$ mice have elevated cytokine and chemokine levels compared to UbE1L$^{-/-}$ mice despite similar viral loads (Dr. Deborah Lenschow). WT, UbE1L-/- and ISG15-/- adult mice were infected with influenza B virus. **(A)** Lung viral titers were determined on days 3 and 6 post infection via plaque assay. **(B and C)** Serum cytokine (B) and chemokine (C) levels were assessed by bioplex on day 6 post infection.

Figure 4.6

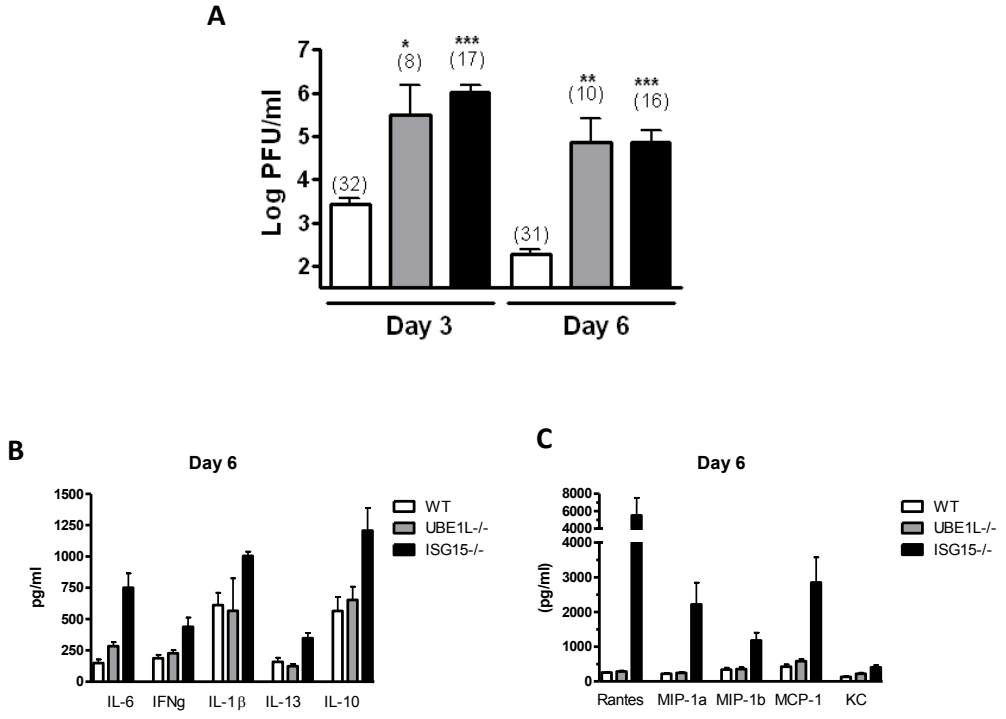
A
Log PFU/ml
7
6
5
4
3
2
(32)
*
(8)
***
(17)
(31)
**
(10)
***
(16)
Day 3
Day 6
B
Day 6
pg/ml
1500
1250
1000
750
500
250
0
IL-6
IFNg
IL-1β
IL-13
IL-10
WT
UBE1L-/-
ISG15-/-
C
Day 6
(pg/ml)
8000
6000
4000
4000
3000
2000
1000
0
Rantes
MIP-1a
MIP-1b
MCP-1
KC
WT
UBE1L-/-
ISG15-/-

References

1. Bessaud, M., C. N. Peyrefitte, B. A. Pastorino, F. Tock, O. Merle, J. J. Colpart, J. S. Dehecq, R. Girod, M. C. Jaffar-Bandjee, P. J. Glass, M. Parker, H. J. Tolou, and M. Grandadam. 2006. Chikungunya virus strains, Reunion Island outbreak. *Emerg Infect Dis* 12:1604-1606.

2. Her, Z., Y. W. Kam, R. T. Lin, and L. F. Ng. 2009. Chikungunya: a bending reality. *Microbes Infect* 11:1165-1176.

3. Economopoulou, A., M. Dominguez, B. Helynck, D. Sissoko, O. Wichmann, P. Quenel, P. Germonneau, and I. Quatresous. 2009. Atypical Chikungunya virus infections: clinical manifestations, mortality and risk factors for severe disease during the 2005-2006 outbreak on Reunion. *Epidemiol Infect* 137:534-541.

4. Lemant, J., V. Boisson, A. Winer, L. Thibault, H. Andre, F. Tixier, M. Lemercier, E. Antok, M. P. Cresta, P. Grivard, M. Besnard, O. Rollot, F. Favier, M. Huerre, J. L. Campinos, and A. Michault. 2008. Serious acute chikungunya virus infection requiring intensive care during the Reunion Island outbreak in 2005-2006. *Crit Care Med* 36:2536-2541.

5. Ernould, S., H. Walters, J. L. Alessandri, B. Llanas, M. C. Jaffar, S. Robin, T. Attali, D. Ramful, and J. C. Combes. 2008. [Chikungunya in paediatrics: epidemic of 2005-2006 in Saint-Denis, Reunion Island]. *Arch Pediatr* 15:253-262.

6. Gerardin, P., G. Barau, A. Michault, M. Bintner, H. Randrianaivo, G. Choker, Y. Lenglet, Y. Touret, A. Bouveret, P. Grivard, K. Le Roux, S. Blanc, I. Schuffenecker, T. Couderc, F. Arenzana-Seisdedos, M. Lecuit, and P. Y. Robillard. 2008. Multidisciplinary prospective study of mother-to-child chikungunya virus infections on the island of La Reunion. *PLoS Med* 5:e60.

7. Couderc, T., F. Chretien, C. Schilte, O. Disson, M. Brigitte, F. Guivel-Benhassine, Y. Touret, G. Barau, N. Cayet, I. Schuffenecker, P. Despres, F. Arenzana-Seisdedos, A. Michault, M. L. Albert, and M. Lecuit. 2008. A mouse model for Chikungunya: young age and inefficient type-I interferon signaling are risk factors for severe disease. *PLoS Pathog* 4:e29.

8. Schilte, C., T. Couderc, F. Chretien, M. Sourisseau, N. Gangneux, F. Guivel-Benhassine, A. Kraxner, J. Tschopp, S. Higgs, A. Michault, F. Arenzana-Seisdedos, M. Colonna, L. Peduto, O. Schwartz, M. Lecuit, and M. L. Albert. 2010. Type I IFN controls chikungunya virus via its action on nonhematopoietic cells. *J Exp Med* 207:429-442.

9. Paun, A., and P. M. Pitha. 2007. The innate antiviral response: new insights into a continuing story. *Adv Virus Res* 69:1-66.

10. Lenschow, D. J., C. Lai, N. Frias-Staheli, N. V. Giannakopoulos, A. Lutz, T. Wolff, A. Osiak, B. Levine, R. E. Schmidt, A. Garcia-Sastre, D. A. Leib, A. Pekosz, K. P. Knobeloch, I. Horak, and H. W. t. Virgin. 2007. IFN-stimulated gene 15 functions as a critical antiviral molecule against influenza, herpes, and Sindbis viruses. *Proc Natl Acad Sci U S A* 104:1371-1376.

11. Giannakopoulos, N. V., E. Arutyunova, C. Lai, D. J. Lenschow, A. L. Haas, and H. W. Virgin. 2009. ISG15 Arg151 and the ISG15-conjugating enzyme UbE1L are important for innate immune control of Sindbis virus. *J Virol* 83:1602-1610.

12. Lai, C., J. J. Struckhoff, J. Schneider, L. Martinez-Sobrido, T. Wolff, A. Garcia-Sastre, D. E. Zhang, and D. J. Lenschow. 2009. Mice lacking the ISG15 E1 enzyme UbE1L demonstrate increased susceptibility to both mouse-adapted and non-mouse-adapted influenza B virus infection. *J Virol* 83:1147-1151.

13. D'Cunha, J., E. Knight, Jr., A. L. Haas, R. L. Truitt, and E. C. Borden. 1996. Immunoregulatory properties of ISG15, an interferon-induced cytokine. *Proc Natl Acad Sci U S A* 93:211-215.

14. Padovan, E., L. Terracciano, U. Certa, B. Jacobs, A. Reschner, M. Bolli, G. C. Spagnoli, E. C. Borden, and M. Heberer. 2002. Interferon stimulated gene 15 constitutively produced by melanoma cells induces e-cadherin expression on human dendritic cells. *Cancer Res* 62:3453-3458.

15. Owhashi, M., Y. Taoka, K. Ishii, S. Nakazawa, H. Uemura, and H. Kambara. 2003. Identification of a ubiquitin family protein as a novel neutrophil chemotactic factor. *Biochem Biophys Res Commun* 309:533-539.

16. Bogunovic, D., M. Byun, L. A. Durfee, A. Abhyankar, O. Sanal, D. Mansouri, S. Salem, I. Radovanovic, A. V. Grant, P. Adimi, N. Mansouri, S. Okada, V. L. Bryant, X. F. Kong, A. Kreins, M. M. Velez, B. Boisson, S. Khalilzadeh, U. Ozcelik, I. A. Darazam, J. W. Schoggins, C. M. Rice, S. Al-Muhsen, M. Behr, G. Vogt, A. Puel, J. Bustamante, P. Gros, J. M. Huibregtse, L. Abel, S. Boisson-Dupuis, and J. L. Casanova. 2012. Mycobacterial disease and impaired IFN-gamma immunity in humans with inherited ISG15 deficiency. *Science* 337:1684-1688.

17. Xia, Z. P., L. Sun, X. Chen, G. Pineda, X. Jiang, A. Adhikari, W. Zeng, and Z. J. Chen. 2009. Direct activation of protein kinases by unanchored polyubiquitin chains. *Nature* 461:114-119.

18. Jiang, X., L. N. Kinch, C. A. Brautigam, X. Chen, F. Du, N. V. Grishin, and Z. J. Chen. 2012. Ubiquitin-induced oligomerization of the RNA sensors RIG-I and MDA5 activates antiviral innate immune response. *Immunity* 36:959-973.

19. Zhao, C., C. Denison, J. M. Huibregtse, S. Gygi, and R. M. Krug. 2005. Human ISG15 conjugation targets both IFN-induced and constitutively expressed proteins functioning in diverse cellular pathways. *Proc Natl Acad Sci U S A* 102:10200-10205.

20. Giannakopoulos, N. V., J. K. Luo, V. Papov, W. Zou, D. J. Lenschow, B. S. Jacobs, E. C. Borden, J. Li, H. W. Virgin, and D. E. Zhang. 2005. Proteomic identification of proteins conjugated to ISG15 in mouse and human cells. *Biochem Biophys Res Commun* 336:496-506.

21. Hicke, L., H. L. Schubert, and C. P. Hill. 2005. Ubiquitin-binding domains. *Nat Rev Mol Cell Biol* 6:610-621.

22. Hurley, J. H., S. Lee, and G. Prag. 2006. Ubiquitin-binding domains. *Biochem J* 399:361-372.

23. Matute, J. D., A. A. Arias, M. C. Dinauer, and P. J. Patino. 2005. p40phox: the last NADPH oxidase subunit. *Blood Cells Mol Dis* 35:291-302.

24. Makeyev, A. V., and S. A. Liebhaber. 2002. The poly(C)-binding proteins: a multiplicity of functions and a search for mechanisms. *RNA* 8:265-278.

25. You, F., H. Sun, X. Zhou, W. Sun, S. Liang, Z. Zhai, and Z. Jiang. 2009. PCBP2 mediates degradation of the adaptor MAVS via the HECT ubiquitin ligase AIP4. *Nat Immunol* 10:1300-1308.

26. Zhou, X., F. You, H. Chen, and Z. Jiang. 2012. Poly(C)-binding protein 1 (PCBP1) mediates housekeeping degradation of mitochondrial antiviral signaling (MAVS). *Cell Res* 22:717-727.

27. McGough, I. J., and P. J. Cullen. 2011. Recent advances in retromer biology. *Traffic* 12:963-971.

28. Cullen, P. J., and H. C. Korswagen. 2012. Sorting nexins provide diversity for retromer-dependent trafficking events. *Nat Cell Biol* 14:29-37.

29. Levine, B., J. E. Goldman, H. H. Jiang, D. E. Griffin, and J. M. Hardwick. 1996. Bc1-2 protects mice against fatal alphavirus encephalitis. *Proc Natl Acad Sci U S A* 93:4810-4815.

30. Nava, V. E., A. Rosen, M. A. Veliuona, R. J. Clem, B. Levine, and J. M. Hardwick. 1998. Sindbis virus induces apoptosis through a caspase-dependent, CrmA-sensitive pathway. *J Virol* 72:452-459.

31. Orvedahl, A., S. MacPherson, R. Sumpter, Jr., Z. Talloczy, Z. Zou, and B. Levine. 2010. Autophagy protects against Sindbis virus infection of the central nervous system. *Cell Host Microbe* 7:115-127.

32. Joubert, P. E., S. W. Werneke, C. de la Calle, F. Guivel-Benhassine, A. Giodini, L. Peduto, B. Levine, O. Schwartz, D. J. Lenschow, and M. L. Albert. 2012. Chikungunya virus-induced autophagy delays caspase-dependent cell death. *J Exp Med* 209:1029-1047.

33. Cadwell, K., J. Y. Liu, S. L. Brown, H. Miyoshi, J. Loh, J. K. Lennerz, C. Kishi, W. Kc, J. A. Carrero, S. Hunt, C. D. Stone, E. M. Brunt, R. J. Xavier, B. P. Sleckman, E. Li, N. Mizushima, T. S. Stappenbeck, and H. W. t. Virgin. 2008. A key role for autophagy and the autophagy gene Atg16l1 in mouse and human intestinal Paneth cells. *Nature* 456:259-263.

34. Levine, B., and G. Kroemer. 2008. Autophagy in the pathogenesis of disease. *Cell* 132:27-42.

35. Deretic, V. 2012. Autophagy as an innate immunity paradigm: expanding the scope and repertoire of pattern recognition receptors. *Curr Opin Immunol* 24:21-31.

36. Komatsu, M., H. Kurokawa, S. Waguri, K. Taguchi, A. Kobayashi, Y. Ichimura, Y. S. Sou, I. Ueno, A. Sakamoto, K. I. Tong, M. Kim, Y. Nishito, S. Iemura, T. Natsume, T. Ueno, E. Kominami, H. Motohashi, K. Tanaka, and M. Yamamoto. 2010. The selective autophagy substrate p62 activates the stress responsive transcription factor Nrf2 through inactivation of Keap1. *Nat Cell Biol* 12:213-223.

37. Fan, W., Z. Tang, D. Chen, D. Moughon, X. Ding, S. Chen, M. Zhu, and Q. Zhong. 2010. Keap1 facilitates p62-mediated ubiquitin aggregate clearance via autophagy. *Autophagy* 6:614-621.

38. Jesenberger, V., and S. Jentsch. 2002. Deadly encounter: ubiquitin meets apoptosis. *Nat Rev Mol Cell Biol* 3:112-121.

39. Klimstra, W. B., K. D. Ryman, K. A. Bernard, K. B. Nguyen, C. A. Biron, and R. E. Johnston. 1999. Infection of neonatal mice with sindbis virus results in a systemic inflammatory response syndrome. *J Virol* 73:10387-10398.

40. Wang, E., E. Volkova, A. P. Adams, N. Forrester, S. Y. Xiao, I. Frolov, and S. C. Weaver. 2008. Chimeric alphavirus vaccine candidates for chikungunya. *Vaccine* 26:5030-5039.

41. Billiau, A. 2006. Anti-inflammatory properties of Type I interferons. *Antiviral Res* 71:108-116.

42. Guarda, G., M. Braun, F. Staehli, A. Tardivel, C. Mattmann, I. Forster, M. Farlik, T. Decker, R. A. Du Pasquier, P. Romero, and J. Tschopp. 2011. Type I interferon inhibits interleukin-1 production and inflammasome activation. *Immunity* 34:213-223.

43. Mohler, K. M., D. S. Torrance, C. A. Smith, R. G. Goodwin, K. E. Stremler, V. P. Fung, H. Madani, and M. B. Widmer. 1993. Soluble tumor necrosis factor (TNF) receptors are effective therapeutic agents in lethal endotoxemia and function simultaneously as both TNF carriers and TNF antagonists. *J Immunol* 151:1548-1561.

44. Merrill, J. C., J. You, C. Constable, S. E. Leeman, and S. Amar. 2011. Whole-body deletion of LPS-induced TNF-alpha factor (LITAF) markedly improves experimental endotoxic shock and inflammatory arthritis. *Proc Natl Acad Sci U S A* 108:21247-21252.

45. Trgovcich, J., K. Ryman, P. Extrom, J. C. Eldridge, J. F. Aronson, and R. E. Johnston. 1997. Sindbis virus infection of neonatal mice results in a severe stress response. *Virology* 227:234-238.

46. Durfee, L. A., N. Lyon, K. Seo, and J. M. Huibregtse. 2010. The ISG15 conjugation system broadly targets newly synthesized proteins: implications for the antiviral function of ISG15. *Mol Cell* 38:722-732.